

**DOKUZ EYLÜL UNIVERSITY**  
**GRADUATE SCHOOL OF NATURAL AND APPLIED SCIENCES**

**INDOOR DISTANCE BASED POSITIONING BY  
USING METRICS OF STANDARD  
COMMUNICATION TECHNOLOGIES**

by  
**Türker TÜRKORAL**

**March, 2017**

**İZMİR**

**INDOOR DISTANCE BASED POSITIONING BY  
USING METRICS OF STANDARD  
COMMUNICATION TECHNOLOGIES**

**A Thesis Submitted to the  
Graduate School of Natural and Applied Sciences of Dokuz Eylül University  
In Partial Fulfillment of the Requirements for the Degree of Master of Science  
in Mechatronics Engineering Program**

**by  
Türker TÜRKORAL**

**March, 2017**

**İZMİR**

## M.Sc THESIS EXAMINATION RESULT FORM

We have read the thesis entitled “**INDOOR DISTANCE BASED POSITIONING BY USING METRICS OF STANDARD COMMUNICATION TECHNOLOGIES**” completed by **TÜRKER TÜRKORAL** under supervision of **ASST. PROF. DR. ÖZGÜR TAMER** and we certify that in our opinion it is fully adequate, in scope and in quality, as a thesis for the degree of Master of Science.



Asst. Prof. Dr. Özgür TAMER

Supervisor



Asst. Prof. Dr. Berna ÖZLER

(Jury Member)



Asst. Prof. Dr. Ahmet ÖZKULAK

(Jury Member)



Prof. Dr. Emine İlknur CÖCEN  
Director  
Graduate School of Natural and Applied Sciences

## ACKNOWLEDGEMENTS

First, I would like to thank to my supervisor Asst. Prof. Özgür TAMER for his supervision, support, guidance and contributions to my thesis from the beginning. He made sure that I am worthy to the title.

I would like to thank to my teacher Assoc. Prof. Dr. Levent ÇETİN for his inducements from the beginning.

I would like to thank to my friends and colleagues Suat YETİŞ, Tunca KÖKLÜ, Recep ÖZTÜRK and Enes İNANÇ for their contribution, support and motivation.

I would like to express my sincere gratitude to my family for their unlimited support, everlasting patience and guidance.

Lastly, I would like to thank to my wife, my friend, my life and my love İlke TÜRKORAL for being my eternal companion.

This work has been supported by The Scientific and Technological Research Council of Turkey (TUBITAK) under Grant No. 114E659.

Türker TÜRKORAL

# **INDOOR DISTANCE BASED POSITIONING BY USING METRICS OF STANDARD COMMUNICATION TECHNOLOGIES**

## **ABSTRACT**

In recent years, indoor localization problem is a highly preferred topic to study. In this thesis, a positioning system based on wireless communication metrics is proposed and implemented for a 4 client robotic team in an indoor environment. It is aimed to estimate the distances between the clients by using the received signal strength measurements. By using the estimated distances, the relative positions of the clients are identified by the proposed no initial indoor positioning algorithm.

In this thesis, besides the preferred wireless communication metric, Received Signal Strength Indicator (RSSI), the other metrics, Time Difference of Arrival (TDoA), Time of Arrival (ToA) and Two-Way ToA are also examined. With the selected hardware it is considered to use RSSI instead of time based metrics in order to implement a short range low cost indoor positioning system. The RSSI measurements are recorded more than once for two different indoor environments and four different client layouts. By using those recordings the distances between the clients are estimated. For 4 clients, 6 different distance values are estimated by using 3 different Received Signal Strength (RSS) based distance estimation methods namely International Telecommunication Union (ITU) Indoor Path Loss Model, Two-Ray Ground Reflected Path Loss Model and the Experimentally Derived Signal Strength Distance Relation (EDR) Model. The distance estimations for 4 clients, 3 distance estimation methods and two environments are recorded to be used in No Initial Indoor Positioning algorithm, the NOIP. The proposed positioning algorithm, the NOIP, is a triangulation based positioning algorithm that needs no initial conditions.

The position estimations of the clients for all the client layouts are presented for the specific hardware and environment selection. The usability of the system is

discussed and some additional information is provided to improve the quality, efficiency and availability of the system.

**Keywords:** RSSI, TDoA, ToA, triangulation, indoor positioning.



# STANDART İLETİŞİM TEKNOLOJİLERİ METRİKLERİ KULLANILARAK İÇ MEKAN MESAFE TABANLI KONUMLAMA

## ÖZ

Son yıllarda, kapalı alan konumlandırma problemi çalışmak için oldukça sık tercih edilen bir konu olmuştur. Bu tezde, kapalı bir mekanda 4 üyeli bir robot takımı için kablosuz haberleşme metriklerini temel alan bir pozisyon belirleme sistemi sunulmuş ve gerçekleştirilmiştir. Üyeler arasındaki mesafelerin alıcıya gelen sinyal şiddeti ölçümleri ile tahmin edilmesi amaçlanmıştır. Tahmin edilen mesafelerin kullanılmasıyla, üyelerin göreceli konumları başlangıç koşulsuz pozisyon belirleme algoritması ile belirlenmiştir.

Bu tezde, tercih edilen kablosuz haberleşme metriği, Alınan İşaret Şiddet Göstergesi'nin (RSSI) yanı sıra diğer metrikler, Varış Süre Farkı (TDoA), Varış Süresi (ToA) ve İki Yönlü Varış Süresi (Two-Way ToA) de incelenmiştir. Seçilen donanım ile, kısa mesafe düşük maliyetli kapalı alan pozisyon belirleme sisteminin gerçekleştirilebilmesi için zaman temelli metriklerin yerine RSSI metriğinin kullanılması düşünülmüştür. RSSI ölçümleri, 4 üye dizilimi ve 2 farklı ortam için birden fazla kez kaydedilmiştir. Bu kayıtlar kullanılarak üyeler arasındaki mesafeler tahmin edilmiştir. 4 üye için 6 farklı mesafe değeri, ITU Kapalı Alan Mesafe Kayıp Modeli, İki Işınlı Yerden Yansımali Mesafe Kayıp Modeli ve Deneysel Olarak Türetilmiş İşaret Şiddeti Mesafe Alaka (EDR) Modeli ile olmak üzere 3 farklı Alınan İşaret Şiddeti (RSS) temelli mesafe kestirim yöntemi kullanılarak tahmin edilmiştir. Mesafe kestirimleri, Başlangıç Koşulsuz İç Mekan Pozisyon Belirleme algoritmasında, yani NOIP'te kullanılmak üzere, 4 üye, 3 mesafe kestirim yöntemi ve 2 ortam için yapılmıştır. Sunulan pozisyon belirleme algoritması, NOIP, başlangıç koşuluna ihtiyaç duymayan üçgenleme temelli bir pozisyon belirleme algoritmasıdır.

Üyelerin pozisyon tahminleri, spesifik donanım ve ortam seçimleri ile 4 farklı üye dizilimi için sunulmuştur. Sistemin kullanılabilirliği tartışılmış, kalitesini, verimliliğini ve geçerliliğini arttırmak için bazı ek bilgiler sağlanmıştır.

**Anahtar kelimeler:** RSSI, TDoA, ToA, üçgenleme, iç mekan konumlama.



## CONTENTS

	<b>Page</b>
M.Sc THESIS EXAMINATION RESULT FORM.....	ii
ACKNOWLEDGEMENTS .....	iii
ABSTRACT.....	iv
ÖZ .....	vi
LIST OF FIGURES .....	xi
LIST OF TABLES .....	xiv
<b>CHAPTER ONE - INTRODUCTION .....</b>	<b>1</b>
<b>CHAPTER TWO - INDOOR LOCALIZATION PROBLEM.....</b>	<b>6</b>
2.1 Wireless Communication Infrastructures .....	7
2.2 Wireless Communication Metrics .....	7
2.2.1 Received Signal Strength Indicator .....	8
2.2.2 Time Difference of Arrival .....	9
2.2.3 Time of Arrival .....	10
2.2.4 Two-Way Time of Arrival .....	12
2.3 Distance Estimation Methods and Positioning.....	12
2.3.1 Received Signal Strength Based Distance Estimation and Positioning..	12
2.3.2 Time Based Distance Estimation and Positioning.....	16
<b>CHAPTER THREE - DISTANCE ESTIMATION AND NO INITIAL INDOOR POSITIONING.....</b>	<b>19</b>
3.1 Distance Estimation Process .....	19
3.1.1 Measurement Process .....	19
3.1.1.1 1 <sup>st</sup> Measurement Method – Measuring between 1 Receiver and 1 Transmitter (1 <sup>st</sup> MM) .....	19

3.1.1.2 2 <sup>nd</sup> Measurement Method – Measuring between 1 Receiver and 3 Transmitters (2 <sup>nd</sup> MM).....	20
3.1.2 Received Signal Strength (RSS) Based Distance Estimation Models.....	21
3.1.2.1 International Telecommunication Union (ITU) Indoor Path Loss Model.....	21
3.1.2.2 Two-Ray Ground Reflected Path Loss Model.....	23
3.1.2.3 Distance Estimation with the Experimentally Derived Signal Strength – Distance Relation (EDR) Model .....	24
3.2 No Initial Indoor Positioning (the NOIP).....	25

## **CHAPTER FOUR - RESULTS ..... 30**

4.1 Simulation Results.....	30
4.1.1 Simulated Results of the 1 <sup>st</sup> Client Layout .....	32
4.1.2 Simulated Results of the 2 <sup>nd</sup> Client Layout .....	35
4.1.3 Simulated Results of the 3 <sup>rd</sup> Client.....	38
4.1.4 Simulated Results of the 4 <sup>th</sup> Client Layout.....	41
4.1.5 Extensive Numerical Error Analysis of Simulation Procedure .....	44
4.2 Experimental Results.....	50
4.2.1 Measurement Process and the Results.....	51
4.2.1.1 Hardware Process of the Measurement Process .....	51
4.2.1.2 Software Process of the Measurement Process.....	55
4.2.1.3 Measurement Results of the Received Signal Strength Indicator (RSSI) Metrics .....	55
4.2.1.3.1 Results of the 1st Measurement Method.....	55
4.2.1.3.2 Results of the 2nd Measurement Method.....	58
4.2.2 Results of the Distance Estimation Process.....	62
4.2.2.1 Distance Estimation Results of ITU Indoor Path Loss Model.....	62
4.2.2.2 Distance Estimation Results of Two-Ray Ground Reflected Path Loss Model.....	65
4.2.2.3 Distance Estimation Results of Experimentally Derived Signal Strength-Distance Relation (EDR) Model.....	68

4.2.2.4 Performance Comparison of the Distance Estimation Methods .....	70
4.2.3 Results of the Positioning Process .....	71
4.2.3.1 Positioning Results of the 1 <sup>st</sup> Client Layout .....	71
4.2.3.2 Positioning Results of the 2 <sup>nd</sup> Client Layout .....	74
4.2.3.3 Positioning Results of the 3 <sup>rd</sup> Client Layout .....	77
4.2.3.4 Positioning Results of the 4 <sup>th</sup> Client Layout .....	79
4.2.3.5 Performance Comparison of the Positioning Results .....	82
<b>CHAPTER FIVE - CONCLUSION .....</b>	<b>84</b>
<b>REFERENCES .....</b>	<b>87</b>
<b>APPENDICES .....</b>	<b>93</b>

## LIST OF FIGURES

	<b>Page</b>
Figure 2.1 TDoA hyperbolas and location estimation .....	10
Figure 2.2 ToA and TDoA measurements, hyperbolas and circles .....	11
Figure 2.3 Two-Ray model signal paths .....	14
Figure 2.4 ToA or Two-Way ToA metric measurements .....	17
Figure 3.1 RSSI recording method of 1, in the office building .....	20
Figure 3.2 2 <sup>nd</sup> MM, measurements by the layouts .....	21
Figure 3.3 EDR Model derivation for a specific example .....	24
Figure 3.4 Setting the relative coordinate plane.....	25
Figure 3.5 Locating client <i>c</i> with the intersection of the measurement circles.....	26
Figure 3.6 Conditions of non-intersecting MCs.....	27
Figure 3.7 Locating client <i>d</i> .....	28
Figure 3.8 All intersections of MCs and the position estimations of the clients .....	29
Figure 4.1 1 <sup>st</sup> client layout, coordinates and distances.....	32
Figure 4.2 Position estimations of CL1 when <i>iterations</i> =10 and SNR=2 .....	33
Figure 4.3 Position estimations of CL1 when <i>iterations</i> =50 and SNR=5 .....	33
Figure 4.4 Position estimations of CL1 when <i>iterations</i> =100 and SNR=10 .....	34
Figure 4.5 Actual and the estimated positions of the clients for the 3 ISCs for CL1..	34
Figure 4.6 2 <sup>nd</sup> client layout, coordinates and distances .....	35
Figure 4.7 Position estimations of CL2 when <i>iterations</i> =10 and SNR=2 .....	36
Figure 4.8 Position estimations of CL2 when <i>iterations</i> =50 and SNR=5 .....	36
Figure 4.9 Position estimations of CL2 when <i>iterations</i> =100 and SNR=10 .....	37
Figure 4.10 Actual and the estimated positions of the clients for the 3 ISCs for CL2 .....	37
Figure 4.11 3 <sup>rd</sup> client layout, coordinates and distances .....	38
Figure 4.12 Position estimations of CL3 when <i>iterations</i> =10 and SNR=2 .....	39
Figure 4.13 Position estimations of CL3 when <i>iterations</i> =50 and SNR=5 .....	39
Figure 4.14 Position estimations of CL3 when <i>iterations</i> =100 and SNR=10 .....	40
Figure 4.15 Actual and the estimated positions of the clients for the 3 ISCs for CL3 .....	40

Figure 4.16 4 <sup>th</sup> client layout, coordinates and distances .....	41
Figure 4.17 Position estimations of CL4 when <i>iterations</i> =10 and SNR=2 .....	42
Figure 4.18 Position estimations of CL4 when <i>iterations</i> =50 and SNR=5 .....	42
Figure 4.19 Position estimations of CL4 when <i>iterations</i> =100 and SNR=10 .....	43
Figure 4.20 Actual and the mean of the estimated positions of the clients for the 3 ISCs for CL4 .....	43
Figure 4.21 Error performance – <i>iterations</i> correlations of the 4 CLs with respect to SNR values .....	48
Figure 4.22 Error performance – SNR correlations of the 4 CLs with respect to <i>iterations</i> .....	49
Figure 4.23 Raspberry Pi .....	51
Figure 4.24 Schematic diagram of the first SID design .....	52
Figure 4.25 Schematic design of the second SID .....	52
Figure 4.26 The 1 <sup>st</sup> (a) and the 2 <sup>nd</sup> (b) layout designs of the SID .....	53
Figure 4.27 First implementation of the SID .....	53
Figure 4.28 Second and the final version of the SID .....	54
Figure 4.29 The connection of RPi and the SID, a ‘client’, 1 <sup>st</sup> version .....	54
Figure 4.30 The 2 <sup>nd</sup> and the final version of a ‘client’ .....	54
Figure 4.31 A hypothetical RSSI-Distance curve .....	56
Figure 4.32 Measurement environment for the 1 <sup>st</sup> MM .....	57
Figure 4.33 First MM and the distances between the clients .....	57
Figure 4.34 The RSSI recordings of the 1 <sup>st</sup> MM .....	58
Figure 4.35 Remaining 3 CLs, 2 <sup>nd</sup> CL, 3 <sup>rd</sup> CL and the 4 <sup>th</sup> CL .....	59
Figure 4.36 The illustration of the 2 <sup>nd</sup> MM .....	59
Figure 4.37 Example of the signal strengths seen by the 1st SID .....	60
Figure 4.38 The 4 clients .....	60
Figure 4.39 The environment where the recordings take place by the 2 <sup>nd</sup> MM .....	61
Figure 4.40 A closer look to the clients during the recordings .....	61
Figure 4.41 ITU exponents vs. the distance error .....	62
Figure 4.42 ITU estimations and the actual distances for the 1 <sup>st</sup> environment .....	64
Figure 4.43 ITU estimations and the actual distances for the 2 <sup>nd</sup> environment .....	65
Figure 4.44 Two-Ray Model distance estimations for the 1 <sup>st</sup> MM .....	66

Figure 4.45 Two-Ray Model distance estimations for the 2 <sup>nd</sup> MM.....	67
Figure 4.46 Derivation of the 1 <sup>st</sup> EDR Model.....	68
Figure 4.47 Derivation of the 2 <sup>nd</sup> EDR Model.....	69
Figure 4.48 Distance Estimations of the 1 <sup>st</sup> EDR Model for the 1 <sup>st</sup> MM .....	69
Figure 4.49 Distance Estimations of the 2 <sup>nd</sup> EDR Model for the 2 <sup>nd</sup> MM.....	70
Figure 4.50 Positioning results of CL1 for the distance estimations of ITU Model..	72
Figure 4.51 Positioning results of CL1 for the distance estimations of Two-Ray Model .....	72
Figure 4.52 Positioning results of CL1 for the distance estimations of EDR Model..	73
Figure 4.53 Mean positioning results of CL1 for all the distance estimation methods .....	73
Figure 4.54 Positioning results of CL2 for the distance estimations of ITU Model..	74
Figure 4.55 Positioning results of CL2 for the distance estimations of Two-Ray Model .....	75
Figure 4.56 Positioning results of CL2 for the distance estimations of EDR Model..	75
Figure 4.57 Mean positioning results of CL2 for all the distance estimation methods .....	76
Figure 4.58 Positioning results of CL3 for the distance estimations of ITU Model..	77
Figure 4.59 Positioning results of CL3 for the distance estimations of Two-Ray Model .....	77
Figure 4.60 Positioning results of CL3 for the distance estimations of EDR Model.	78
Figure 4.61 Mean positioning results of CL3 for all the distance estimation methods .....	78
Figure 4.62 Positioning results of CL4 for the distance estimations of ITU Model..	79
Figure 4.63 Positioning results of CL4 for the distance estimations of Two-Ray Model .....	80
Figure 4.64 Positioning results of CL4 for the distance estimations of EDR Model..	80
Figure 4.65 Mean positioning results of CL4 for all the distance estimation methods .....	81

## LIST OF TABLES

	<b>Page</b>
Table 4.1 Generated noisy $L_{ab}$ distances for $iterations=10$ and $SNR=2$ .....	30
Table 4.2 Different generations of noisy $L_{ab}$ distances.....	31
Table 4.3 Numerical error analysis of the 3 ISCs for the 1 <sup>st</sup> CL.....	35
Table 4.4 Numerical error analysis of the 3 ISCs for the 2 <sup>nd</sup> CL.....	38
Table 4.5 Numerical error analysis of the 3 ISCs for the 3 <sup>rd</sup> CL.....	41
Table 4.6 Numerical error analysis of the 3 ISCs for the 4 <sup>th</sup> CL.....	44
Table 4.7 Positioning error values of CL1 for 25 ISCs.....	44
Table 4.8 Positioning error values of CL2 for 25 ISCs.....	45
Table 4.9 Positioning error values of CL3 for 25 ISCs.....	46
Table 4.10 Positioning error values of CL4 for 25 ISCs.....	47
Table 4.11 The Mean values of the RSSI recordings taken in the 1 <sup>st</sup> and 2 <sup>nd</sup> environments.....	63
Table 4.12 Mean distance error values of all the estimation methods.....	70
Table 4.13 Positioning errors of CL1.....	74
Table 4.14 Positioning errors of CL2.....	76
Table 4.15 Positioning errors of CL3.....	79
Table 4.16 Positioning errors of CL4.....	81
Table 4.17 Actual and estimated distance comparison for the 4 <sup>th</sup> CL.....	82
Table 4.18 Error comparison of all CLs for all the distance estimation methods.....	82
Table 4.19 Individual and mean error performance comparison of the CLs.....	83

## **CHAPTER ONE**

### **INTRODUCTION**

For about the last decade, team robotics has gained a considerable importance. Robots entered our lives and they now are used for a large number of tasks even at home with the self-moving cleaning robots, robotic pets and user controlled robotics toys i.e. Sony AIBO is a great example to this type of robotic use for both the robots at home and team robotics applications. As an example, Quinlan et. al. (2003) used Sony AIBO to improve the locomotion and vision of the robot in the RoboCup Legged League by applying the Support Vector Machines and Hill Climbing techniques (Quinlan, Chalup, & Middleton, 2003). Besides the robotics in industry, this improvement of robotics enlarges the usage of robots, even for cleaning a house, delivering a cargo and also the entertainment of a child etc.

In recent technologies the position information of either a person or a robot that in a team becomes very important for monitoring or doing the assigned task. In team robotics, any robot is assigned a different task or they have been given only one mission. To accomplish the given task successfully, the robots have to know the position of themselves and each other. For a factory building, again the position information is a must know information and also the factory workers' positions may be wanted to monitored to increase the efficiency.

In any case, the positions of the clients, either a robot or a person, have a significant value to complete a mission. To specify the significance of the position information of the client in robotics, autonomous team robots would be a reliable example. With the educational mini robots, e-pucks, one can make a team and assign a task for them. Mondada et al. (2006) presented the design of a robot, e-pucks, for the specific target of engineering education in university level (Mondada et al., 2006).

Regardless of the task, a robot or a number of robots have to know some initial information to complete a given task. And here, position information has a great

importance within the communication infrastructures. In the work of Liu et al. (2007), an overview of the existing wireless indoor positioning techniques and solutions are provided and also a specific method of positioning, triangulation, is said to be that needs multiple reference points in order to locate a point (Liu, Darabi, Banerjee, & Liu, 2007). A robot cannot be located without an established communication, either one way communication or two ways. To establish a data transaction with the robots, a wireless communication infrastructure needs to be integrated or a wired system may be set up but it is not preferable in this technological era, especially for robots. Larranaga et al. (2010) preferred ZigBee for an adaptive indoor positioning algorithm in 2010 (Larranaga, Muguira, Lopez-Garde, & Vazquez, 2010), Kovacs et al. (2011) used Bluetooth for a multi-robot exploration algorithm in 2011 (Kovács, Pásztor, & Istenes, 2011) and in the work of Winfield and Holland (2000) the wireless communication infrastructure is WLAN for the control of mobile robots even in 2000 (Winfield & Holland, 2000). Wired systems complicate the whole system and limit the movement of robots and flexibility of the system.

There are a large number of wireless communication infrastructures such as Wi-Fi, Bluetooth, ZigBee, Radio, Microwave, IR etc. to use but two of them are the most known and preferred ones which are Wi-Fi and Bluetooth. These wireless communication infrastructures have a big role in our lives besides the industrial and academic usage of them. Almost everywhere, including the streets (for some) a Wi-Fi connection can be established or a Bluetooth pairing can be completed regardless of the environment just considering the range of the clients trying to connect their devices over Bluetooth.

The intensity of the usage of these wireless infrastructures, made the choice easier. In the work of Galvan et al. (2012) a combined positioning algorithm is proposed which is based on Bluetooth and Wi-Fi both (Galvan T., Galvan-Tejada, Sandoval, & Brena, 2012). To accomplish a communication and locate the clients, these two wireless communication infrastructures are preferred in this work.

After the communication infrastructures are set to be used, the next option in line until reaching the position information of a client is the metrics which are internally given by the Wi-Fi and Bluetooth Integrated Circuit (IC) (in our case it is a FN-Link Device containing Realtek RTL8723BU Wi-Fi & Bluetooth IC). Few of the many wireless communication metrics are RSSI (Received Signal Strength Indicator), TDoA (Time Difference of Arrival), ToA (Time of Arrival), Two-Way ToA (Two Way Time of Arrival) etc. While some of these metrics are automatically given by the wireless communication infrastructure, some are not. But with an additional hardware implementation the other metrics can also be added to the list of usable metrics. Grossman et al. (2008) used RSSI within a digital museum guide (Grossmann, Gansemer, & Suttorp, 2008), Gaber and Omar (2015) used TDoA along with DoA (Direction of Arrival) for a wireless indoor positioning study which has an achievable result of 1.5 cm for 2D indoor positioning (Gaber & Omar, 2015), in the work of Li et al. (2016) an indoor ultrasonic positioning system based on ToA for IoT (Internet of Things) is emphasized and the results are as precise as in the cm level for the moving objects in an indoor environment (Li, Han, Zhu, & Sun, 2016), and lastly, McCrady et al. (2000) chose Two-Way ToA in order to exceed synchronization problem between the master and slave clients in their work (McCrady, Doyle, Forstrom, Dempsey, & Martorana, 2000). In this work, all the mentioned wireless communication metrics are studied and with one (RSSI) simulation and experimental procedure is realized with the reasons due to its preference.

The next step in line to reach the position information of a client is the distance estimation procedure with using the selected wireless communication metric. RSSI is the preferred metric in this work and it gives the power of the signal that arrives to the belonging receiver. Kumar et al. (2009) used RSS based measurements, RSSI, in order to approximate the distances between the nodes in a wireless sensor network (WSN) (Kumar, Reddy, & Varma, 2009). But only RSSI information has no use when searching for the distance information between the clients. We need to establish a relation between RSSI and the distance between the clients.

To acquire the distance information between the clients, the relation models are examined in literature and two of them were selected. With the use of these relation models the estimation of a distance between the clients can be found by using RSSI data. Besides the selected 2 models, an experimental power-distance relation model that is called EDR (Experimental Signal Strength - Distance Relation Model) Model is also provided in this study. The relation models are;

- International Telecommunication Union (ITU) Indoor Path Loss Model
- Two-Ray Ground Reflected Propagation Model
- Experimental Signal Strength – Distance Relation (EDR) Model

With the use of these three signal strength-distance relation (SSDR) models the distances between the clients can be estimated by using RSSI data as an input. ITU indoor path loss model is emphasized for the measurements taken in indoor office environment for site-specific validation of the model in the work of Chrysikos et. al. (2009) (Chrysikos, Georgopoulos, & Kotsopoulos, 2009). The basis of the second model, Two-Ray, commonly known as Friis Equation, can also be used as a relation model and in the work of Lassabe et. al. (2005) it is used to locate Wi-Fi terminals in an indoor environment (Lassabe, Canalda, Chatonnay, Spies, & Baala, 2005). They also compare the accuracy results of their work with the other solutions. Friis Equation deals with only one, line of sight signal but Two-Ray Ground Reflected Propagation model adds the second signal which is the reflected signal from the ground as it is said in the name of the model, Two-Ray. Sommer and Dressler (2011) examined the Two-Ray Ground path loss models and they proposed an alternative model, not being for indoor positioning but it is for vehicles on the road, Inter-Vehicle Communication Protocols (Sommer & Dressler, 2011). The last model that is proposed to be used in this work is the EDR model. This model is based on RSSI measurements and the real distances that RSSI measurements are recorded. Türkoral et al. (2016) proposed this experimental method as an alternative to the other indoor distance estimation techniques for a specific hardware implementation (Türkoral, Tamer, Yetiş, İnanç, & Çetin, 2016).

The distance values between the clients only are not enough for locating them. To do that, a positioning algorithm is proposed in this thesis called the NOIP (No Initial Indoor Positioning). This algorithm is based on the triangulation method but has no need for the initial position information of the first three clients. Triangulation is locating a point by using the distance information of three other initially known points (Türkorall, Tamer, Yetiş, & Çetin, 2017). Also Liu et. al. (2007) examine both the metrics and the trilateration methods as well as triangulation (Liu et al., 2007).

To estimate the position of a client, there are several other methods can be used besides the distance based location estimation techniques. Nuaimi and Kamel (2011) completed a survey on indoor positioning systems and algorithms and they mainly focused on two types of positioning; Fixed Indoor Positioning and Indoor Pedestrian Positioning (Nuaimi & Kamel, 2011). The subsections of the first method, Fixed Indoor Positioning Systems; Infrared Positioning Systems, Ultrasonic Positioning Systems, RF Positioning Systems and Optical Positioning Systems are also defined in their work. Where Nuaimi and Kamel did a survey on indoor positioning techniques, Moghtadaiee et al. (2011) used FM Radio Signals for indoor localization with a fingerprinting approach (Moghtadaiee, Dempster, & Lim, 2011). Also Guerrieri et al. (2006) used RFID tags in their indoor localization and communication systems for the first responders (Guerrieri et al., 2006). In the variety of these positioning techniques, we decided to construct a distance based indoor positioning system.

Overall, the aim here is to design a communication system and a distance based positioning algorithm for a robotic team number of 4 for indoor environments.

## **CHAPTER TWO**

### **INDOOR LOCALIZATION PROBLEM**

Indoor localization is a highly preferable subject to be studied in academics. It is also studied in commercial applications to increase efficiency and to reduce the cost. Not being directly related with these concepts but localization problem lies under in any robotic system that needs to be located, or the location information of them is must to be known.

In all the robotic systems containing movable clients, the position information is an essential factor. Regardless from the concept of the task they are given, all the clients are moving in an environment and in order to complete the mission they must operate in harmony. To do that, a communication method must be set between them. Even though they can communicate, that is not enough to complete the task. The missions of mobile robotic systems make the clients to move and moving are essential in the task, which is why the clients are mobile. Hence, the clients must know the positions of one another.

The locations of the nodes, clients or another thing in an indoor environment can be found in several ways. There are a large number of methods are used to locate a node in a robotic team with being under the categories of Non-Radio Technologies (NRT) and Wireless Technologies (WT) (“Indoor Positioning System,” n.d.). Magnetic Positioning, Inertial Measurements, Positioning with Visual Markers and Positioning with Known Visual Features are the methods belonging to NRT.

However, with the improvement of wireless technologies, especially in the last two decades, positioning methods that belong to WT have been developed. Received Signal Strength Indication, Time of Arrival and Angle of Arrival are the three subsections of WT (“Indoor Positioning System,” n.d.). By using a wireless infrastructure, say Wi-Fi or Bluetooth, wanting to construct an indoor positioning system, for a low cost, easy to access and feasible system, one can choose the RSS or Time based wireless communication metrics. To use AoA, extra devices must be

implemented containing antennas and the positioning process would not be as applicable as it would be with the other metrics.

To estimate the locations of the members of a robotic team, wireless communication infrastructures and metrics, distance estimation models and positioning algorithms can be used as well.

## **2.1 Wireless Communication Infrastructures**

To establish a communication between the clients in an indoor environment, several wireless communication infrastructures can be preferred with being easily accessible, considerably cheap, easy to use and above for all, should be universal in order to access the devices that are going to be used.

In all wireless communication infrastructures that are mentioned in the previous chapter, two of them are the most recognized namely Wi-Fi and Bluetooth.

We may prefer Wi-Fi and/or Bluetooth to connect the clients to one another and obtain the necessary measurements. When choosing the wireless communication infrastructure, one must note that the wireless communication metrics that are needed to be recorded are internally given by the chosen structures or not besides all the definitions.

## **2.2 Wireless Communication Metrics**

As mentioned in the previous section, the most common metrics are RSSI, TDoA ToA, Two-Way ToA with being used the metric RSSI in this study, and the other metrics are also examined.

### ***2.2.1 Received Signal Strength Indicator***

RSSI is the power indicator value of a received signal that is sent from a client. RSSI metric is provided by the chosen wireless infrastructure. With a proper coding, one can list the wireless devices that are in the range and the signal strengths of them on a screen.

To acquire proper RSSI values, a line of sight between the elements is needed, reflections must be prevented and the Automatic Gain Control (AGC) of the devices (if exists and if active) must be deactivated in order to link RSSI values directly with the distance values a priori. It can be said that the mentioned channel characteristics must be known since the measurements are depending on them. Signal strength algorithms that are used to locate a client are very sensitive to the estimations of that channel characteristics (Arslan, Chen, & Di Benedetto, 2006).

RSSI is a highly preferable metric for indoor positioning. It is used in many applications so far and will be used continually. The wireless communication metrics can be used in both hybrid and non-hybrid localization techniques. RSSI is used along with TDoA and ToA in the work of Laaraiedh et al. (2011) to compare the hybrid localization schemes (Laaraiedh, Yu, Avrillon, & Uguen, 2011). In the work of Xiao et al. (2011), indoor wireless positioning techniques, such as ToA, TDoA, AoA and RSSI, are compared and where the positioning precision of TDoA for an UWB system is defined as ‘a few centimeters to tens of centimeters’, it is ‘tens of centimeters to tens of meters’ for RSSI for a Bluetooth system (Xiao, Liu, Yang, Liu, & Xu, 2011). Even though it is said that TDoA based location estimations have advantages over RSSI based applications but Hara and Anzai (2008) compared the experimental results of both estimation methods and the results showed that, for a crowded area where LOS between clients has frequently cut RSSI has advantages over TDoA (Hara & Anzai, 2008).

### 2.2.2 Time Difference of Arrival

TDoA is the time difference between the signals coming from different transmitters to one receiver.

$$x_{tdoa} = |t_{yx} - t_{zx}| \quad (2.1)$$

where  $x_{tdoa}$  is the TDoA metric of the belonging client  $x$ ,  $t_{yx}$  and  $t_{zx}$  are the time of arrivals of the signals sent by the other clients  $Y$  and  $Z$  respectively.

In order to use this method time synchronization of the reference nodes must be set because TDoA schemes require at least three base stations for two dimensional localization (Cong & Weihua, 2002). But if all the positioning work will be proceed over TDoA measurements, every client in the robotic team must be synchronized on the same clock. In this context, Yamasaki et al. (2005) used an additional synchronizing component to their Access Points where they are implementing a TDoA localization system for IEEE 802.11b WLAN (Yamasaki et al., 2005). In Gustafsson and Gunnarsson's work (2003) it can be observed that the TDoA measurements are used for positioning also (Gustafsson & Gunnarsson, 2003).

Usually, this method is used in systems that contain both mobile and steady members. Steady members represent the sensors, beacons etc. and the mobile ones are the robots most of the time. The position of the mobile member can be estimated through a number of TDoA measurements with having the position information of the steady members. In that case, with using TDoA measurements, a location estimator can be developed based on the triangulation of hyperbolic asymptotes (Doğançay, 2005).

In Figure 2.1, an illustration of the two hyperbolas formed from the TDoA measurements at three fixed receivers is shown (Rappaport, Reed, & Woerner, 1996).

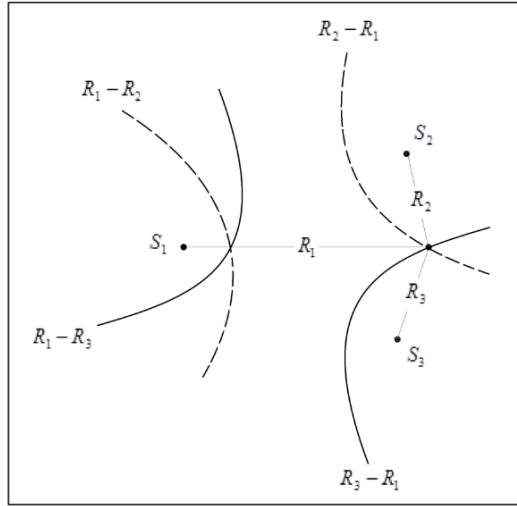


Figure 2.1 TDoA hyperbolas and location estimation

In Figure 2.1,  $S_1$ ,  $S_2$  and  $S_3$  represent the fixed receiver locations,  $R_1$ ,  $R_2$  and  $R_3$  are the estimated distances calculated with using TDoA measurements and the representations of the hyperbolas drawn by TDoA measurements are  $R_1-R_2$ ,  $R_1-R_3$ ,  $R_2-R_1$  and  $R_3-R_1$ . Also Eq. 2.2 is used to determine the two hyperbolas (Rappaport et al., 1996).

$$R_{i,j} = \sqrt{(X_i - x)^2 + (Y_i - y)^2 + (Z_i - z)^2} - \sqrt{(X_j - x)^2 + (Y_j - y)^2 + (Z_j - z)^2} \quad (2.2)$$

where  $(X_i, Y_i, Z_i)$  and  $(X_j, Y_j, Z_j)$  represent the coordinates of the fixed receivers,  $i$  and  $j$  (Rappaport et al., 1996).

### 2.2.3 Time of Arrival

ToA is also a time based metric representing the time between the signal's departure from the transmitter and the arrival to the receiver, commonly known as the travel time. To use ToA metrics in a localization algorithm, first the distance information must be extracted from the propagation delay between TX and RX (Güvenç & Chong, 2009). For the measurements of ToA metrics, there is also a need for synchronizing both the clients but if again the other measurements will be taken over this metric, other clients are also needed to be synchronized on the same clock (Arslan et al., 2006).

Whereby the TDoA metrics the distances are estimated with using the hyperbolas, for ToA metrics it is the circles (see Figure 2.2, (Kaune, 2012)). For a properly synchronized team of robots, the ToA metric represents time difference of a signal's departure and arrival difference of one client to another.

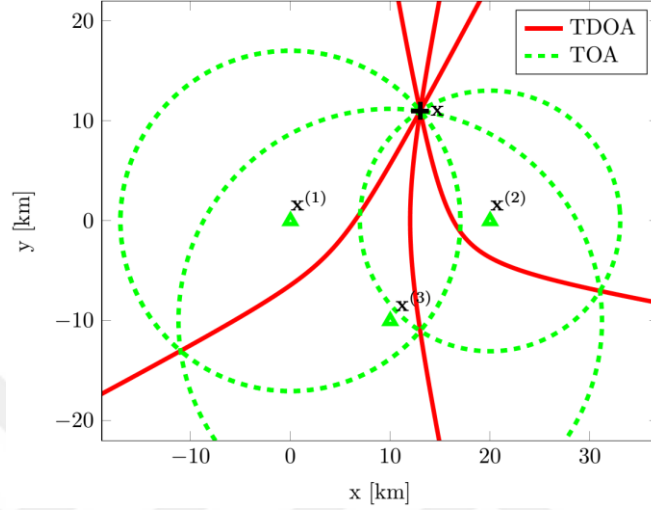


Figure 2.2 ToA and TDoA measurements, hyperbolas and circles, (Kaune, 2012)

For a perfectly synchronized ToA system that contains three receivers and one transmitter at a time, the distance between the clients are expressed as;

$$d_3 = c(t_3 - t_0) \quad , \quad d_2 = c(t_2 - t_0) \quad \text{and} \quad d_1 = c(t_1 - t_0) \quad (2.3)$$

where  $c$  is the speed of light and  $t_0$  is the time of signal departure. Now, for a 2D map, by using the calculated set of distances the transmitter's position  $T_p = [x_t, y_t]$  can be derived as;

$$\begin{cases} \sqrt{(x_1 - x_t)^2 + (y_1 - y_t)^2} = d_1 \\ \sqrt{(x_2 - x_t)^2 + (y_2 - y_t)^2} = d_2 \\ \sqrt{(x_3 - x_t)^2 + (y_3 - y_t)^2} = d_3 \end{cases} \quad (2.4)$$

where  $(x_1, y_1)$ ,  $(x_2, y_2)$  and  $(x_3, y_3)$  are the positions of the receivers. From that point the location of the transmitter can be estimated by a selected algorithm, such as Least Squares (Kietlinski-Zaleski, Yamazato, & Katayama, 2010).

#### ***2.2.4 Two-Way Time of Arrival***

This metric is based on the flight time of the signal but to use this type of metric there is no need for time synchronization. Because the initial transmitter is the secondary receiver, so the first receiver basically reflects the arrived signal. The initial transmitter then receives the signal back and records the time between. That metric is called Two-Way ToA. The distance estimation algorithms of this metric are the same as ToA distance estimation algorithms but if the time delay on the initial receiver which reflects the signal. The time that is spent on the initial receiver must be taken into account calculated carefully in order to record a meaningful Two-Way ToA measurement.

### **2.3 Distance Estimation Methods and Positioning**

The wireless communication metrics are all based on two main titles; signal strength based and time based. For all the metrics which belong to the same category, the same estimation model can be used (in theory). Hence, the distance estimation methods and the positioning techniques are all observed under these two titles.

#### ***2.3.1 Received Signal Strength Based Distance Estimation and Positioning***

Received Signal Strength (RSS) based positioning techniques rely on a path-loss model and location estimations depend on the energy of the signal measured on one end of a client (Arslan et al., 2006).

To begin with, RSSI metric is the first step of understanding the RSS based wireless communication metrics. With the proper settings of the channels, and the reliable recordings of the measurements, one can draw a map of signal strength – distance (SSD) relations. With the recordings of the measurements, power related distance estimation methods will be used to take on to the next step, positioning. Two of the many distance estimation methods are ITU Indoor Path-Loss Model and

Two-Ray Ground Reflected Propagation Model. Also with the EDR model that is experimentally derived in this work the estimation models becomes three.

- International Telecommunication Union (ITU) Indoor Path Loss Model

ITU Model is an indoor propagation path loss model (Equation 2.5) (International Telecommunication Union, 2015; Seybold, 2005).

$$P_L = P_t - P_{RSSI} = 20 \log_{10}(f) + N \log_{10}(d) + L_f(n) - 28dB \quad (2.5)$$

In Equation 2.5;

$P_L$  is the power loss and equals to the absolute difference of transmitted signal strength  $P_t$  and the measured RSSI metric  $P_{RSSI}$ ,

$N$  represents the distance power loss coefficient,

$L_f(n)$  is the loss factor of the floor penetration,

$f$  is the frequency, which is 2.4 GHz ,

$d$  is the distance in meters,

$n$  is the number of floors between the receiver and transmitter.

This estimation model depends on the floors between the receiver and transmitter, working frequency, and ambient conditions. For different frequencies, different environmental materials, these factors change and the total loss differs from one another.

For an indoor environment, the estimated distance values of the RSSI measurements via ITU model can be used in a positioning algorithm. Türkoral et al. (2016) presented the simulation results of this model for different SNR values and the number of iterations (Türkoral, Tamer, Yetiş, & Çetin, 2016).

- Two-Ray Ground Reflected Path Loss Model

The second distance estimation method is based on the Two-Ray Ground Reflected Path Loss Model. This model is based on a free space propagation model commonly known as the Friis Equation but where Friis Equation handles only one

LOS (line of sight) signal, Two-Ray Model utilizes the second signal which is the ground reflected one of the same source.

In Equation 2.6, the free space path loss formula can be seen. It is the same for the losses for the combination of all the paths. In this case the number of paths is two; hence, the path loss is represented with  $L_{tr}$ .

$$P_{RSSI} = P_t + G_r + G_t - L_{tr} \quad (2.6)$$

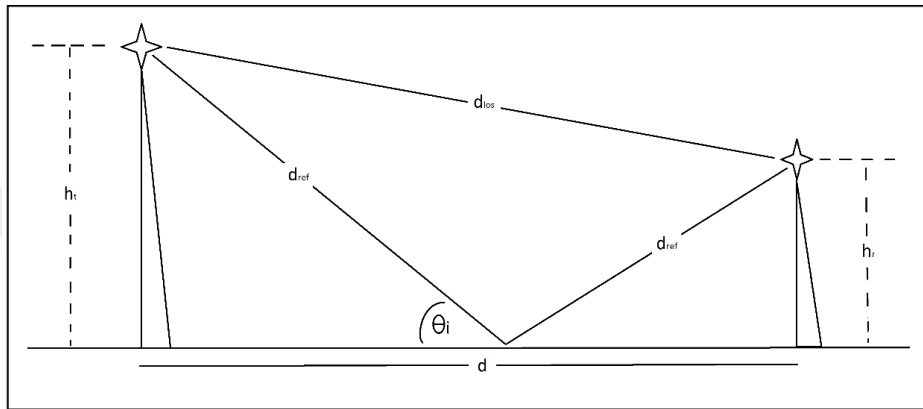


Figure 2.3 Two-Ray model signal paths

Assuming free space loss, beginning with only one path, the path loss can be written as the function of distance ( $d$ ) between the antennas and the wavelength ( $\lambda$ );

$$L_{loss} = 20 \log\left(4\pi \frac{d}{\lambda}\right) \quad (2.7)$$

However, this loss considers only the LOS signal, we need to add the formula at least one distorting signal, namely the ground reflection signal, therefore, the ground reflected model formula yields itself (Sommer & Dressler, 2011);

$$L_{tr} = 20 \log\left(4\pi \frac{d}{\lambda} \left|1 + \Gamma_{gnd} e^{i\varphi}\right|^{-1}\right) \quad (2.8)$$

by using the equations presented in the following.

$$\varphi = 2\pi \frac{d_{los} - d_{ref}}{\lambda} , \quad \Gamma_{gnd} = \frac{\sin \theta_i - \sqrt{\epsilon_r + \cos^2 \theta_i}}{\sin \theta_i + \sqrt{\epsilon_r + \cos^2 \theta_i}} \quad (2.9)$$

$$d_{los} = \sqrt{d^2 + (h_t - h_r)^2} , \quad d_{ref} = \sqrt{d^2 + (h_t + h_r)^2} \quad (2.10)$$

$$\sin \theta_i = \frac{(h_t + h_r)}{d_{ref}} , \quad \cos \theta_i = \frac{d}{d_{ref}} \quad (2.11)$$

As can be clearly seen, this calculation is a complex and not an easily/quickly solvable one (Sommer & Dressler, 2011). However the formulas are simplified assuming a perfect polarization and reflection (Rappaport, 1996). Hence, simplified Two-Ray Ground Reflected path loss formula becomes;

$$L_{lr} = 20 \log\left(\frac{d^2}{h_t h_r}\right) \quad (2.12)$$

The resulting path loss model of this method relies on the height of the antennas ( $h_t, h_r$ ) and the direct distance between them (see Equation 2.12).

- Experimentally Derived Signal Strength – Distance Relation (EDR) Path Loss Model

This model is a unique, self-derived model that relies on the actual RSSI measurements (Türköral, Tamer, Yetiş, İnanç, & Çetin, 2016). Equation 2.13 shows the mathematical formula of the presented SSDR model.

$$d = a.e^{b.P_{RSSI}} \quad (2.13)$$

EDR model is basically the fitted curve of the actual measurement-distance results. It is an exponential function containing two parameters besides the measurements and the desired values.

With the use of these distance estimation models, recordings of the measurements, in other words, RSSI values can be used to estimate distance between clients. After the distances between the clients are all estimated, one of the positioning algorithms

(triangulation based algorithms are very common) that relies on the distance values can be used to locate the clients. Triangulation is a common positioning algorithm which estimates the position of a client by using three or more positions of the other clients. Triangulation based location estimation methods needs at least three reference points. From the distances of the client which the user wants to locate from these reference points, the positioning process can be completed (Arslan et al., 2006).

### ***2.3.2 Time Based Distance Estimation and Positioning***

Time based wireless communication metrics, ToA, Two-Way ToA etc., are alike the RSSI metric but this time distance and position estimation process is being done with the measurements in time, not signal strength. To do that, several techniques may be selected from a variant of approaches; Conventional Correlation Based Approaches, Two-Step ToA Estimations, Maximum Likelihood Methods, Low-Complexity Timing Offset Estimations etc. (Arslan et al., 2006).

The idea of estimating the distance over a time based metric may rely on the time of flight of a received signal. For ToA metric the distance is estimated by;

$$d = \frac{ToA}{T_f} \quad (2.14)$$

where  $ToA$  and  $T_f$  represent the flight time of the signal and the timer frequency respectively. To use this method the clients must be synchronized because the metric gives the difference between the departure and arrival times of the signal. If the clients are operating at different clocks, the metric would not contain only the time of flight, it also contains the difference of the clocks. Also for TDoA metric, the transmitters must be synchronized for considering only one measurement, if all the system relies on TDoA measurements, every client must be synchronized on the same clock.

Without synchronization, the only time based metric to use is the Two-Way ToA. The processor records the time of departure of a signal, then the signal reaches a

receiver and be reflected back again to the initial transmitter. The time difference between the departure and arrival time represents the Two-Way ToA metric. But this time metric also contains the time delay between the arrival and departure time of the signal on the receiver. This delay time must be extracted from the metric to make the metric directly bounded to the distance.

$$d = \frac{TWToA - T_{delay}}{2 * T_f} \quad (2.15)$$

where the delay time and the time based metric are represented with  $T_{delay}$  and  $TWToA$  respectively.

If a time based metric is used to estimate the distance, the speed of the signal would be used. This speed is equal to the speed of light,  $c$ , which is  $3 * 10^8$  m/sec. This means that, if one would try to measure distance over a time based metric directly with a Wireless & Bluetooth device (SID) without using any extra component or device, the main processor should be operate at 300 MHz in order to compensate 1 machine cycle with the speed of light for a distance resolution of 1 m.

$$d = \frac{c}{f} = \frac{3 * 10^8}{300 * 10^6} = 1m \quad (2.16)$$

At that frequency, 1 cycle difference means 1 m distance but it is not enough to select a CPU operating over 300 MHz.

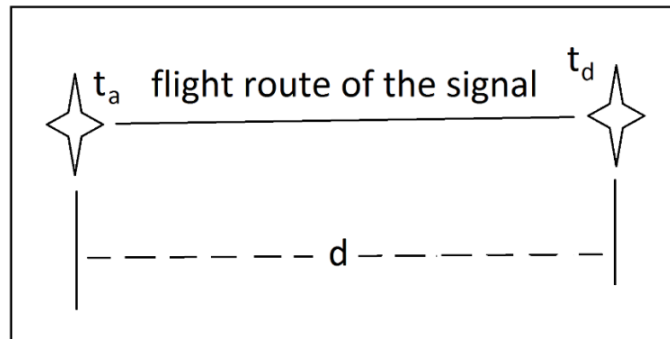


Figure 2.4 ToA or Two-Way ToA metric measurements

For a ToA measurement the distance is expressed as;

$$d = c(t_a - t_d) \quad (2.17)$$

where  $t_d$  and  $t_a$  represent the departure and the arrival time of the signal respectively. The same procedure stands for also a Two-Way ToA measurement. Only difference is the distance is doubled and a delay time is added to the metric which is the time that is spent on the 1<sup>st</sup> receiver/2<sup>nd</sup> transmitter. But this time the departure and the arrival of the signal happens on the same client. The 2<sup>nd</sup> client only reflects the signal.

$$2d = c(t_a - t_d - t_{delay}) \quad (2.18)$$

In Equation 2.18,  $t_a$  and  $t_d$  are the time stamp values which represent the exact times of signal arrival and departure respectively. The selected processor must include a timer operating over at least 300 MHz in order to maintain 1 m resolution on distance measuring. The selected SBC of the project includes a timer operating at maximum 10 KHz. So, without adding an extra component or device to the system, it is not possible to use time based indoor positioning methods for the task. If it was used, the resulting distance resolution would be 30km for a ToA and 15 Km for a Two-Way ToA system considering the capacity of the timer because whatever the actual metric is, processor always senses the metric as the timer lets, 1 clock, 0.0001 sec in an indoor environment.

$$d = 3 * 10^8 * (0.0001) \quad (2.19)$$

If the time stamps were enough sufficient to be used, one can use Equation 2.18 estimate the distances between the clients. Having the distances between the clients, one can also estimate the position of a client with various positioning algorithms, such as triangulation.

## **CHAPTER THREE**

### **DISTANCE ESTIMATION AND NO INITIAL INDOOR POSITIONING**

To accomplish a wireless communication between all the clients in a robotic team and locate any client in an indoor environment we present an algorithm which relies on RSSI measurements taken over Wi-Fi, three different signal strength based distance estimation methods and the positioning process based on triangulation but needs no initial conditions.

Hence, the two main titles in this chapter are the distance estimation process and the no initial indoor positioning (the NOIP) process.

#### **3.1 Distance Estimation Process**

The first major part of the project is estimating the distances between the clients over RSSI measurements. In order to estimate the distance, we need to record the RSSI measurements.

##### ***3.1.1 Measurement Process***

The measurement process contains the method of RSSI recordings. These metrics are provided by wireless communication infrastructures which are Wi-Fi and Bluetooth both operating at 2.4 GHz frequency. RSSI recordings are the measurements that to be estimated into distance. These recordings are taken in two different indoor environments, one office building and a school basement. For that two environment two different measurement methods are used.

###### ***3.1.1.1 1<sup>st</sup> Measurement Method – Measuring between 1 Receiver and 1 Transmitter (1<sup>st</sup> MM)***

This method relies on the measurements between only one receiver and one transmitter. The measuring process of this method is presented in Figure 3.1.

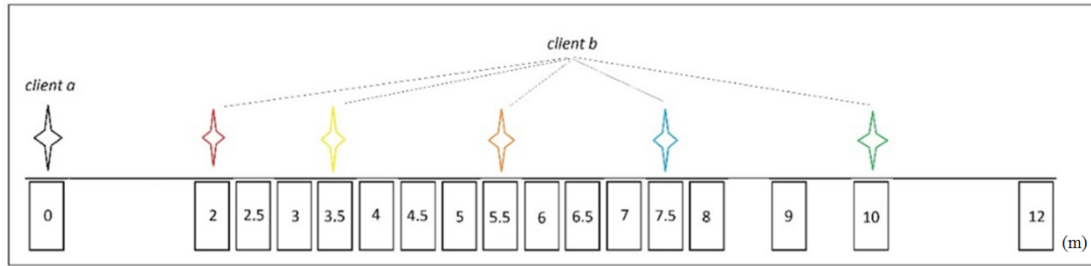


Figure 3.1 RSSI recording method of 1, in the office building

In Figure 3.1, the 1<sup>st</sup> measurement method is presented. In an office building, one client is set to origin and the other is moved by the selected measurement points. In Section 4.2.1.3.1 it is explained why the measurements are limited with those distances shown in Figure 3.1.

The advantage of this method is that one can use the measurements for locating the clients which are located in an unlimited number of layout variations. But, besides the first two clients, *a* and *b*, which actually has the real measurements, the distances between the other clients are generated from the measurements taken between the first 2 ones. This approach contains both simulation and experimental RSSI data.

### 3.1.1.2 2<sup>nd</sup> Measurement Method – Measuring between 1 Receiver and 3 Transmitters (2<sup>nd</sup> MM)

Unlike the first measurement method (1<sup>st</sup> MM), the 2<sup>nd</sup> measurement method (2<sup>nd</sup> MM) depends on the actual measurements taken between all the clients on by one for the selected layout variations. This method contains only the experimental RSSI data but the layout variations of the clients on the map are limited with the selected 3 layouts.

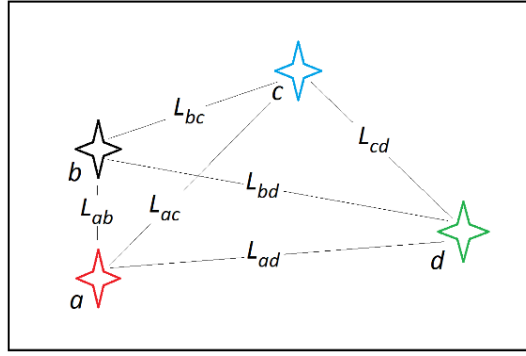


Figure 3.2 2<sup>nd</sup> MM, measurements by the layouts

The half of these measurement set is unique for the measuring point. The other half is basically the repetition. In example, when recording the first set of measurements  $L_{ab}$  distance is recorded from client 'a', in the second set the same measurement is taken from client 'b', hence, the measurement between 2 clients are repeated. The data is still real but for a 4 client robotic team there are 6 different one-to-one RSSI measurements.

### 3.1.2 Received Signal Strength (RSS) Based Distance Estimation Models

After the measurement procedure, now we pass into the distance estimation models. In this process, three different RSS based path loss models; namely, ITU Indoor Path Loss Model, Two-Ray Ground Reflected Path Loss Model and the experimentally derived EDR Model are presented.

#### 3.1.2.1 International Telecommunication Union (ITU) Indoor Path Loss Model

ITU Indoor Path Loss Model is an indoor propagation path loss model as previously described. This model relies on some exponents and constants. These constants also depend on the ambient conditions.

$$P_t - P_{RSSI} = 20 \log_{10}(2.4 \times 10^9) + N \log_{10}(d) + L_f(0) - 28dB \quad (3.1)$$

Before the estimation process with ITU Model, these constants must be set depending on the environment. RSSI measurements are all taken when the receiver

and the transmitter(s) are all in the same floor. Hence, the representation of the receiver-transmitter floor difference,  $n$ , equals to zero (see Equation 3.1). In some sources these exponents are explained and defined for some operating frequencies and ambient conditions. For the conditions of the measurements take place, the power loss coefficient,  $N$ , is given as 28; and the floor penetration loss factor,  $Lf(n)$ , can be chosen between 11 and 16 because there is no definite answer for 2.4 GHz (International Telecommunication Union, 2015). Also by adding the transmitted signal power the formula of the indoor path loss propagation model becomes;

$$13 - P_{RSSI} = 20 \log_{10}(2.4 \times 10^9) + 28 \log_{10}(d) + 11 - 28 \quad (3.2)$$

The first operating conditions are set by replacing the constants with these values; therefore, the only unknown parameter left is the distance which is desired to be found. The final working conditions are presented in the results section of this model (see Section 4.2.2.1).

Since all the conditions are set, the desired value, distance, can be evaluated as;

$$28 \log_{10}(d) = -P_{RSSI} - 20 \log_{10}(2.4 \times 10^9) - 11 + 28 + 13 \quad (3.3)$$

$$28 \log_{10}(d) = -P_{RSSI} - 20 \log_{10}(2.4 \times 10^9) - 11 + 28 + 13 \quad (3.4)$$

$$28 \log_{10}(d) = -P_{RSSI} - 68.44 - 11 + 28 + 13 \quad (3.5)$$

$$28 \log_{10}(d) = -P_{RSSI} - 38.44 \quad \text{so} \quad 28 \log_{10}(d) = -(P_{RSSI} + 38.44) \quad (3.6)$$

$$\log_{10}(d) = -\frac{(P_{RSSI} + 38.44)}{28} \quad (3.7)$$

$$d = 10^{\frac{-(P_{RSSI} + 38.44)}{28}} \quad (3.8)$$

Equation 3.8 shows the resulting estimation formula for the first model of distance estimation. For every RSSI data this process is repeated and recorded to be used in the positioning process.

### 3.1.2.2 Two-Ray Ground Reflected Path Loss Model

Depending on free space path loss, this model deals with both the LOS and the reflected signal path losses. The formula of the model contains the transmitted signal strength, received signal strength, both antenna gains and the logarithmic path loss in dBs.

$$P_{RSSI} = P_t + G_r + G_t - 20 \log\left(\frac{d^2}{h_t h_r}\right) \quad (3.9)$$

In the model,  $G_r$  and  $G_t$  represent the antenna gains,  $P_t$  and  $P_{RSSI}$  represents the transmitted and received signal strength. Received signal strength is provided by RSSI measurements, transmitted signal strength depends on the wireless communication device output and the antenna.

Since all the wireless devices are identical in this thesis, the heights and the gains of any antenna are also equal to one another. Hence, the formula becomes;

$$P_{RSSI} = P_t + 2G - 20 \log\left(\frac{d^2}{h^2}\right) \quad \text{where } h_t = h_r \quad \text{and} \quad G_t = G_r \quad (3.10)$$

Now, all the constants are known except for the distance, the desired value. To leave the distance, 'd', alone in the one side of the equality;

$$20 \log\left(\frac{d^2}{h^2}\right) = P_t + 2G - P_{RSSI} \quad (3.11)$$

$$40 \log\left(\frac{d}{h}\right) = P_t + 2G - P_{RSSI} \quad (3.12)$$

$$\log\left(\frac{d}{h}\right) = \frac{P_t + 2G - P_{RSSI}}{40} \quad (3.13)$$

$$\left(\frac{d}{h}\right) = 10^{\frac{P_t + 2G - P_{RSSI}}{40}} \quad (3.14)$$

$$d = h.10^{\frac{P_t + 2G - P_{RSSI}}{40}} \quad (3.15)$$

For every RSSI measurement, this process is repeated and the resulting distance estimations are recorded to be applied to the positioning algorithm.

### 3.1.2.3 Distance Estimation with the Experimentally Derived Signal Strength – Distance Relation (EDR) Model

The EDR Model that relies on the actual measurements and the location of that measurements take place is described as;

$$d = a.e^{b.P_{RSSI}} \quad (3.16)$$

It was said that this function is an exponential function that fitted on the actual measurement-distance values. For a specific result set these values are found by;

$$a = 0.09878 \quad \text{and} \quad b = -0.06658 \quad (3.17)$$

hence, the formula becomes;

$$d = 0.09878.e^{-0.06658.P_{RSSI}} \quad (3.18)$$

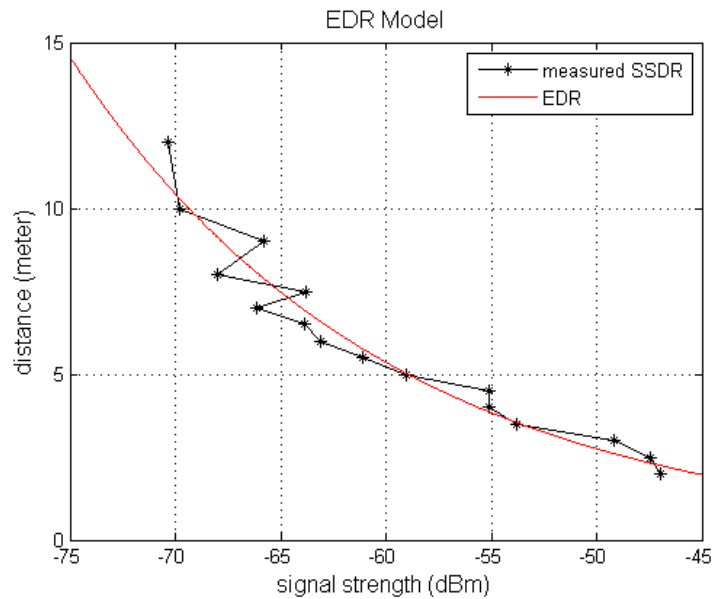


Figure 3.3 EDR Model derivation for a specific example

This formula is a specific one for a specific set of measurement set. It can vary by the measurements, environment, ambient conditions of the area etc. If the conditions are the same every time the model can be applied for any other measurement set and the results should be expected to be equal as well. Figure 3.3 illustrates the derivation the SSSR model for the specific example.

The estimations can also be repeated for any measurement set and the resulting data set can be applied to the positioning process.

### 3.2 No Initial Indoor Positioning (the NOIP)

The novelty of the presented no initial indoor positioning algorithm (the NOIP) is, there is no need for an initial construction or an initial position information of the clients, sensors etc. By the measurements, the distance estimations are recorded and with that recordings the NOIP sets its' own coordinate system for localization by using the  $L_{ab}$  distance set estimated between the 1<sup>st</sup> two clients,  $a$  and  $b$  (see Figure 3.4).

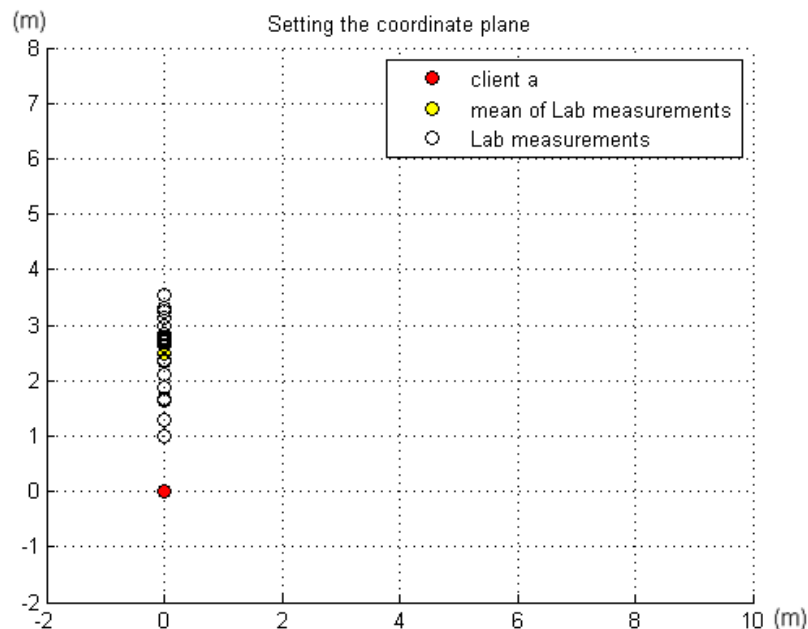


Figure 3.4 Setting the relative coordinate plane

Client  $a$  is always located in the origin of the relative coordinate plane (RCP). Then with the distance estimations of the RSSI measurements between the clients  $a$  and  $b$ , the relative location set of client  $b$  is set on  $y$  plane. As can be seen from Figure 3.4 the RCP is set on the 1<sup>st</sup> two clients.

After the RCP is set, by the measurements of  $L_{ab}$ ,  $L_{ac}$  and  $L_{bc}$ , the location of the 3<sup>rd</sup> client,  $c$ , can be estimated via finding the intersections of the measurement circles (see Figure 3.5).

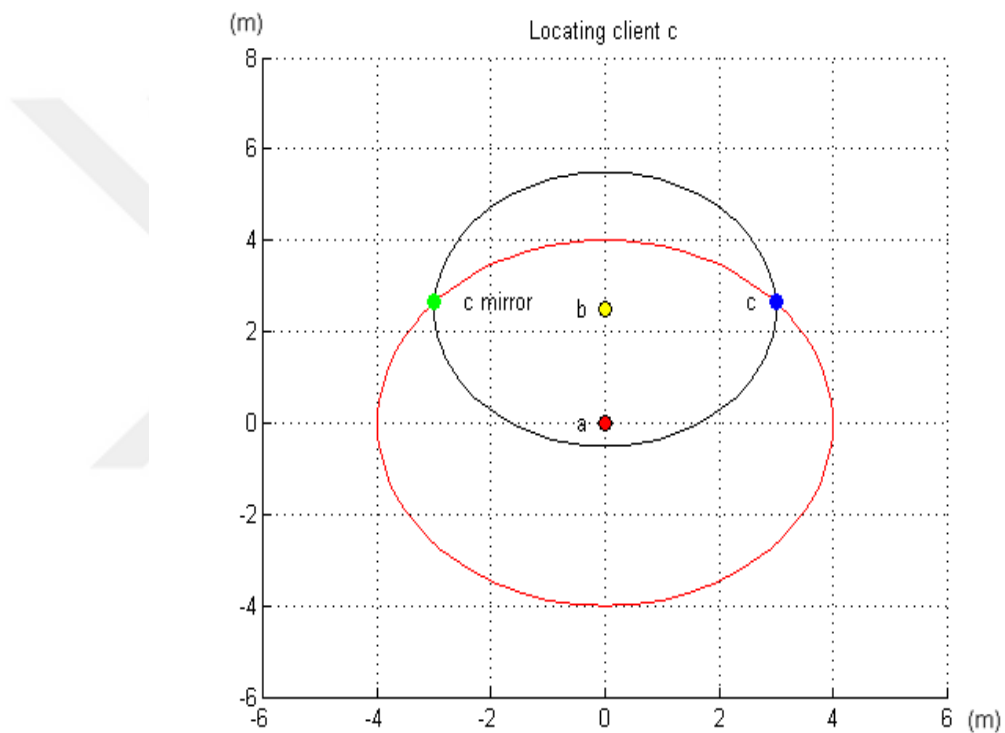


Figure 3.5 Locating client  $c$  with the intersection of the measurement circles

As can be seen in Figure 3.5, there are 2 intersections of the measurement circles (MC). For all the measurements, it is assumed that the client's position will always be on the right side of the map. This assumption can be supported automatically with additive information that provides the aspect of the client's position which is estimated.

However, there are 3 exceptions that the MCs would not intersect. These exceptions are defined as;

$$L_{ab} \geq L_{ac} + L_{bc} \quad , \quad L_{ac} \geq L_{ab} + L_{bc} \quad \text{and} \quad L_{bc} \geq L_{ab} + L_{ac} \quad (3.19)$$

where  $L_{ab}$ ,  $L_{ac}$  and  $L_{bc}$  represent the distance estimations between the clients. These conditions are illustrated in Figure 3.6.

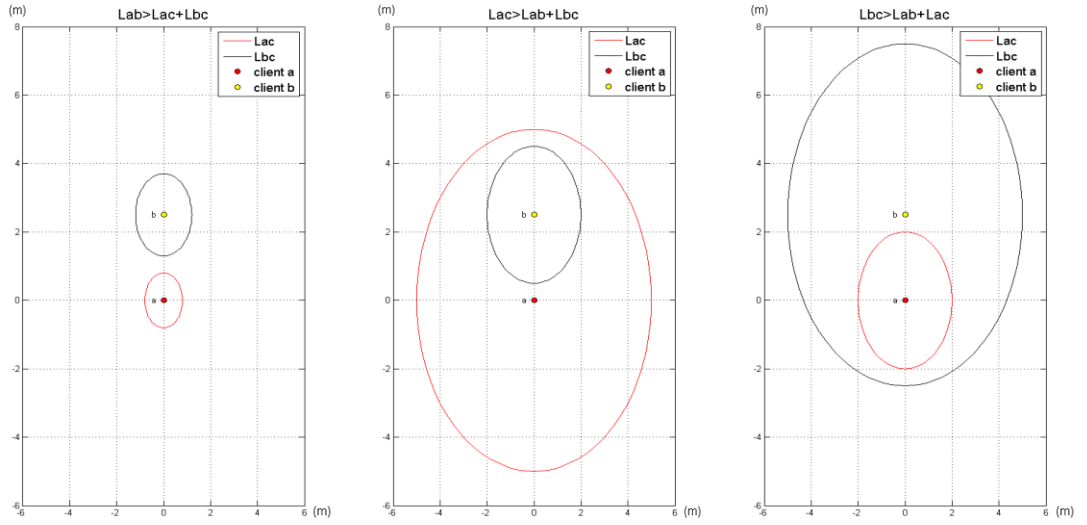


Figure 3.6 Conditions of non-intersecting MCs

If one of these three conditions happens, the location of client  $c$  cannot be estimated for that measurement. Therefore, that non-intersecting MC result is excluded from the positioning process. For example, if 6 non-intersecting MCs appear in one measurement set containing 15 measurements, the mean value of 9 intersecting MCs are derived to estimate the position of the belonging client.

The same positioning process is applied to the last client,  $d$ , as it was for client  $c$ . This time, the measurements sets  $L_{ab}$ ,  $L_{ad}$  and  $L_{bd}$  are used.

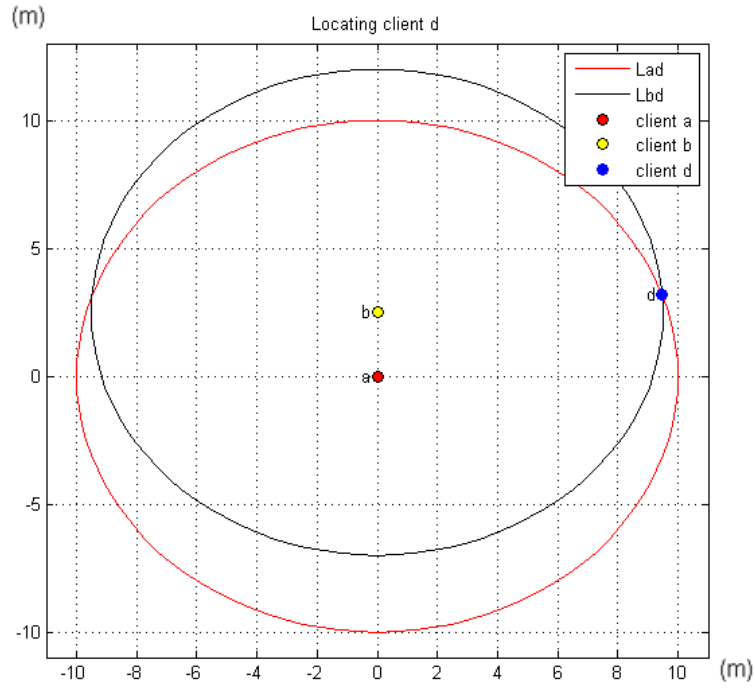


Figure 3.7 Locating client  $d$

When all the intersected measurement circles are recorded, the possible positions of the clients are estimated regarding to the belonging measurement. The resulting estimated position of a client is found via;

$$EP_x = \frac{\sum MC_{int}(x)}{\#NZI} \quad \text{and} \quad EP_y = \frac{\sum MC_{int}(y)}{\#NZI} \quad (3.20)$$

where,

$EP_x$  is the estimated  $x$  plane value of the belonging client,

$EP_y$  is the estimated  $y$  plane value of the belonging client,

NZI is the number of intersected MCs for,

$\sum MC_{int}(x)$  is the summation of  $x$  plane values of the intersected MCs,

$\sum MC_{int}(y)$  is the summation of  $y$  plane values of the intersected MCs.

Figure 3.8 shows the whole process with an illustration of the estimated positions of the clients and the intersection points of every MCs.

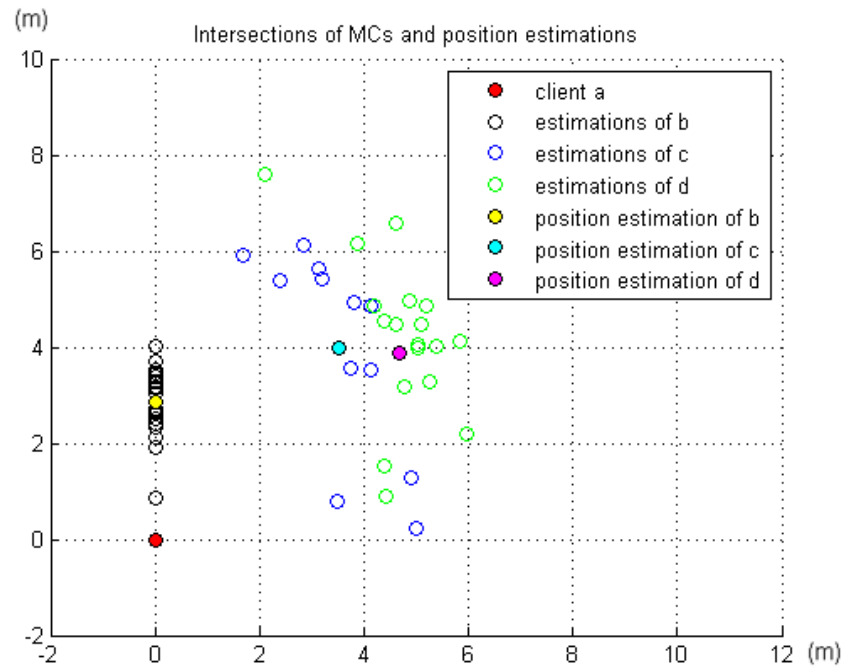


Figure 3.8 All intersections of MCs and the position estimations of the clients

Overall, the NOIP sets the RCP, derives all the intersections of all the related MCs, estimates all possible locations of the clients, then defines the final position estimations of all the clients from the derivation of the intersected MCs.

Besides the illustrations of the position estimations, the NOIP also gives the results of numerical error analysis for the selected conditions.

## CHAPTER FOUR

### RESULTS

This chapter contains both the simulation and experimental results of the study. Here, the distance estimations and the positioning process both have results related with each other.

At first, the simulation results of the positioning process will be shown, then the experimental results will be shared for both distance estimations and positioning process for different distances and layouts.

#### 4.1 Simulation Results

The positioning results for different number of iterations and SNR (Signal to Noise Ratio) values are shown in this section. Iterations represent the simulated version of RSSI measurements. Namely, the actual distances between the clients are calculated and in addition to those values Additive White Gaussian Noise (*awgn*) function is used in MATLAB for different SNRs. These resulting values are the distance estimations of the two belonging clients. This procedure and the positioning algorithm are applied for 4 different client layouts.

For example, for the 1<sup>st</sup> client layout (CL), the distances between the clients are shown in Figure 4.1. With *awgn* function, a random noise is added to the replicated distances by the iteration number with a user defined SNR value. A specific example is shown in Table 4.1 when *iterations*=10 and SNR=2.

Table 4.1 Generated noisy  $L_{ab}$  distances for *iterations*=10 and SNR=2

$L_{ab\_noisy} (m)$									
2.7018	2.9789	3.1349	1.9022	2.0171	2.2092	3.6369	2.3153	4.086	3.2464

These imitations of noisy measurements are derived with the following code lines in MATLAB;

```

iterations=10; % number of iterations
snr=2; % signal to noise ratio
Lab=2.5; % the distance between client a and b
ab_noisy=ones(iterations,1)*Lab; % 10-1 matrix containing all Lab
values
Lab_noisy=awgn(ab_noisy,snr) % noisy Lab matrix

```

When one runs these code lines in MATLAB, he/she gets the results alike in Table 4.1.

Note that the simulated results can change when the algorithm is replied even if the conditions are the same. Because, *awgn* function generates the noisy measurement imitations randomly. Every time the run button is hit, a different noisy  $L_{ab}$  distance set is generated (see Table 4.2).

Table 4.2 Different generations of noisy  $L_{ab}$  distances

Lab_noisy	run #1	run #2	run #3	run #4	run #5	run #6	run #7	run #8	run #9	run #10
iteration #1	2.0921	0.6592	4.6828	1.2175	2.0920	3.6554	2.1036	2.9521	1.9490	2.5876
iteration #2	2.0446	3.1690	2.1199	2.7784	3.7689	1.8301	2.0011	2.5785	2.5697	4.0049
iteration #3	3.0429	0.8813	2.1802	3.3997	1.8978	3.3318	1.9110	2.1482	3.0897	2.0857
iteration #4	3.7160	3.1301	3.7322	2.7924	0.7196	2.9263	1.8241	2.1026	2.7637	4.2222
iteration #5	1.3007	1.9469	3.8333	2.7654	1.5973	2.0216	2.0693	1.7634	2.3534	2.8316
iteration #6	3.1782	2.3775	1.5266	4.1233	1.3780	3.0614	4.0998	1.8716	1.0406	2.3174
iteration #7	1.4901	1.8249	2.5729	2.0697	2.7245	3.7486	2.8100	0.7480	2.3899	2.2867
iteration #8	2.5571	3.3502	2.9240	1.6337	2.4869	3.9655	1.7146	3.0165	2.6712	2.2158
iteration #9	3.1141	1.3379	2.2050	2.4802	2.4880	1.6973	3.3600	1.8965	1.8649	2.5802
iteration #10	1.8063	2.4292	2.0528	1.3604	3.0025	1.3978	3.1233	2.6264	1.5009	1.4062

However, the figures and the error values are recorded at the same time, hence, for the same conditions the illustrations and the numerical errors presented in the following belong to each other.

The simulated results are recorded for 3 different *iterations* – SNR combinations (ISC) and the illustrations are shown for that belonging ISC. Also an extended positioning error analysis is presented in Section 4.1.5 for a variety of ISCs for the 4 CLs.

### 4.1.1 Simulated Results of the 1<sup>st</sup> Client Layout

CL1 is illustrated in Figure 4.1.

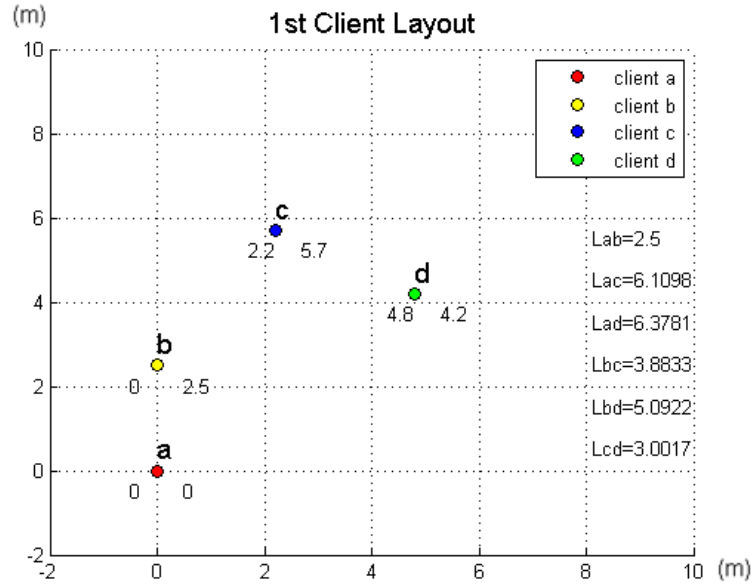


Figure 4.1 1<sup>st</sup> client layout, coordinates and distances

For the 1<sup>st</sup> layout, the coordinates and the distances between the clients are presented in Figure 4.1. For this case, the distances can be estimated by applying actual distances between, *iterations* and SNR.

For three different combinations of SNR and *iterations*, the positioning results are presented in the following figures. In all the figures (Figures 4.2, 4.3, 4.4, 4.7, 4.8, 4.9, 4.12, 4.13, 4.14, 4.17, 4.18 and 4.19) containing the positioning results, black blank circles, blue blank circles and green blank circles are the representation of the position estimations of client *b*, client *c* and client *d* respectively mean of the estimations are shown with respectively yellow filled, cyan filled and magenta filled circles for the corresponding clients. Actual positions of the clients are also illustrated with the same colors but they also have a black wall on them (see Figure 4.3).

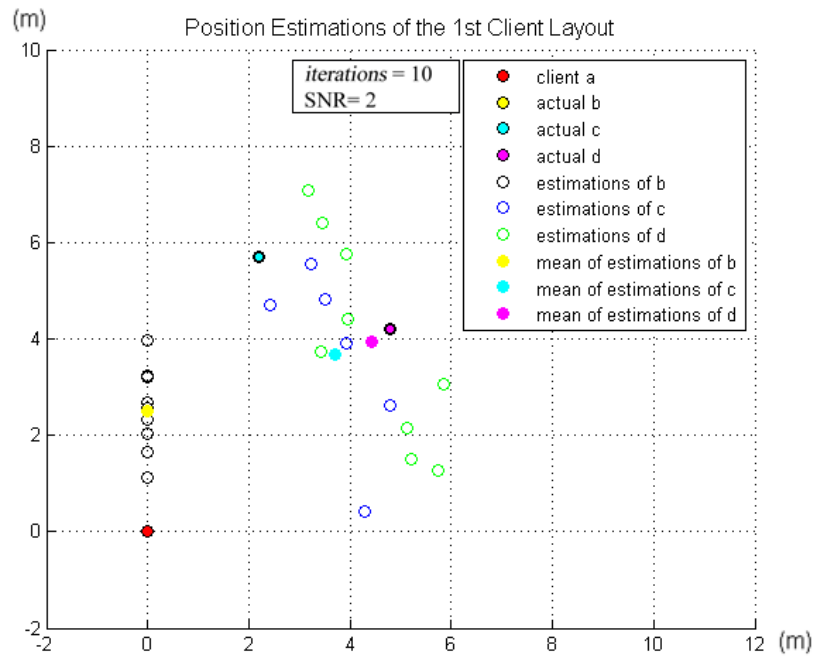


Figure 4.2 Position estimations of CL1 when  $iterations=10$  and  $SNR=2$

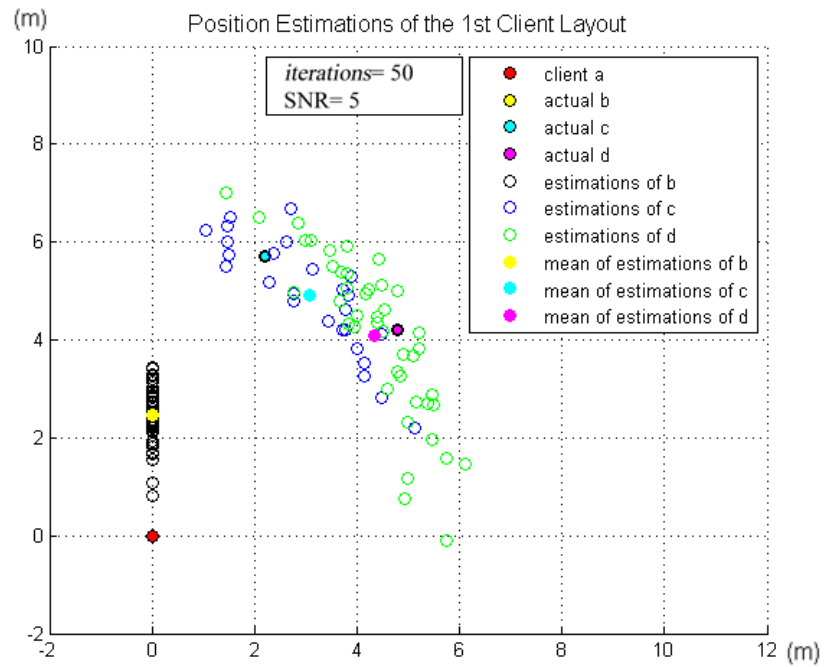


Figure 4.3 Position estimations of CL1 when  $iterations=50$  and  $SNR=5$

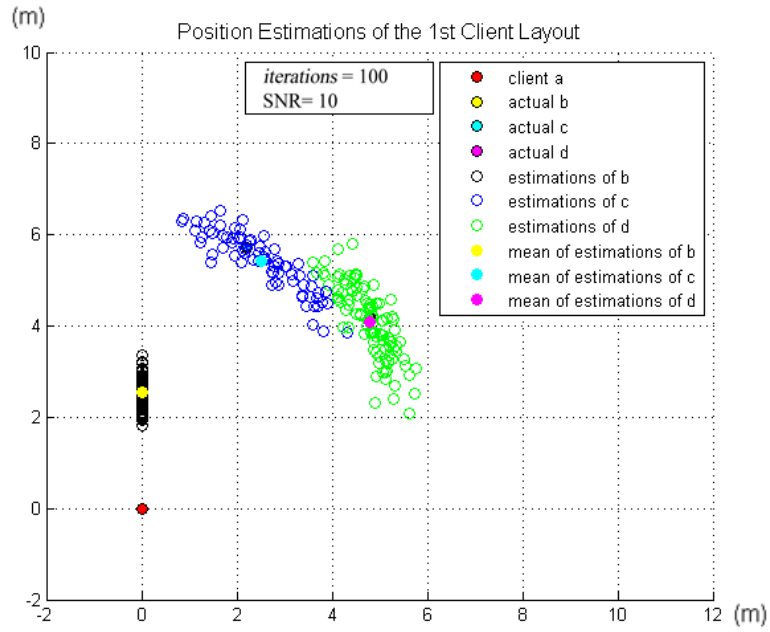


Figure 4.4 Position estimations of CL1 when  $iterations=100$  and  $SNR=10$

Figures 4.2, 4.3 and 4.4 illustrate the simulated positioning results of CL1 for different  $iterations$  and SNR values. Figure 4.5 below shows the results of these three combinations in one plot.

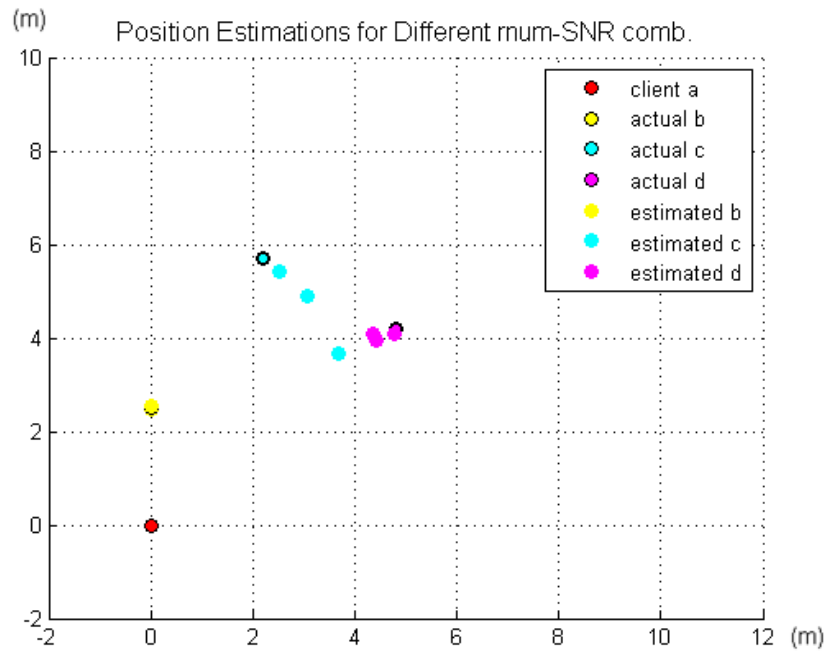


Figure 4.5 Actual and the estimated positions of the clients for the 3 ISCs for CL1

Also the numerical error analysis is illustrated with Table 4.3.

Table 4.3 Numerical error analysis of the 3 ISCs for the 1<sup>st</sup> CL

Positioning Error Analysis of Client Layout 1					
iterations	SNR	pos. error b (m)	pos. error c (m)	pos. error d (m)	mean pos. error (m)
10	2	0.0110	2.5141	0.4539	0.9930
50	5	0.0435	1.1731	0.4651	0.5606
100	10	0.0449	0.4212	0.1127	0.1929

Positioning error is defined by the difference of the client's actual position and the mean of the estimated positions (see Equation 4.1). The mathematical expression of the positioning error is;

$$P_{err} = \sqrt{(mP_x - aP_x)^2 + (mP_y - aP_y)^2} \quad (4.1)$$

where,  $P_{err}$ ,  $mP_x$ ,  $mP_y$ ,  $aP_x$  and  $aP_y$  are the positioning error,  $x$ -axis value of the mean estimated position,  $y$ -axis value of the mean estimated position,  $x$ -axis value of the actual position and  $y$ -axis value of the actual position respectively.

#### 4.1.2 Simulated Results of the 2<sup>nd</sup> Client Layout

CL2 is illustrated in Figure 4.6.

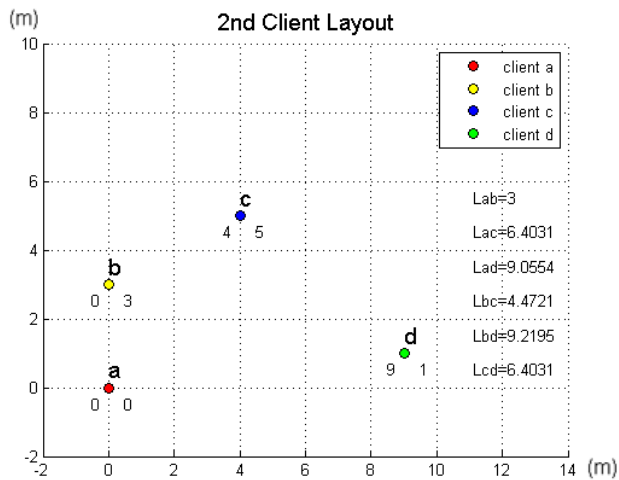


Figure 4.6 2<sup>nd</sup> client layout, coordinates and distances

For the same 3 ISCs, the positioning results are illustrated in the following.

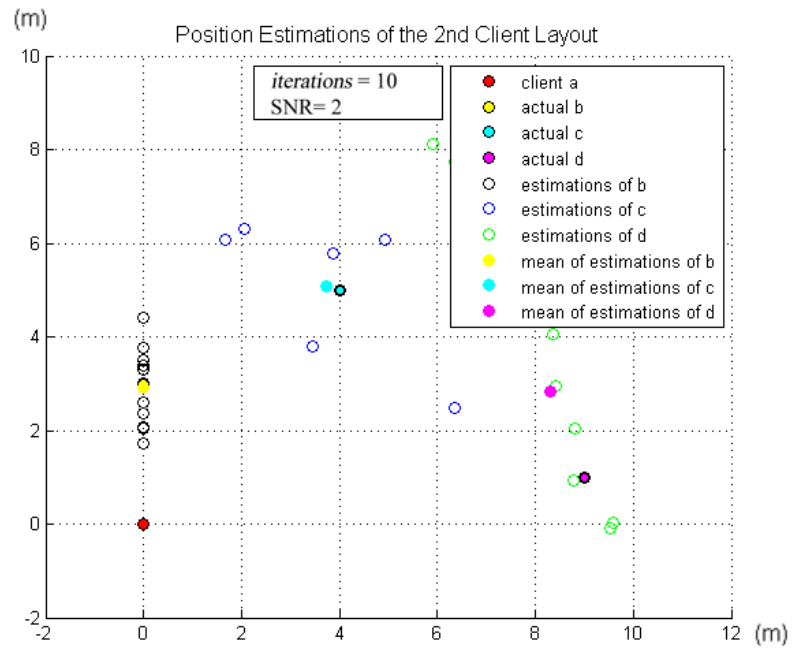


Figure 4.7 Position estimations of CL2 when  $iterations=10$  and  $SNR=2$

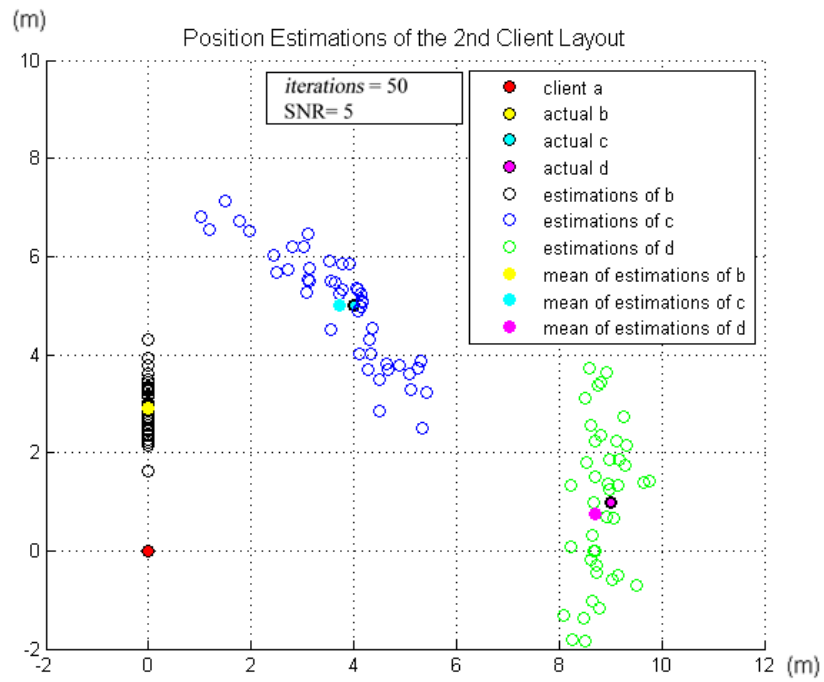


Figure 4.8 Position estimations of CL2 when  $iterations=50$  and  $SNR=5$

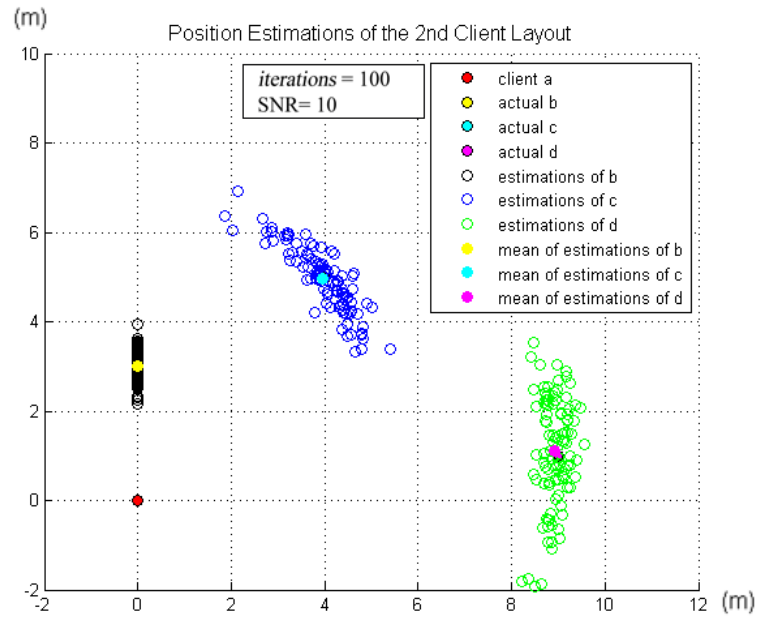


Figure 4.9 Position estimations of CL2 when  $iterations=100$  and  $SNR=10$

The actual positions and the three estimated positions of the clients are illustrated in one plot in Figure 4.10.

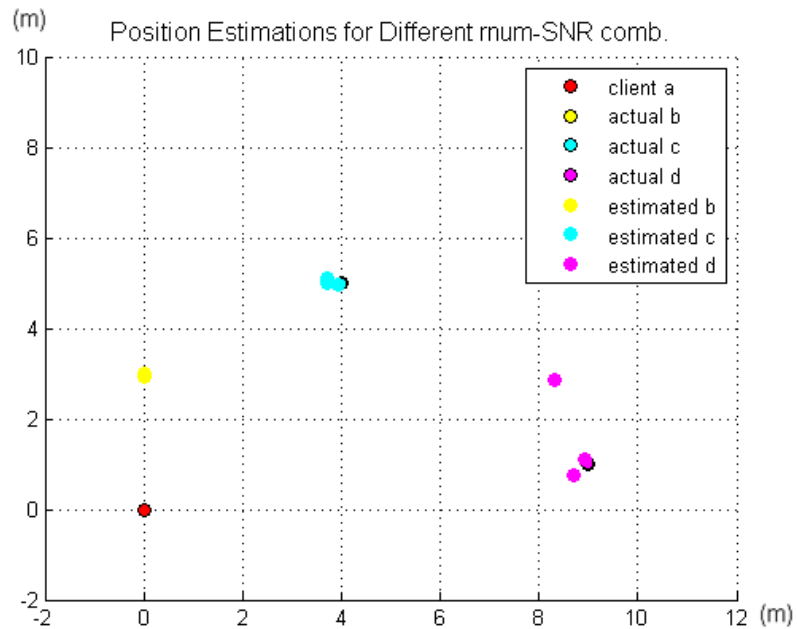


Figure 4.10 Actual and the estimated positions of the clients for the 3 ISCs for CL2

Table 4.4 shows the numerical error analysis of CL2 estimations.

Table 4.4 Numerical error analysis of the 3 ISCs for the 2<sup>nd</sup> CL

Positioning Error Analysis of Client Layout 2					
iterations	SNR	pos. error b (m)	pos. error c (m)	pos. error d (m)	mean pos. error (m)
10	2	0.0805	0.2893	1.9688	0.7795
50	5	0.0781	0.2875	0.3970	0.2542
100	10	0.0016	0.0600	0.1317	0.0644

#### 4.1.3 Simulated Results of the 3<sup>rd</sup> Client

CL3 is illustrated in Figure 4.11.

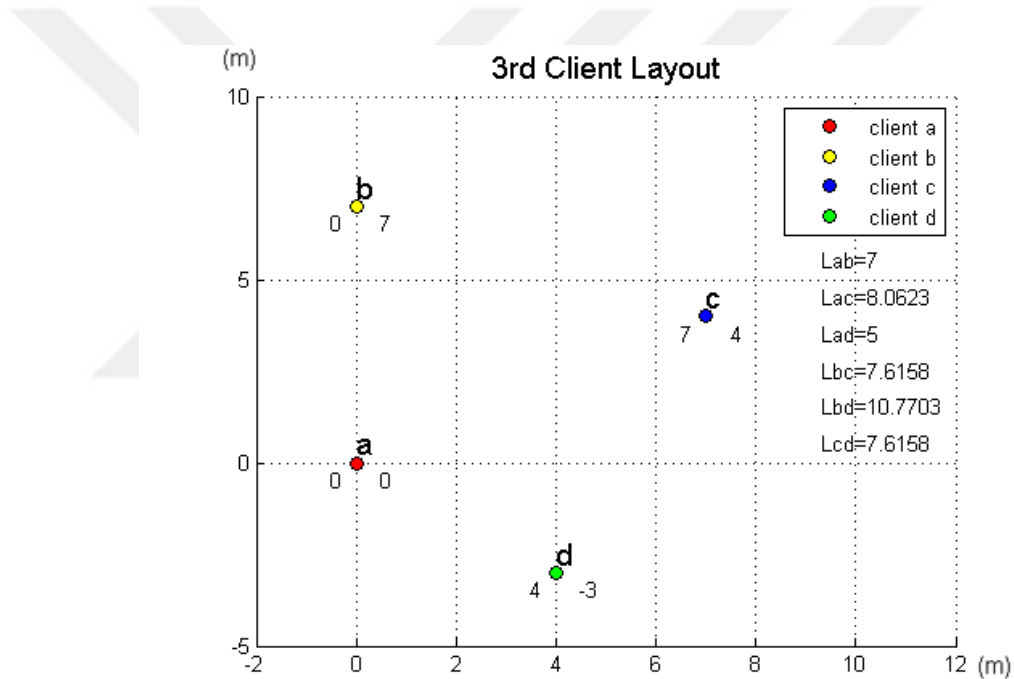


Figure 4.11 3<sup>rd</sup> client layout, coordinates and distances

The position estimations of CL3 are presented with the following figures containing the results for the same 3 ISCs.

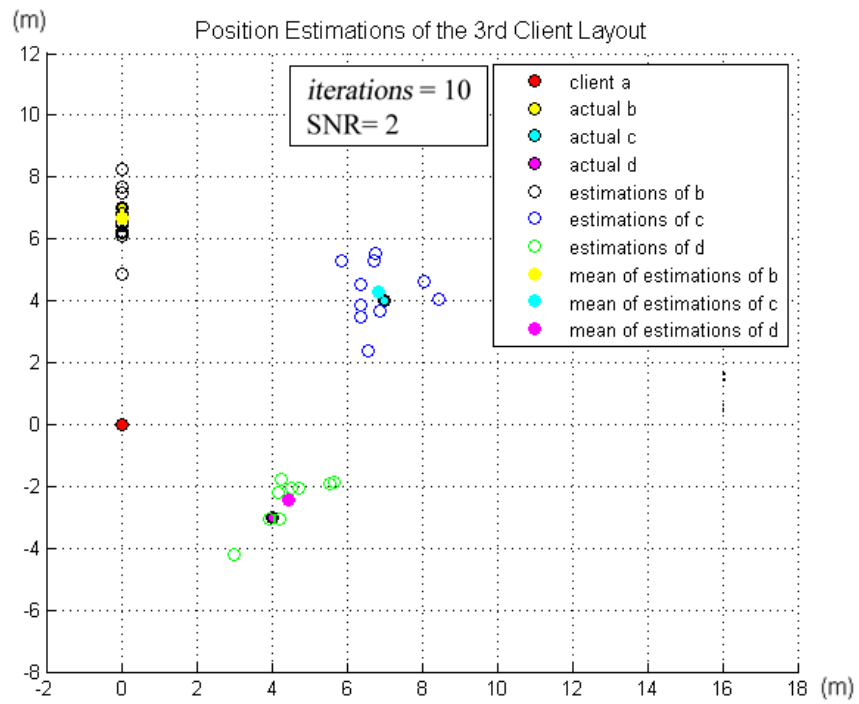


Figure 4.12 Position estimations of CL3 when *iterations*=10 and SNR=2

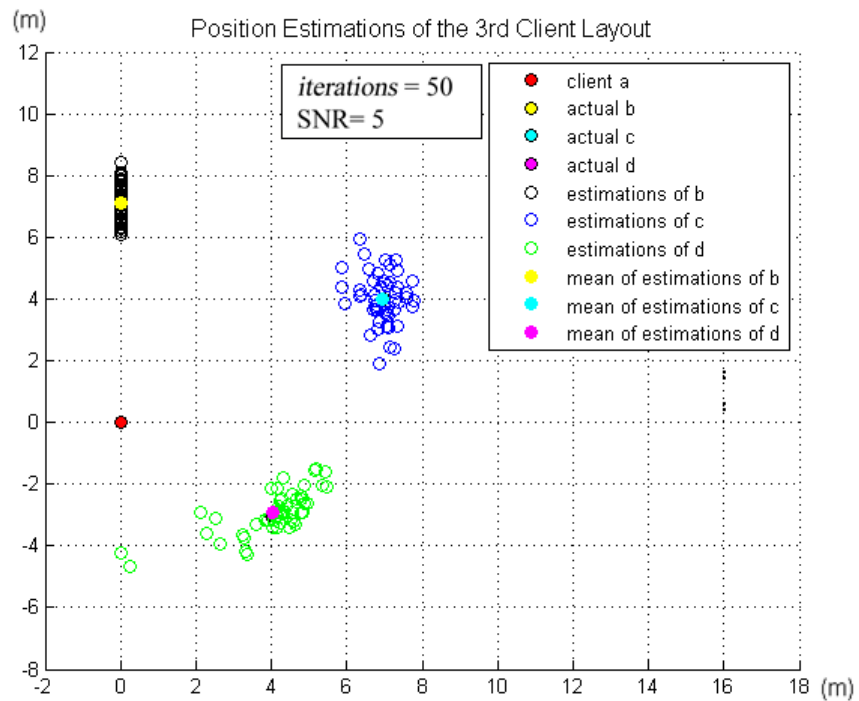


Figure 4.13 Position estimations of CL3 when *iterations*=50 and SNR=5

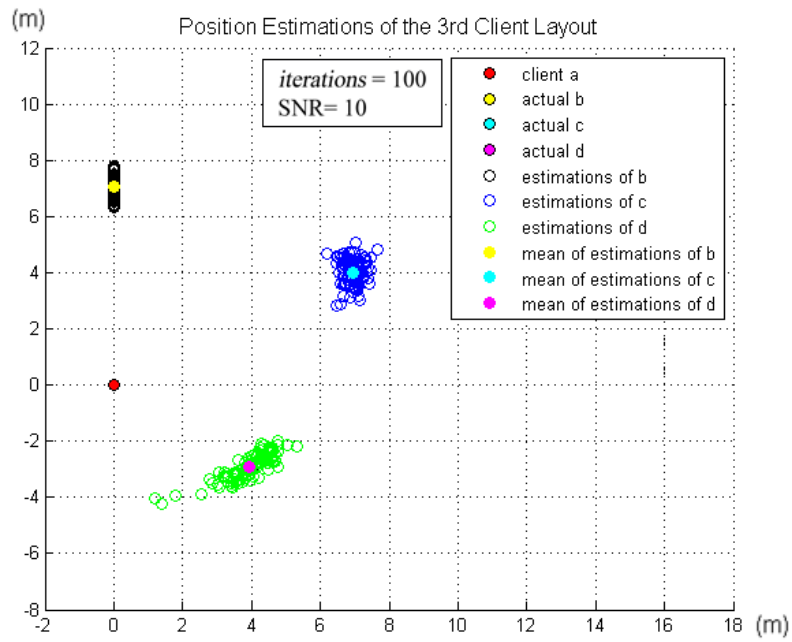


Figure 4.14 Position estimations of CL3 when  $iterations=100$  and  $SNR=10$

The three mean position estimations and the actual positions of the clients are illustrated in Figure 4.15 for the 3<sup>rd</sup> CL.

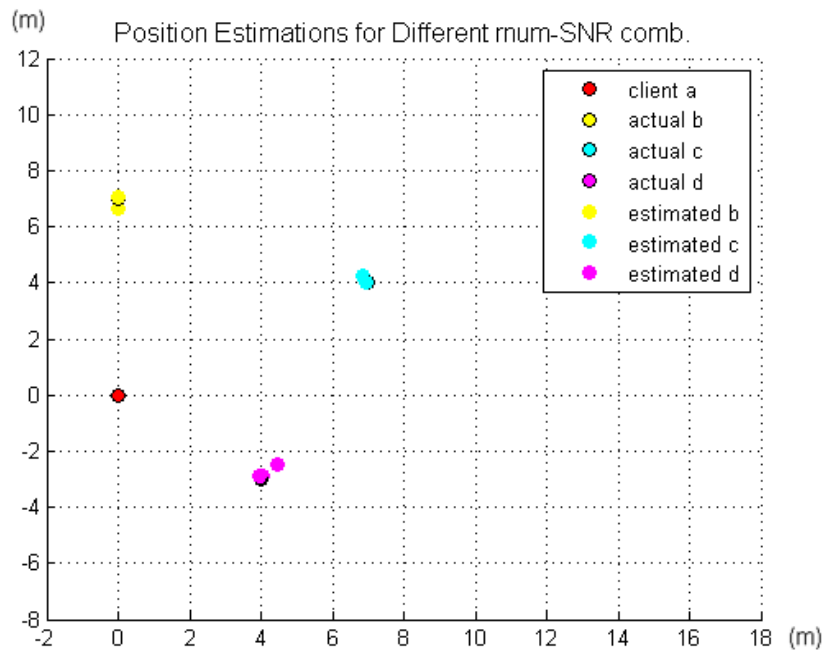


Figure 4.15 Actual and the estimated positions of the clients for the 3 ISCs for CL3

The positioning errors of the 3<sup>rd</sup> CL are shown in Table 4.5.

Table 4.5 Numerical error analysis of the 3 ISCs for the 3<sup>rd</sup> CL

Positioning Error Analysis of Client Layout 3					
iterations	SNR	pos. error b (m)	pos. error c (m)	pos. error d (m)	mean pos. error (m)
10	2	0.3375	0.3089	0.7037	0.4500
50	5	0.0853	0.0517	0.1034	0.0801
100	10	0.0726	0.0506	0.1180	0.0804

#### 4.1.4 Simulated Results of the 4<sup>th</sup> Client Layout

CL4 is illustrated in Figure 4.16.

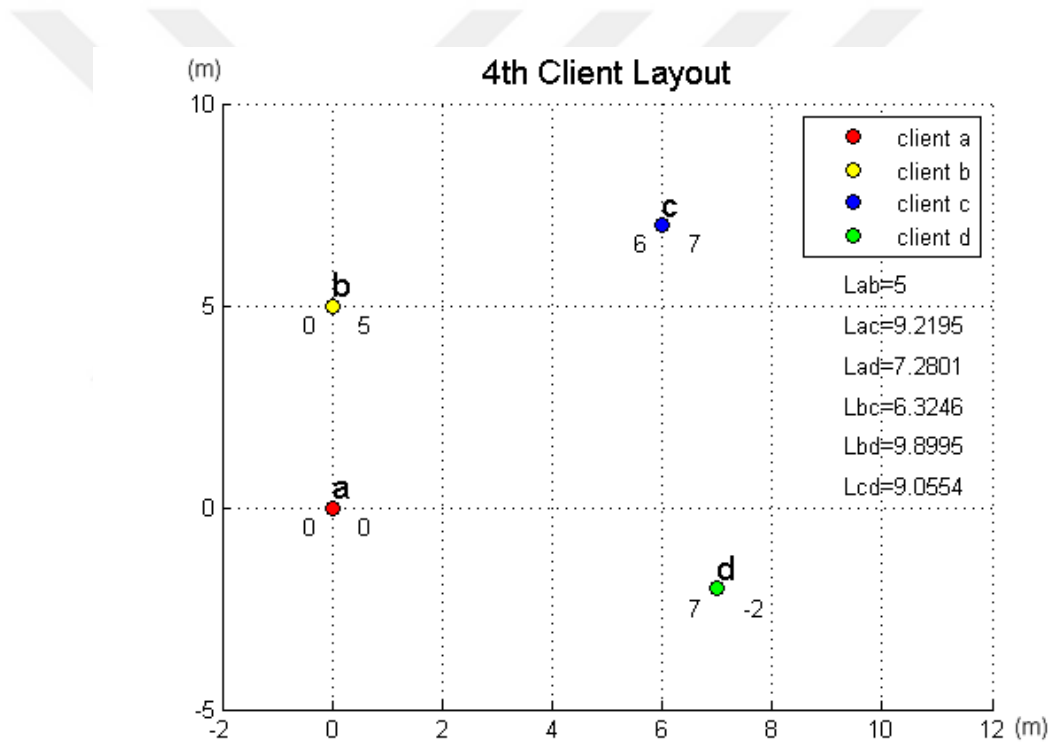


Figure 4.16 4<sup>th</sup> client layout, coordinates and distances

Positioning results for this layout are presented in the following figures for 3 ISCs.

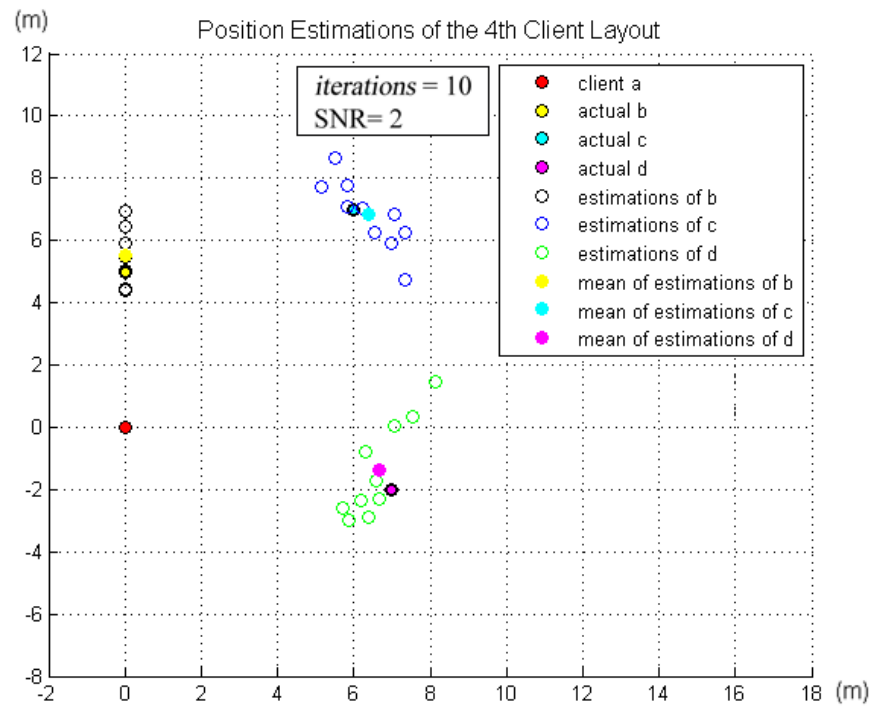


Figure 4.17 Position estimations of CL4 when *iterations*=10 and SNR=2

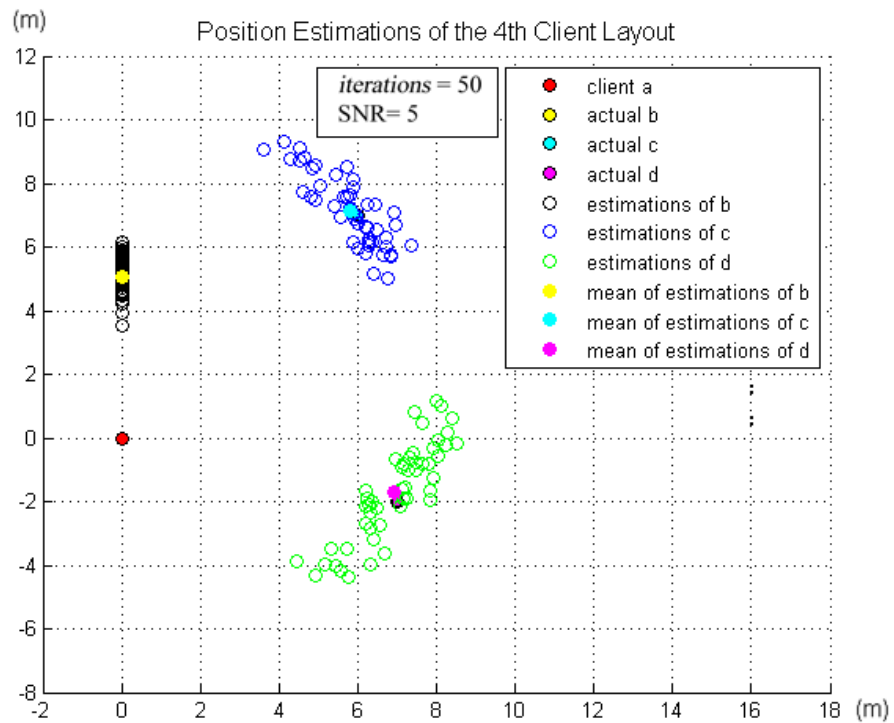


Figure 4.18 Position estimations of CL4 when *iterations*=50 and SNR=5

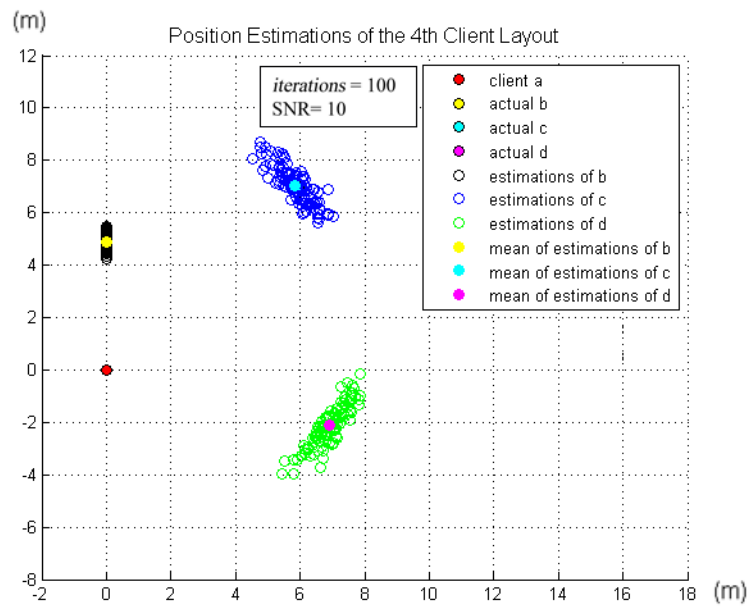


Figure 4.19 Position estimations of CL4 when  $iterations=100$  and  $SNR=10$

The resulting mean position estimations and the actual position of the last CL is presented in Figure 4.20 below.

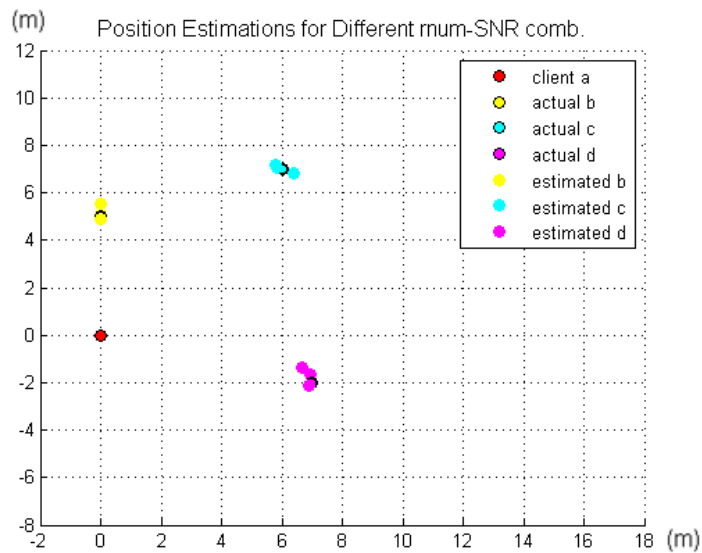


Figure 4.20 Actual and the mean of the estimated positions of the clients for the 3 ISCs for CL4

The positioning errors of this layout are presented in Table 4.6.

Table 4.6 Numerical error analysis of the 3 ISCs for the 4<sup>th</sup> CL

<b>Positioning Error Analysis of Client Layout 4</b>					
<i>iterations</i>	SNR	pos. error b (m)	pos. error c (m)	pos. error d (m)	mean pos. error (m)
<b>10</b>	<b>2</b>	0.5251	0.4231	0.7058	0.5513
<b>50</b>	<b>5</b>	0.0838	0.2457	0.3255	0.2183
<b>100</b>	<b>10</b>	0.0944	0.1548	0.1544	0.1345

#### ***4.1.5 Extensive Numerical Error Analysis of Simulation Procedure***

In this section, the extensive error analysis of the 4 CLs are presented. Both the numerical position error values and the graphical examinations of them are illustrated in the following.

Table 4.7 Positioning error values of CL1 for 25 ISCs

<b>Error Analysis of CL1</b>					
<i>iterations</i>	SNR	pos. error b (m)	pos. error c (m)	pos. error d (m)	mean pos. error (m)
<b>10</b>	<b>1</b>	0.2481	1.7178	0.8575	0.9411
<b>10</b>	<b>2</b>	0.0110	2.5141	0.4539	0.9930
<b>10</b>	<b>5</b>	0.0133	0.5270	0.2638	0.2680
<b>10</b>	<b>10</b>	0.0147	0.3348	0.1320	0.1605
<b>10</b>	<b>20</b>	0.0230	0.1203	0.1147	0.0860
<b>20</b>	<b>1</b>	0.1802	1.7868	1.3153	1.0941
<b>20</b>	<b>2</b>	0.1074	1.8105	0.5109	0.8096
<b>20</b>	<b>5</b>	0.2655	1.0734	0.2944	0.5444
<b>20</b>	<b>10</b>	0.1383	1.0690	0.6614	0.6229
<b>20</b>	<b>20</b>	0.0267	0.1202	0.0541	0.0670
<b>30</b>	<b>1</b>	0.2028	2.8819	0.4959	1.1935
<b>30</b>	<b>2</b>	0.0446	2.0153	1.1548	1.0716
<b>30</b>	<b>5</b>	0.0874	1.1247	0.4942	0.5688
<b>30</b>	<b>10</b>	0.0124	0.6260	0.1702	0.2695
<b>30</b>	<b>20</b>	0.0145	0.0620	0.0529	0.0431
<b>50</b>	<b>1</b>	0.0614	2.4751	0.6542	1.0636
<b>50</b>	<b>2</b>	0.0980	2.1320	0.4154	0.8818
<b>50</b>	<b>5</b>	0.0435	1.1731	0.4651	0.5606
<b>50</b>	<b>10</b>	0.0019	0.8984	0.3344	0.4116
<b>50</b>	<b>20</b>	0.0073	0.0591	0.0372	0.0345
<b>100</b>	<b>1</b>	0.0637	1.7127	0.6937	0.8234
<b>100</b>	<b>2</b>	0.0056	1.8667	0.7985	0.8903
<b>100</b>	<b>5</b>	0.0686	1.2161	0.2637	0.5161
<b>100</b>	<b>10</b>	0.0449	0.4212	0.1127	0.1929
<b>100</b>	<b>20</b>	0.0023	0.0361	0.0297	0.0227

Table 4.7 shows the individual position errors of the clients and the mean position errors of all for CL1 and for 5 different number of iterations and 5 different SNR values, hence, 25 different ISCs.

Table 4.8 Positioning error values of CL2 for 25 ISCs

<b>Error Analysis of CL2</b>					
<i>iterations</i>	<b>SNR</b>	<b>pos. error b (m)</b>	<b>pos. error c (m)</b>	<b>pos. error d (m)</b>	<b>mean pos. error (m)</b>
<b>10</b>	<b>1</b>	0.4972	0.7094	1.6630	0.9565
<b>10</b>	<b>2</b>	0.0805	0.2893	1.9688	0.7795
<b>10</b>	<b>5</b>	0.0917	0.4877	0.9073	0.4956
<b>10</b>	<b>10</b>	0.0817	0.1273	0.3544	0.1878
<b>10</b>	<b>20</b>	0.0188	0.0832	0.0779	0.0600
<b>20</b>	<b>1</b>	0.0954	1.2752	1.5797	0.9834
<b>20</b>	<b>2</b>	0.0745	0.5023	0.9803	0.5190
<b>20</b>	<b>5</b>	0.0278	0.3587	0.6767	0.3544
<b>20</b>	<b>10</b>	0.0285	0.1659	0.3137	0.1694
<b>20</b>	<b>20</b>	0.0129	0.0112	0.0637	0.0293
<b>30</b>	<b>1</b>	0.2570	1.5219	0.7518	0.8436
<b>30</b>	<b>2</b>	0.2463	0.2062	0.6078	0.3534
<b>30</b>	<b>5</b>	0.1313	0.5924	0.5153	0.4130
<b>30</b>	<b>10</b>	0.0393	0.1657	0.4299	0.2116
<b>30</b>	<b>20</b>	0.0097	0.0109	0.0273	0.0160
<b>50</b>	<b>1</b>	0.0308	0.5451	0.9389	0.5049
<b>50</b>	<b>2</b>	0.0024	0.7506	0.6968	0.4833
<b>50</b>	<b>5</b>	0.0781	0.2875	0.3970	0.2542
<b>50</b>	<b>10</b>	0.0310	0.2337	0.2195	0.1614
<b>50</b>	<b>20</b>	0.0215	0.0372	0.0469	0.0352
<b>100</b>	<b>1</b>	0.0367	1.1085	0.5888	0.5780
<b>100</b>	<b>2</b>	0.0320	0.3860	1.0406	0.4862
<b>100</b>	<b>5</b>	0.0159	0.4377	0.3986	0.2841
<b>100</b>	<b>10</b>	0.0016	0.0600	0.1317	0.0644
<b>100</b>	<b>20</b>	0.0081	0.0125	0.0832	0.0346

Table 4.9 Positioning error values of CL3 for 25 ISCs

<b>Error Analysis of CL3</b>					
<i>iterations</i>	<b>SNR</b>	<b>pos. error b (m)</b>	<b>pos. error c (m)</b>	<b>pos. error d (m)</b>	<b>mean pos. error (m)</b>
<b>10</b>	<b>1</b>	0.1790	0.5339	0.4359	0.3829
<b>10</b>	<b>2</b>	0.3375	0.3089	0.7037	0.4500
<b>10</b>	<b>5</b>	0.2569	0.2618	0.1488	0.2225
<b>10</b>	<b>10</b>	0.0049	0.1657	0.1687	0.1131
<b>10</b>	<b>20</b>	0.0285	0.0459	0.0253	0.0332
<b>20</b>	<b>1</b>	0.1592	0.4924	0.8291	0.4936
<b>20</b>	<b>2</b>	0.3126	0.2202	0.3860	0.3063
<b>20</b>	<b>5</b>	0.0573	0.1578	0.3824	0.1992
<b>20</b>	<b>10</b>	0.0325	0.1860	0.1571	0.1252
<b>20</b>	<b>20</b>	0.0041	0.0908	0.0489	0.0479
<b>30</b>	<b>1</b>	0.1781	0.2151	0.1864	0.1932
<b>30</b>	<b>2</b>	0.0154	0.0998	0.5836	0.2329
<b>30</b>	<b>5</b>	0.0362	0.0947	0.1613	0.0974
<b>30</b>	<b>10</b>	0.0450	0.0583	0.0920	0.0651
<b>30</b>	<b>20</b>	0.0064	0.0086	0.0253	0.0134
<b>50</b>	<b>1</b>	0.0163	0.1483	0.4414	0.2020
<b>50</b>	<b>2</b>	0.0023	0.2511	0.3215	0.1916
<b>50</b>	<b>5</b>	0.0853	0.0517	0.1034	0.0801
<b>50</b>	<b>10</b>	0.0593	0.1871	0.0409	0.0958
<b>50</b>	<b>20</b>	0.0007	0.0187	0.0367	0.0187
<b>100</b>	<b>1</b>	0.0485	0.1716	0.2265	0.1489
<b>100</b>	<b>2</b>	0.0776	0.0870	0.3882	0.1843
<b>100</b>	<b>5</b>	0.0322	0.0557	0.1266	0.0715
<b>100</b>	<b>10</b>	0.0726	0.0506	0.1180	0.0804
<b>100</b>	<b>20</b>	0.0002	0.0105	0.0120	0.0076

Table 4.10 Positioning error values of CL4 for 25 ISCs

<b>Error Analysis of CL4</b>					
<i>iterations</i>	SNR	pos. error b (m)	pos. error c (m)	pos. error d (m)	mean pos. error (m)
<b>10</b>	<b>1</b>	0.3489	0.4024	0.2608	0.3374
<b>10</b>	<b>2</b>	0.5251	0.4231	0.7058	0.5513
<b>10</b>	<b>5</b>	0.0026	0.1735	0.2612	0.1458
<b>10</b>	<b>10</b>	0.0344	0.0936	0.2427	0.1236
<b>10</b>	<b>20</b>	0.0024	0.1030	0.0641	0.0565
<b>20</b>	<b>1</b>	0.1493	0.7615	0.7393	0.5500
<b>20</b>	<b>2</b>	0.0537	0.4624	0.1336	0.2166
<b>20</b>	<b>5</b>	0.0305	0.0826	0.6235	0.2455
<b>20</b>	<b>10</b>	0.0704	0.0478	0.0333	0.0505
<b>20</b>	<b>20</b>	0.0159	0.0361	0.0439	0.0320
<b>30</b>	<b>1</b>	0.0351	0.6131	0.3258	0.3247
<b>30</b>	<b>2</b>	0.1110	0.2164	0.4491	0.2588
<b>30</b>	<b>5</b>	0.1637	0.1464	0.4306	0.2469
<b>30</b>	<b>10</b>	0.0098	0.0435	0.3094	0.1209
<b>30</b>	<b>20</b>	0.0044	0.0215	0.0330	0.0196
<b>50</b>	<b>1</b>	0.1284	0.3100	0.5867	0.3417
<b>50</b>	<b>2</b>	0.1107	0.5642	0.5112	0.3954
<b>50</b>	<b>5</b>	0.0838	0.2457	0.3255	0.2183
<b>50</b>	<b>10</b>	0.0558	0.0667	0.0307	0.0511
<b>50</b>	<b>20</b>	0.0167	0.0454	0.0327	0.0316
<b>100</b>	<b>1</b>	0.0581	0.5460	0.4855	0.3632
<b>100</b>	<b>2</b>	0.0206	0.3345	0.4246	0.2599
<b>100</b>	<b>5</b>	0.0150	0.1248	0.2503	0.1300
<b>100</b>	<b>10</b>	0.0944	0.1548	0.1544	0.1345
<b>100</b>	<b>20</b>	0.0119	0.0391	0.0406	0.0305

In Table 4.10, the numerical positioning error analysis of the 4 CLs for 25 different ISCs are presented. In Figures 4.21 and 4.22, the graphical illustrations of these error values are shown. There are 2 graphs containing 4 inner graphs each representing the illustrations of mean error performances of the 4 CLs with respect to SNR and *iterations*.

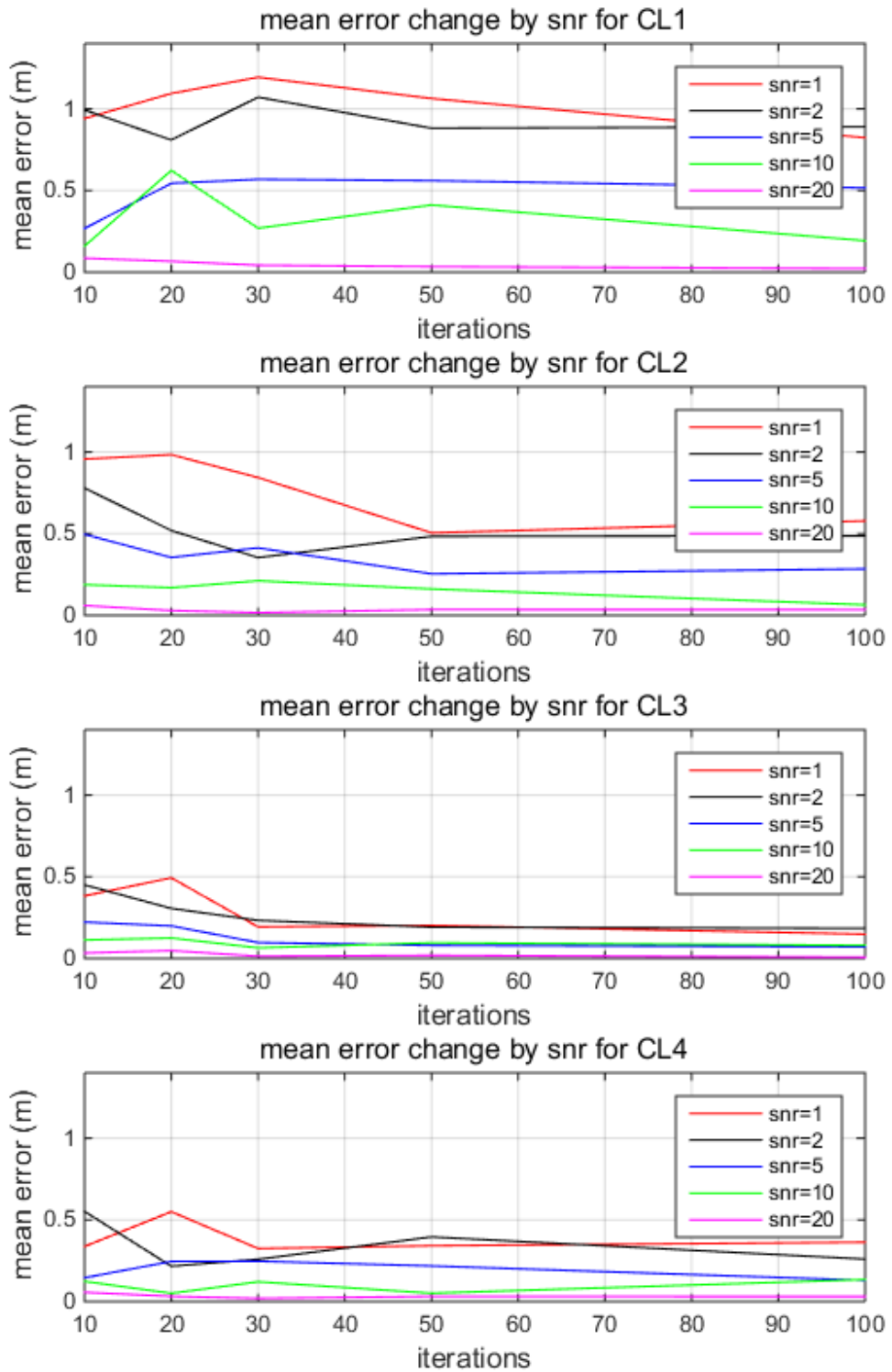


Figure 4.21 Error performance – iterations correlations of the 4 CLs with respect to SNR values

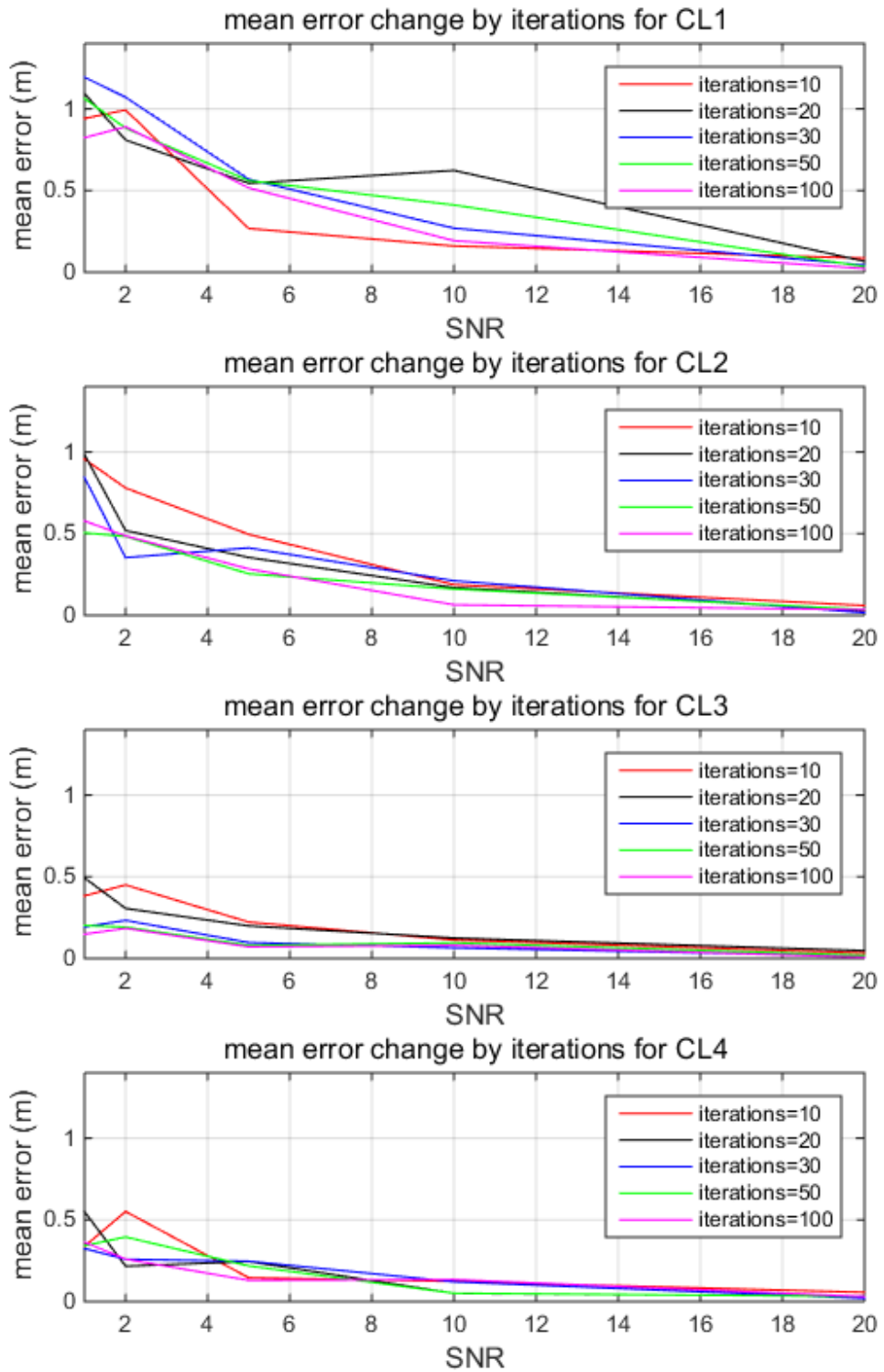


Figure 4.22 Error performance – SNR correlations of the 4 CLs with respect to *iterations*

As can be seen from Figure 4.21, the error performance increases with the number of iterations even if SNR is held constant for all the 4 CLs if we do not take the exceptions caused by the randomly added noises into account. Up to a number of iterations, the error performance of the system seems to be unreliable, however, after 30 repetitions, it was seen that there is a correlation between the error performance and the number of repetitions. The positioning error decreases with the number of iterations. But these are only the simulation results. It can be expected that, for a small number of iterations, even if it was random, the noise may cause the system to be more than anticipated. But after 30 repetitions, one can say that the random error is uniformly distributed. By the increase of *iterations*, it is normal to observe a reduced positioning error.

Figure 4.22 illustrates the error performance of the 4 CLs depending on SNR values. Since SNR is the indicator of the level of the noise added to the system, it is normal to see a decreasing error curve by the increase of SNR. However, SNR is seen to be related with the number of repetitions even if it was not expected. For a small number of *iterations*, error curves for different number of SNRs show that, it is not very reliable to make an assumption like *'the greater the SNR the better the error performance is'* but after about a number of 30 iterations error curves are seen to be in line, as expected. The two error performance curves (Figures 4.21 and 4.22) both show that for a reliable outcome, a reliable measurement set, the number of the repetitions, in another words the number of the RSSI measurements should be greater than 30 in order to maintain a trustworthy system.

## 4.2 Experimental Results

In the previous section, the simulation results of the 4 CLs are presented and the importance of the number of the measurements is defined. Now in this section we present the experimental results of the distance estimations and the NOIP.

To present the distance estimations we first need to share the RSSI measurements and the specific ways of measurements, the correlations of them with the distances

they were taken. Then the distance estimations of the RSSI recordings are presented for all 3 SDR models. Finally the positioning results by the estimated distances are exhibited with using the NOIP.

#### ***4.2.1 Measurement Process and the Results***

Communication of the clients is provided by the built of Wi-Fi and Bluetooth wireless communication infrastructures by using a self-implemented device (SID) but after the examinations of the results it seemed that Bluetooth results are not very reliable. The variation of the signal strength can reach up to 20 dBm even if the distance is not changed. Hence, we are focused on Wi-Fi results which are considerably more consistent.

##### ***4.2.1.1 Hardware Process of the Measurement Process***

The preferred wireless communication metric, RSSI, is being recorded for several distances between the clients. The hardware of each client consists of Raspberry Pi SBC (“Raspberry Pi,” n.d.) and Realtek RTL8723BU (FN-LINK, n.d.) Wi-Fi & Bluetooth IC.

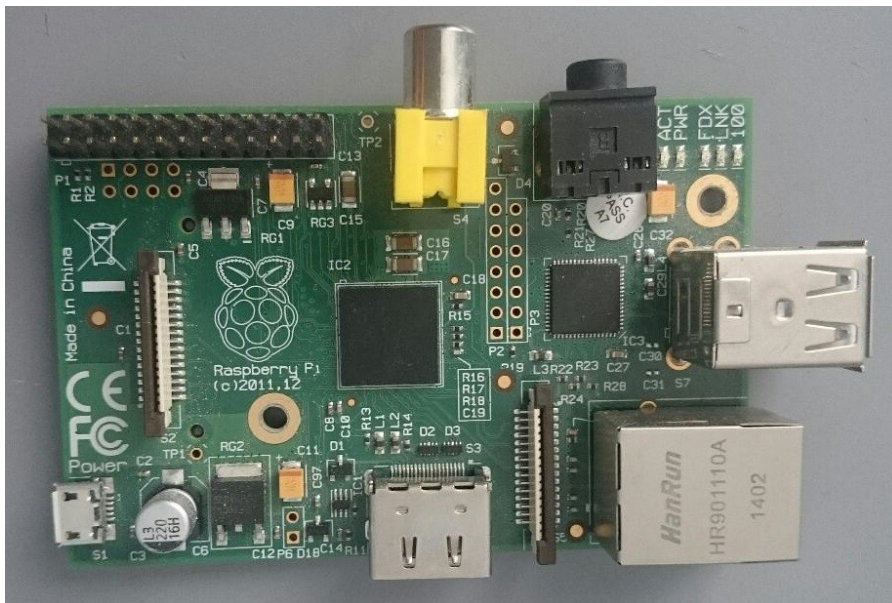


Figure 4.23 Raspberry Pi

To use the Wi-fi & Bluetooth module, two versions of the circuits are designed and implemented which is given in the product datasheet (FN-LINK, n.d.). The schematic diagram of the first design is given below (Figures 4.24 and 4.25).

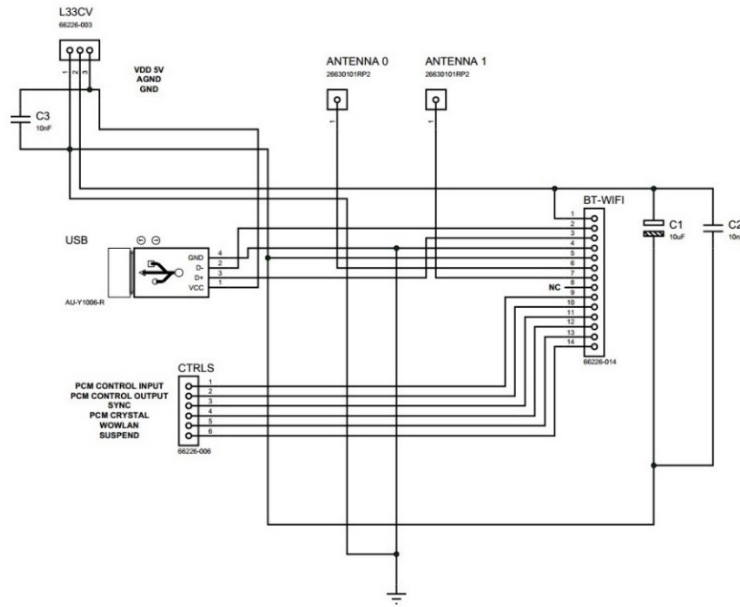


Figure 4.24 Schematic diagram of the first SID design

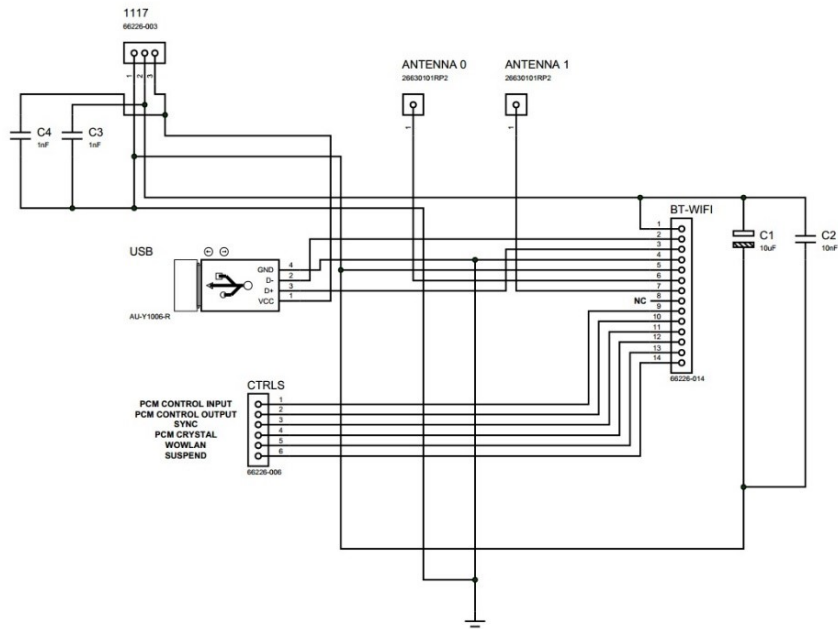


Figure 4.25 Schematic design of the second SID

The only difference between the two designs is a few components; a capacitor and the voltage regulator IC. But the difference would be seen more clearly in the layout designs (see Figure 4.26).

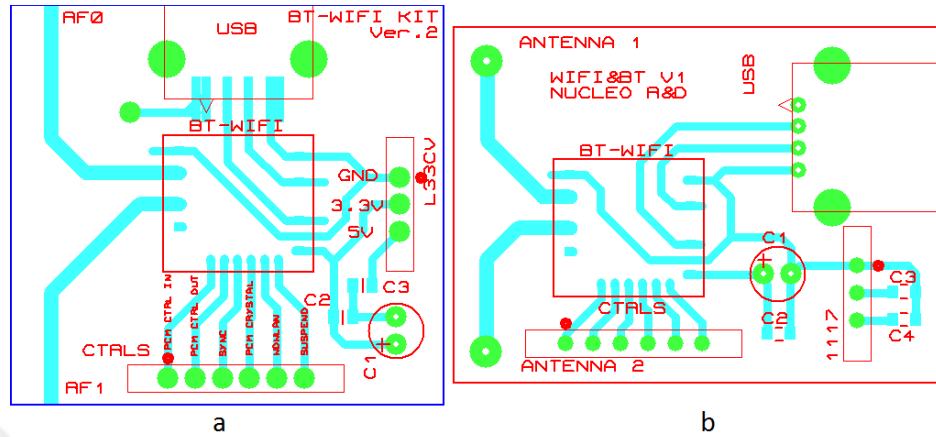


Figure 4.26 The 1<sup>st</sup> (a) and the 2<sup>nd</sup> (b) layout designs of the SID

Besides the datasheet circuit of the SID, a regulator component is added to the resulting device in order to supply the device directly from a USB port of Raspberry Pi (RPi) as can be seen in the previous figures. This component is basically a 3.3V regulator. In the first design and second design two different components are used; L33CV and LM117 as the supply regulating component.

The first version of the SID is presented in Figure 4.27.

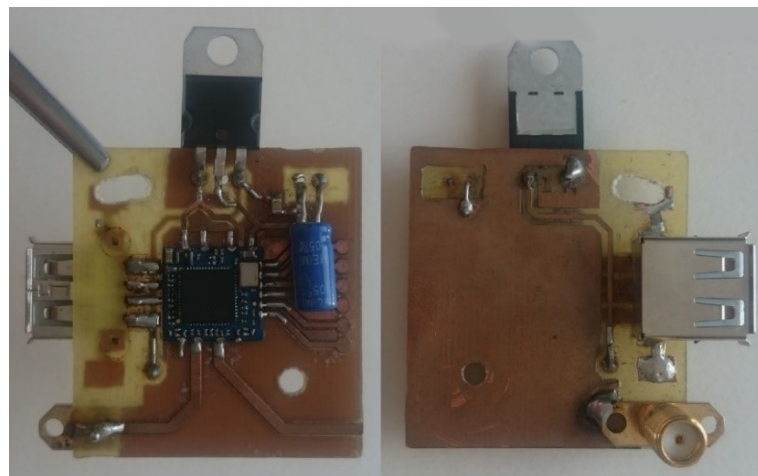


Figure 4.27 First implementation of the SID

The second and the final version of the device are given in Figure 4.28.

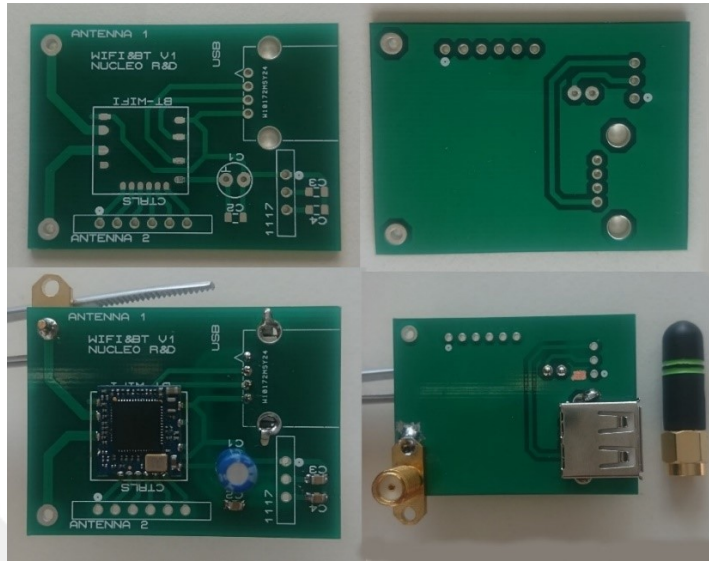


Figure 4.28 Second and the final version of the SID

With the connection of the SID and RPi through a USB-USB cable unveils a 'client' (Figures 4.29 and 4.30).

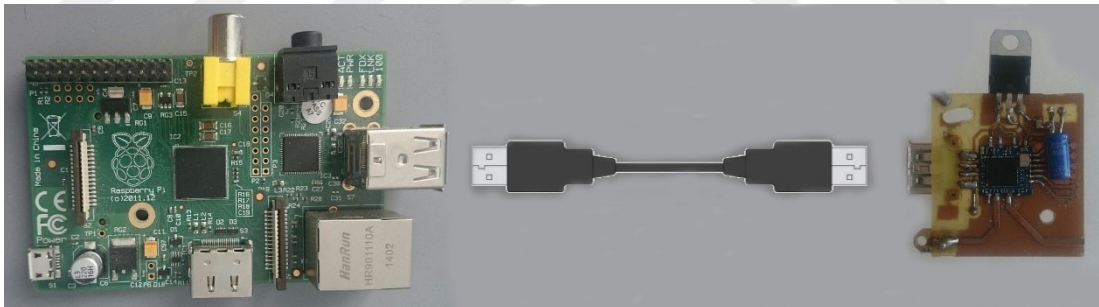


Figure 4.29 The connection of RPi and the SID, a 'client', 1<sup>st</sup> version

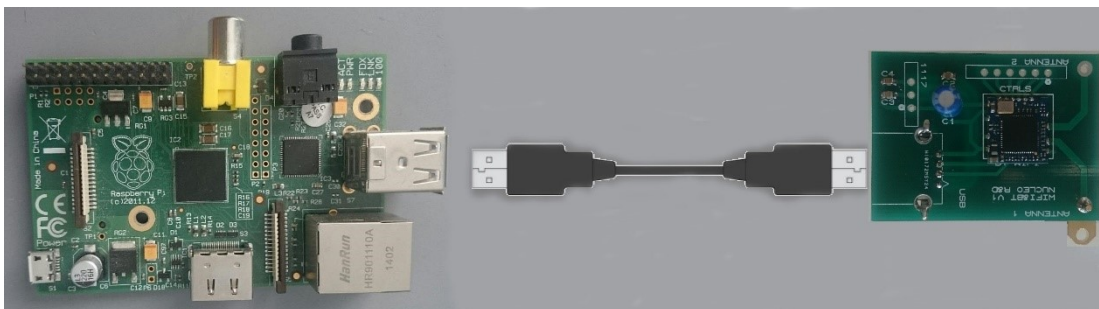


Figure 4.30 The 2<sup>nd</sup> and the final version of a 'client'

After the implementation of the 4 SIDs, we pass into the software process in order to use the devices with RPi.

#### *4.2.1.2 Software Process of the Measurement Process*

All 4 SIDs are set to behave as an Access Point (AP). The device is programmed to record RSSI metrics 15 times a row (1 measurement in 1 second, 15 measurements = 15 seconds) which is visible to the SID in the environment. This is done for eliminating the instant errors that will cause faulty measurements. The mean value of the 15 measurements at a point is the RSSI value of that point for the first recordings. These recordings are only used for the experimental process of the 1<sup>st</sup> CL and the method is called the 1<sup>st</sup> MM as previously described in Section 3.1.1.1. For the experimental procedure of the other 3 CLs, the 2<sup>nd</sup> MM is used. The number of an individual recording is 20 for the 2<sup>nd</sup> MM.

During the measurements it was observed that even if the distance is increased between the clients, the signal strength increases instead of decreasing. To overcome this problem, the driver of the SID is observed and the Automatic Gain Control (AGC) of the device is disabled in order to relate signal strength only with the distance. For the software implementations Debian based operating system Raspbian is used.

#### *4.2.1.3 Measurement Results of the Received Signal Strength Indicator (RSSI) Metrics*

After at least two clients are ready to be used, a measurement process can be started. As described previously, two different measurement method is used, 1<sup>st</sup> MM and 2<sup>nd</sup> MM.

*4.2.1.3.1 Results of the 1st Measurement Method.* This measurement is implemented with only two clients. These clients are set in an office building and for a various distances between them the RSSI metrics are recorded.

After a few recordings it was observed that, the minimum and the maximum visible signal strengths are -70 dBm and -47 dBm respectively. Up to nearly 30 m the SID works perfectly however the RSSI metrics change only between 2 m and 12 m. When the distance between the clients are under 2 m the RSSI metric is always -47 dBm and after 12 m it is always -70 dBm. These are the signal strength limits of the SID.

These ranges can vary device to device, components etc. But, neglecting the maximum and minimum limits of the RSSI metrics, the SDR curve is expected to be similar to a decreasing exponential curve for any device that can provide RSSI outputs (see Figure 4.31).

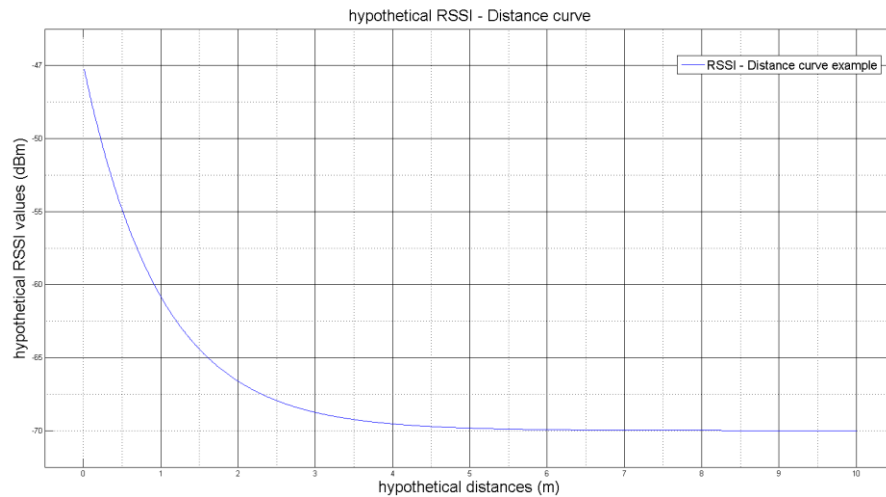


Figure 4.31 A hypothetical RSSI-Distance curve

To record meaningful measurements, we seek to reach a curve alike in Figure 4.31. The measurements take place in an office building illustrated in Figure 4.32 and recordings are taken for 16 different distance values between 2-12 m.



Figure 4.32 Measurement environment for the 1<sup>st</sup> MM

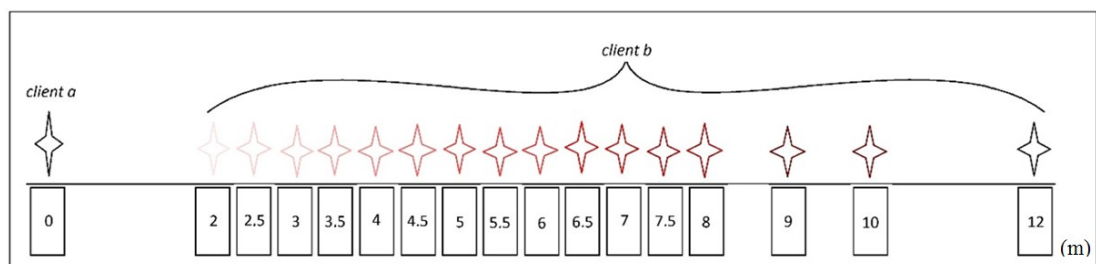


Figure 4.33 First MM and the distances between the clients

There are many recordings that were taken but the best measurement results for this method is illustrated in Figure 4.34.

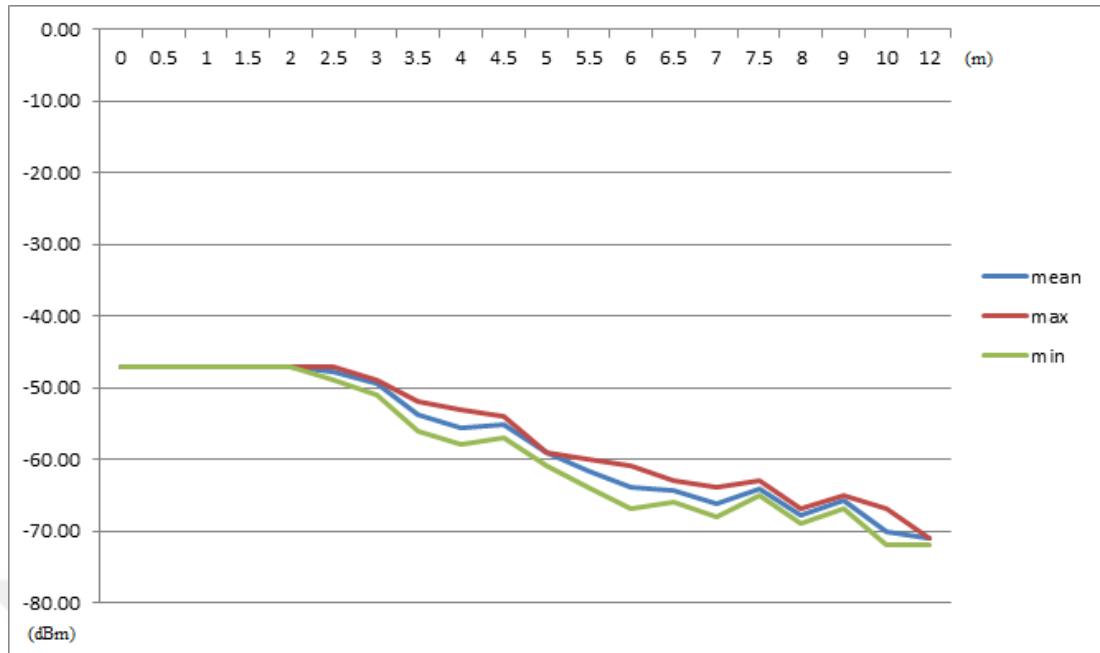


Figure 4.34 The RSSI recordings of the 1<sup>st</sup> MM

In Figure 4.34 *mean*, *max* and *min* represent the mean, maximum and minimum values of the RSSI measurements. As can be seen in Figure 4.34, there is no change until the distance reaches 2 m between the clients. These results are estimated into distance via the 3 distance estimation methods and those results are used for the positioning process of the 1<sup>st</sup> CL.

The actual measurements showed that our curve is different. First of all, the slope of the curve is not exponential, but linear. This situation may be caused by the structure of the device but it is an unknown fact for us to make a comment. However, it is considered that these curve variations can be caused by the structure of the device.

*4.2.1.3.2 Results of the 2nd Measurement Method.* The 2<sup>nd</sup> MM is implemented with all four clients. These clients are set in the basement of a school building and for the remaining 3 CLs the RSSI metrics are recorded 20 times for each measurement. The remaining CLs, 2<sup>nd</sup> CL, 3<sup>rd</sup> CL and the 4<sup>th</sup> CL, are illustrated previously in the simulation results but in Figure 4.35 they are presented again in a single illustration.

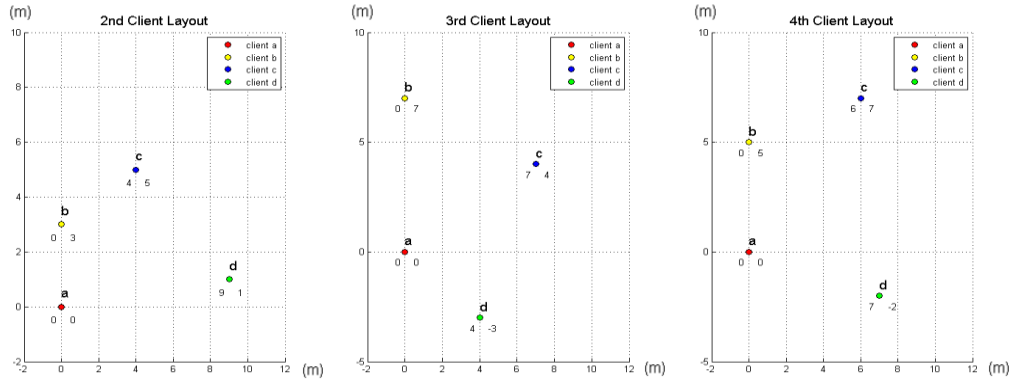


Figure 4.35 Remaining 3 CLs, 2<sup>nd</sup> CL, 3<sup>rd</sup> CL and the 4<sup>th</sup> CL

The RSSI metrics are recorded at first from client *a*, then *b*, *c* and *d*. By doing that, the distance combinations between any of the clients have been recorded twice. For example, when recording the metrics from client *a*, the distance  $L_{ab}$  is saved, then again when recording the metrics from client *b*, the distance  $L_{ab}$  is saved again. Hence, the number of the RSSI recordings taken for each distance becomes 40 instead of 20. And this number of repetitions is enough for a reliable measurement as previously described in Section 4.1.5. The order of recordings is illustrated in Figure 4.36 below.

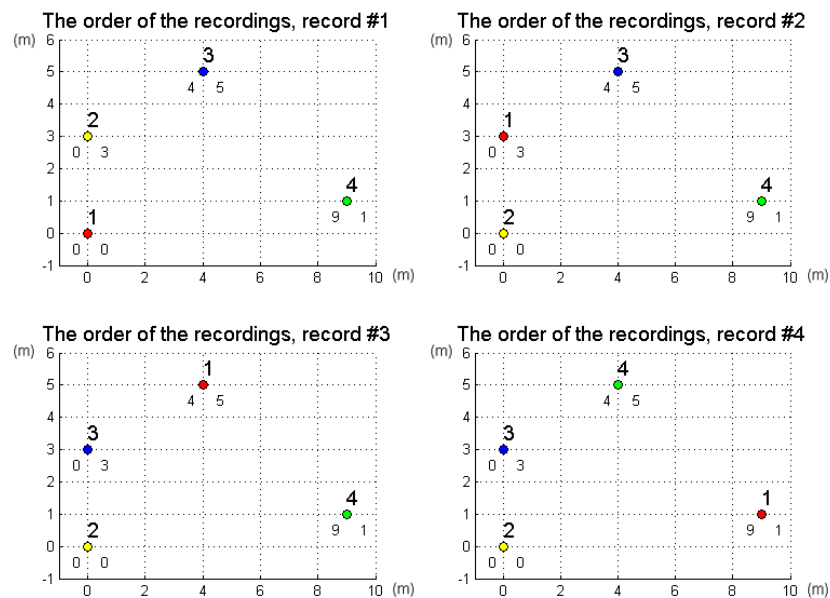


Figure 4.36 The illustration of the 2<sup>nd</sup> MM

This method contains only the experimental RSSI data. For 4 clients and 3 different layouts, 240 RSSI measurements are taken (for 3 layout variations, 4 clients and 20 repetitions, there are 240 RSSI measurements).

```
pi@raspberrypi ~/Desktop/Data $ sudo python deneme.py
Name      Signal
eduroam   -65.00 dBm
eduroam   -69.00 dBm
eduroam   -73.00 dBm
eduroam   -71.00 dBm
Pi_4      -63.00 dBm
Pi_3      -60.00 dBm
Pi_2      -65.00 dBm

pi@raspberrypi ~/Desktop/Data $ sudo python deneme.py
Name      Signal
eduroam   -63.00 dBm
eduroam   -69.00 dBm
eduroam   -73.00 dBm
eduroam   -71.00 dBm
Pi_4      -64.00 dBm
Pi_3      -60.00 dBm
Pi_2      -65.00 dBm
```

Figure 4.37 Example of the signal strengths seen by the 1st SID

In Figure 4.37, Pi\_2, Pi\_3 and Pi\_4 represent the signal strength of the 2<sup>nd</sup>, 3<sup>rd</sup> and the 4<sup>th</sup> clients (2, 3 and 4). In Figure 4.38 the 4 clients can be seen.



Figure 4.38 The 4 clients

The 4 clients presented in Figure 4.38, are placed by the layouts and the RSSI metrics are recorded. The environment of recordings belonging to the 2<sup>nd</sup> MM is illustrated in the following (Figures 4.39 and 4.40).



Figure 4.39 The environment where the recordings take place by the 2<sup>nd</sup> MM

In Figure 4.39 the clients are highlighted in red circles. In Figure 4.40 the clients can be seen closely.

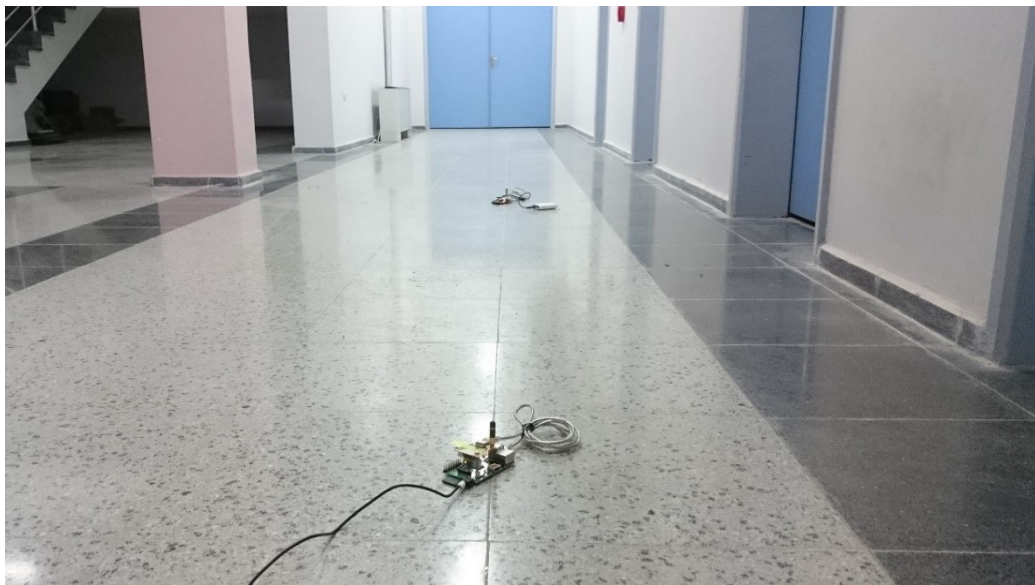


Figure 4.40 A closer look to the clients during the recordings

## 4.2.2 Results of the Distance Estimation Process

After all the RSSI recordings are saved for all the 4 CLs and the 2 MMs, we can estimate the distances between the clients via the 3 RSS based indoor path loss models.

### 4.2.2.1 Distance Estimation Results of ITU Indoor Path Loss Model

ITU is a path loss model based on its' exponents,  $N$  and  $L_f$ . Being consistent with the belonging document of International Telecommunication Union, we derived these exponents by calculating the distance errors for various combinations of them. From 10 to 40, every  $N$  and  $L_f$  combination is calculated and the resulting distance error graph is presented in Figure 4.41. The distance error is defined by the difference of the estimation of ITU model with the actual distance that the RSSI metric was recorded. The distance error is;

$$D_{err} = |D_{ITU} - D_{real}| \quad (4.2)$$

where,  $D_{err}$ ,  $D_{ITU}$  and  $D_{real}$  represent the distance error, ITU estimation and the actual distance respectively.

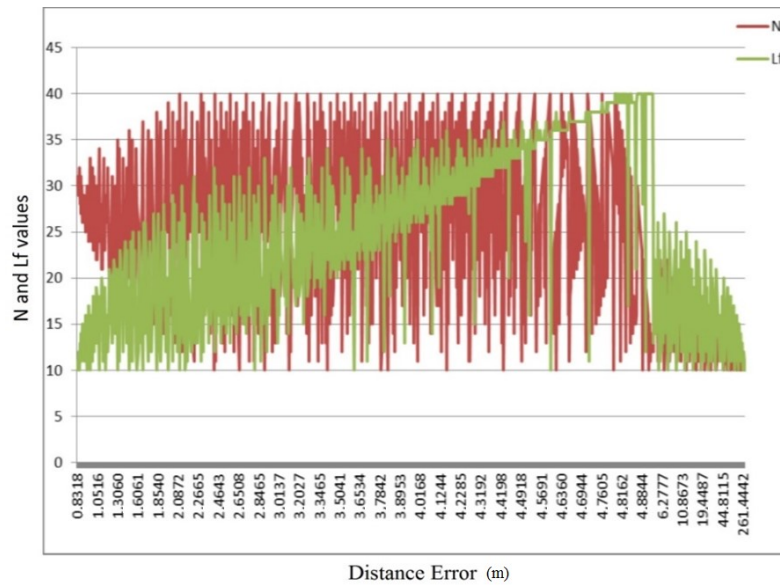


Figure 4.41 ITU exponents vs. the distance error

The resulting error graph yields that the minimum distance error occurs when  $N=28$  and  $L_f=11$ , which is consistent with the literature (International Telecommunication Union, 2015; Seybold, 2005). Hence, the resulting ITU Model formula is given by;

$$d = 10^{\frac{(P_{RSSI}+38.44)}{28}} \quad (4.3)$$

where the only unknown is the distance,  $d$ , being the RSSI recordings.

After the exponents are set, the distance estimation process was started by using ITU model for all the distances that the RSSI recordings are taken. There are 16 and 13 different distances that the RSSI metrics are recorded via the 1<sup>st</sup> MM and the 2<sup>nd</sup> MM respectively (Table 4.11). In Table 4.11, the results of the 2<sup>nd</sup> MM are the combined measurement set for the 2<sup>nd</sup>, 3<sup>rd</sup> and the 4<sup>th</sup> CLs.

Table 4.11 The Mean values of the RSSI recordings taken in the 1<sup>st</sup> and 2<sup>nd</sup> environments

1st MM		2nd MM	
Distance (m)	RSSI (dBm)	Distance (m)	RSSI (dBm)
2.00	-47.00	3.00	-46.68
2.50	-47.47	4.47	-51.23
3.00	-49.20	5.00	-55.91
3.50	-53.80	6.32	-61.63
4.00	-55.10	6.40	-54.75
4.50	-55.07	7.00	-57.13
5.00	-59.06	7.28	-59.58
5.50	-61.07	7.62	-58.30
6.00	-63.07	8.06	-60.60
6.50	-63.87	9.05	-61.95
7.00	-66.13	9.22	-62.00
7.50	-63.80	9.90	-60.58
8.00	-68.00	10.77	-60.05
9.00	-65.80		
10.00	-69.80		
12.00	-70.00		

The recordings are separated in 2 parts because the measurements were taken in 2 different environments. The first measurement set is for the 1<sup>st</sup> CL, and the second set is for the remaining CLs. The ITU results of the 2 MMs showed a large amount

of error. So, we decided to recalculate the environmental conditions by changing the exponents of the model. The distance errors are recalculated and the least error occurred when  $N=25$  and  $L_f=10$  for the 2<sup>nd</sup> environment. Hence, the ITU formula is redefined for the 2<sup>nd</sup> MM (see Equation 4.4).

$$d_2 = 10^{\frac{(P_{RSSI}+37.44)}{25}} \quad (4.4)$$

Now that the exponents are set for the 2 environments, the distance estimation process can be applied for both the results taken via the 1<sup>st</sup> MM and the 2<sup>nd</sup> MM in the 2 environments. In Figure 4.42 and Figure 4.43 the distance estimation results and the mean distance error of ITU Path Loss Model is presented for the RSSI recordings of both environments.

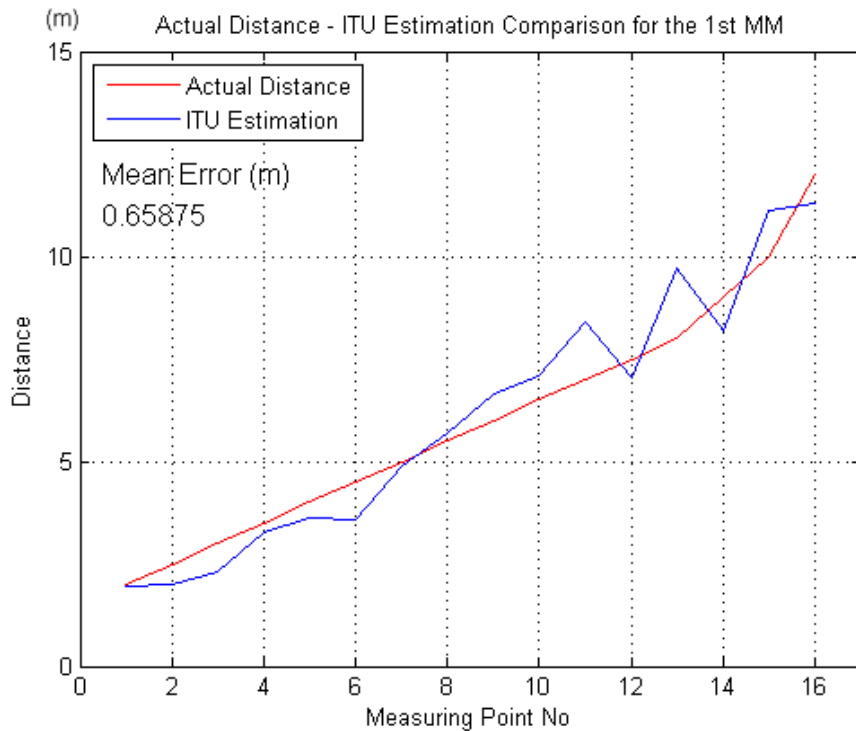


Figure 4.42 ITU estimations and the actual distances for the 1<sup>st</sup> environment

The resulting mean distance error for the 1<sup>st</sup> environment is found approximately 66 cm.

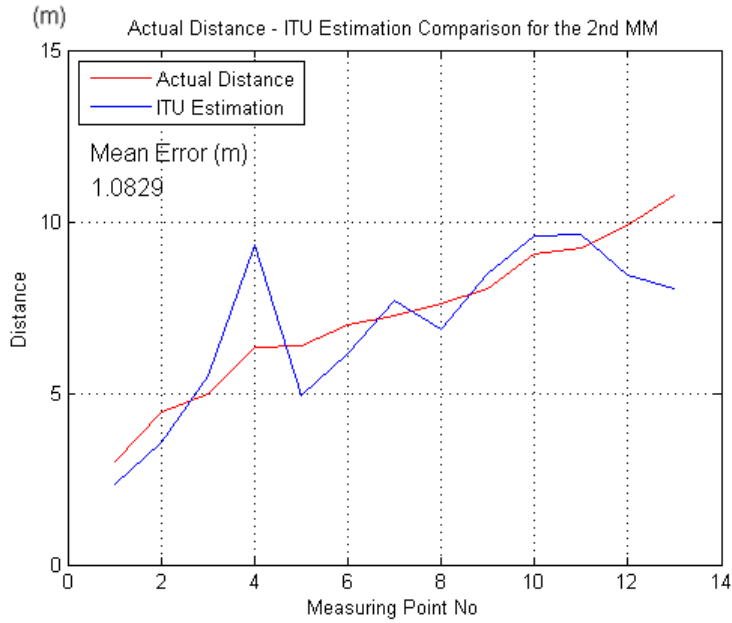


Figure 4.43 ITU estimations and the actual distances for the 2<sup>nd</sup> environment

The mean distance error for the 2<sup>nd</sup> environment is found 108 cm approximately. However, as can be seen from Figure 4.43, this error is highly caused by the results of the 4<sup>th</sup> measurement point. During the measurements in the 2<sup>nd</sup> environment, we paid attention not to intersect the LOSs of the signals with the columns. The large distance estimation error at measurement point 4 belongs to the specific measurement set taken between the 2<sup>nd</sup> and the 3<sup>rd</sup> points.

Hereby, the results of the first path loss model that is used to estimate the distance values are presented in this section. These results will be used to estimate the positions of the clients by their layouts in the positioning algorithm, the NOIP, as inputs.

#### 4.2.2.2 Distance Estimation Results of Two-Ray Ground Reflected Path Loss Model

The second method of RSS based distance estimation is Two-Ray Ground Reflected Path Loss Model. The mathematical expression of this model is;

$$d = h.10^{\frac{P_t + 2G - P_{RSSI}}{40}} \quad (4.5)$$

as defined previously in Section 3.1.2.2.

The distance estimations of the mean values of the RSSI measurements for the belonging distances are illustrated for the two environments in the following.

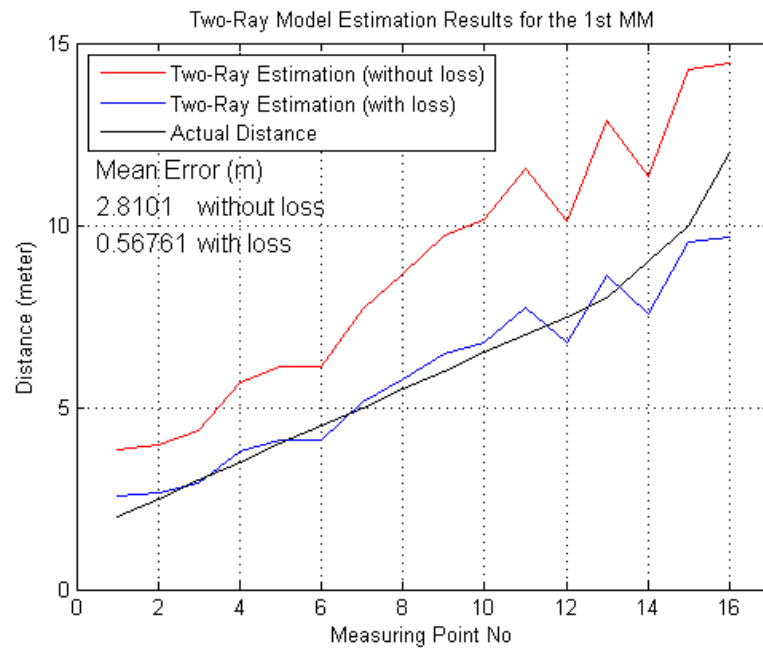


Figure 4.44 Two-Ray Model distance estimations for the 1<sup>st</sup> MM

When the distances are estimated by the resulting RSSI recordings of the 1<sup>st</sup> MM via Two-Ray Model (see Figure 4.44), it was seen that, there is almost a parallel difference between the estimated distance curve (red line) and the actual distance curve (black line). When the mean distance error is calculated, an unacceptable mean error is found, 2.81 m. To overcome this problem, relying on the approximately parallel difference of the distance curves, we defined an extra power loss factor. That power loss ( $P_l$ ) is added to the distance estimation model and the resulting equation is;

$$d = h.10^{\frac{P_t + 2G - P_{RSSI} - P_l}{40}} \quad (4.6)$$

Then we calculated this power loss factor as 7 dBm for the test environment. After the extra power loss is added to the system, the estimated distance curve (blue line in Figure 4.44) and the actual distance curve (black line in Figure 4.44) are nearly overlaid one another. The resulting mean distance error is then recalculated as approximately 56 cm which is nearly the 1/5 of the previous error value.

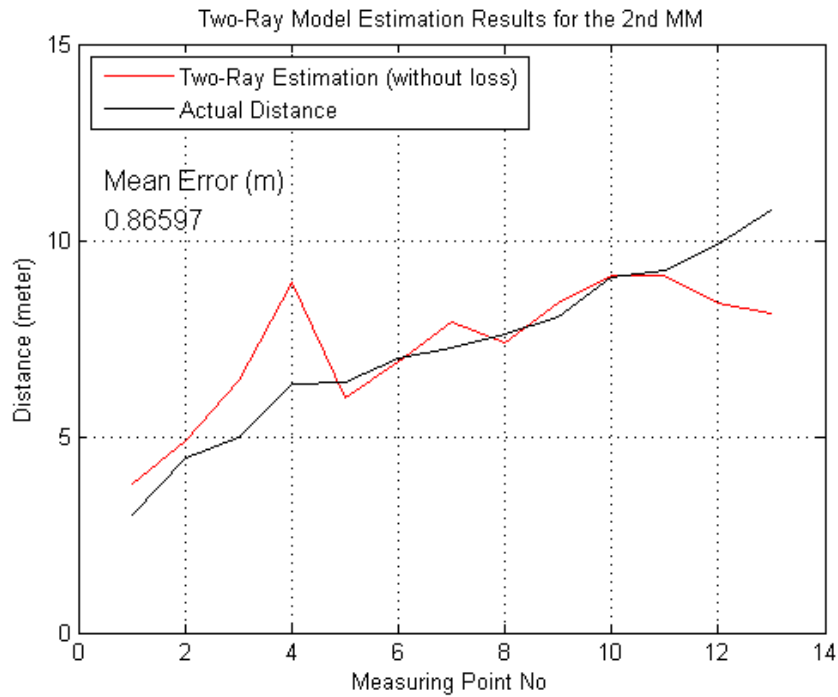


Figure 4.45 Two-Ray Model distance estimations for the 2<sup>nd</sup> MM

The distance estimation results of the 2<sup>nd</sup> MM via Two-Ray Model are seen to be similar to the 1<sup>st</sup> method (with respect to distance errors) even if there is no external power loss is defined for this estimation. The mean distance error is found by approximately 86 cm. However, Figure 4.45 shows that, at the 4<sup>th</sup> and the last two measuring points, the individual distance errors increase. The error on the 4<sup>th</sup> measurement point could be caused by a column which intersects the LOS of the signal when the measurement was recorded. The last two are different because this time there is no power loss, it is power rise that could be caused by the reflections.

Both distance estimation results are recorded to be used in the NOIP as inputs.

#### 4.2.2.3 Distance Estimation Results of Experimentally Derived Signal Strength-Distance Relation (EDR) Model

The 3<sup>rd</sup> and the last model of distance estimation is the EDR Model. EDR Model is based on the specific measurements and the distance values that the measurements were recorded. We first defined a model for a specific measurement set, the results of the 1<sup>st</sup> MM, however, the environmental conditions affected the results of the measurements more than anticipated. Consequently, we defined two separate EDR formulas to estimate the measurements recorded in the 1<sup>st</sup> and the 2<sup>nd</sup> environment. As previously presented, the first one is defined by;

$$d = 0.09878.e^{-0.06658.P_{RSSI}} \quad (4.7)$$

and the second formula is;

$$d = 0.1777.e^{-0.06364.P_{RSSI}} \quad (4.8)$$

The estimation results of both EDR Models are demonstrated in the following with the individual illustrations.

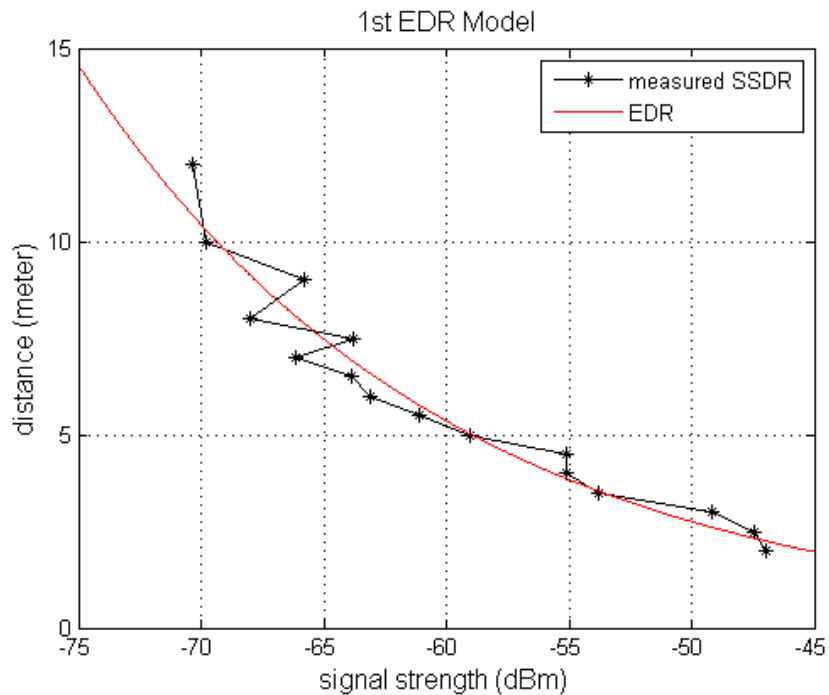


Figure 4.46 Derivation of the 1<sup>st</sup> EDR Model

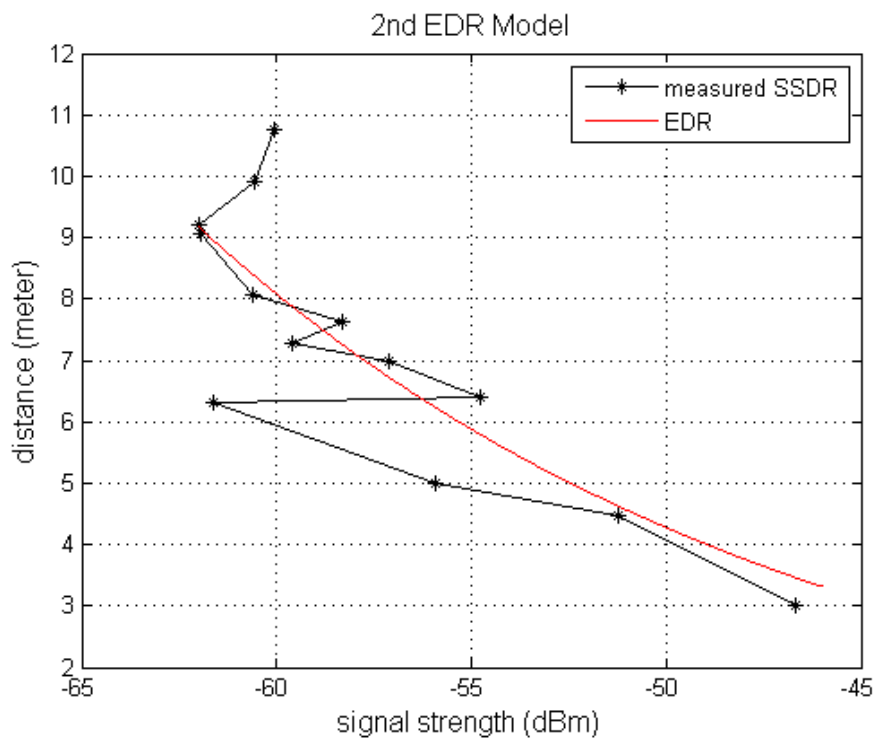


Figure 4.47 Derivation of the 2<sup>nd</sup> EDR Model

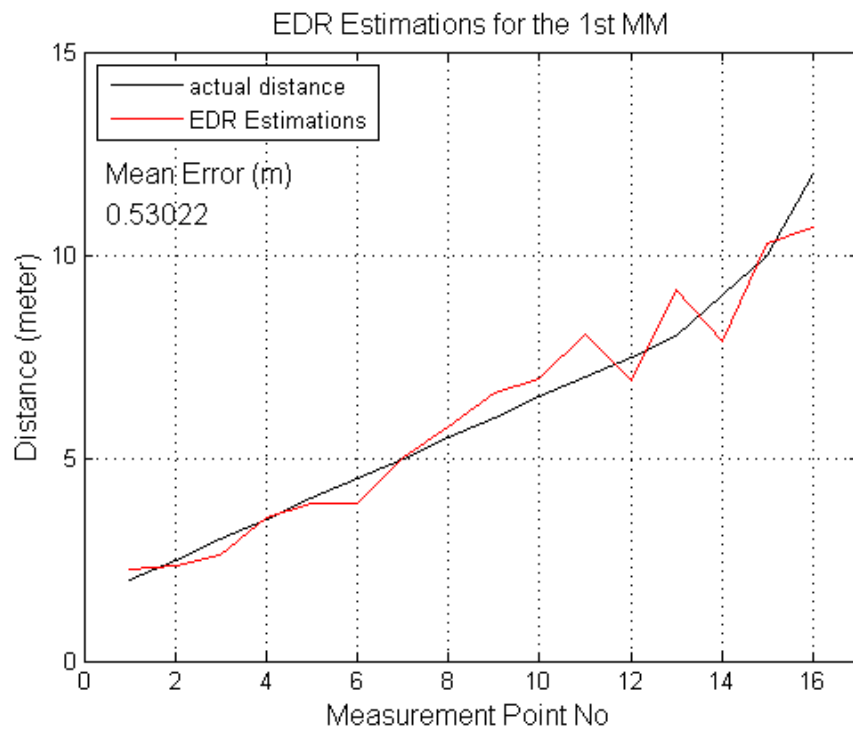


Figure 4.48 Distance Estimations of the 1<sup>st</sup> EDR Model for the 1<sup>st</sup> MM

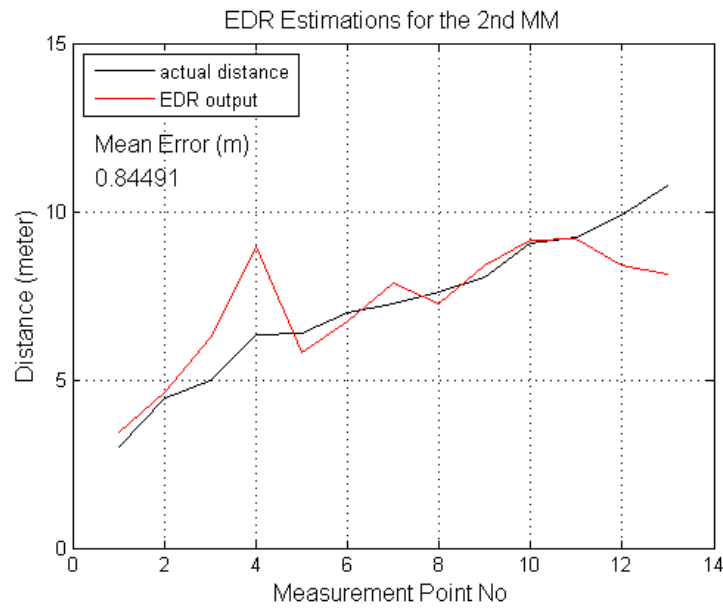


Figure 4.49 Distance Estimations of the 2<sup>nd</sup> EDR Model for the 2<sup>nd</sup> MM

Eventually all the distance estimations are recorded to be used in the positioning algorithm, the NOIP.

#### 4.2.2.4 Performance Comparison of the Distance Estimation Methods

Before starting the positioning process, it is decided to examine the error performances of the distance estimation methods. In Table 4.12, the numerical error analysis of all the distance estimation methods for the recordings taken in 2 different environments is presented.

Table 4.12 Mean distance error values of all the estimation methods

Error Performance Table	Mean Distance Error (m)	
	1st MM	2nd MM
ITU Model	0.6588	1.0829
Two-Ray Model	0.5676	0.8660
EDR Model	0.5302	0.8449

According to Table 4.12, one can say that the distance estimations of the 1<sup>st</sup> MM is expected to be result in a more accurate position estimation. Also the best distance estimation method is seemed to be the EDR Model considering the mean error

values. However, these are the mean distance error values. The positioning results can change due to the distances between the clients. For example, we stated that the 4<sup>th</sup> measurement point of the 2<sup>nd</sup> MM is faulty. If a distance between clients is close to the distance which the measurement #4 is taken, the resulting positions of the clients may be expected to be faulty either. On the other hand, if the distance values between the clients are all coincide to the accurate measurements, even if the mean distance error is high, the positions of the clients can be estimated correctly. This statement will be emphasized after the positioning process again.

### ***4.2.3 Results of the Positioning Process***

The main goal in this thesis is to estimate the positions of the clients in a robotic team in an indoor environment without any initial information. The data set that is used to estimate the positions of the clients contains distance information of any combination between the clients. The data set is derived with 3 different RSS based path loss models by estimating the distance values by using the RSSI measurements recorded. Eventually, the positions of the clients can be estimated by using the distance information. If we consider the measurement, distance estimation and positioning process as one whole process, the only input of the system would be the RSSI metric measurements where the output is the position information of the clients.

The positioning results are presented in the following with respect to both CLs and the distance estimation methods and at least the combined performance comparison is illustrated with figures and numerical error analysis.

#### ***4.2.3.1 Positioning Results of the 1<sup>st</sup> Client Layout***

The results of the NOIP for the 1<sup>st</sup> CL for the distance estimations of ITU Model, Two-Ray Model and EDR Model are respectively presented in the following. Then, the mean estimations of all distance estimation methods are illustrated in order to compare the performances of the distance estimation methods. In the end, the

numerical positioning errors of the 3 distance estimation methods are presented in Table 4.13.

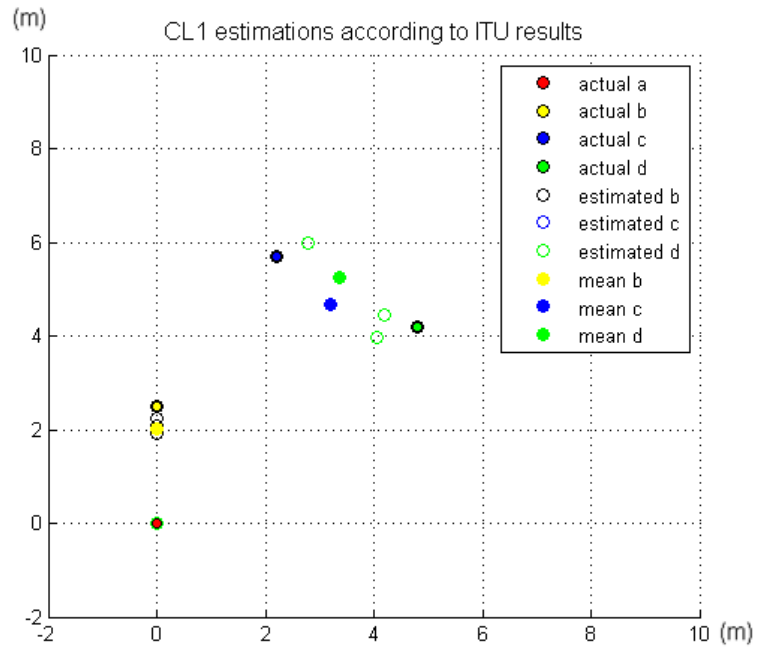


Figure 4.50 Positioning results of CL1 for the distance estimations of ITU Model

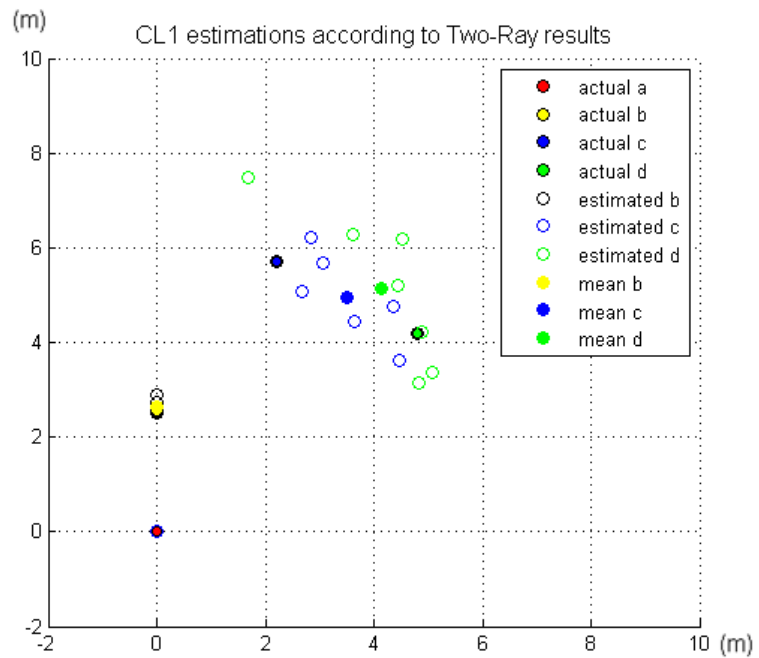


Figure 4.51 Positioning results of CL1 for the distance estimations of Two-Ray Model

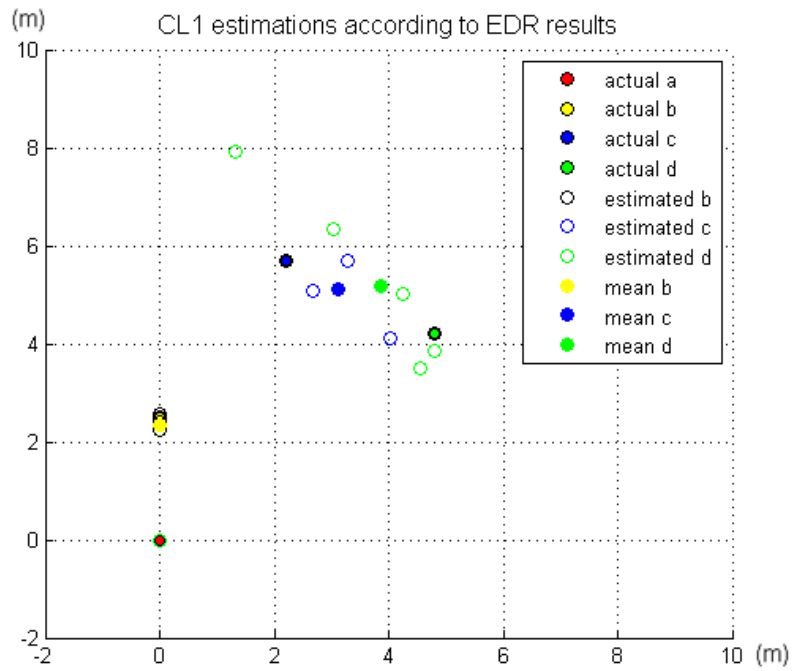


Figure 4.52 Positioning results of CL1 for the distance estimations of EDR Model

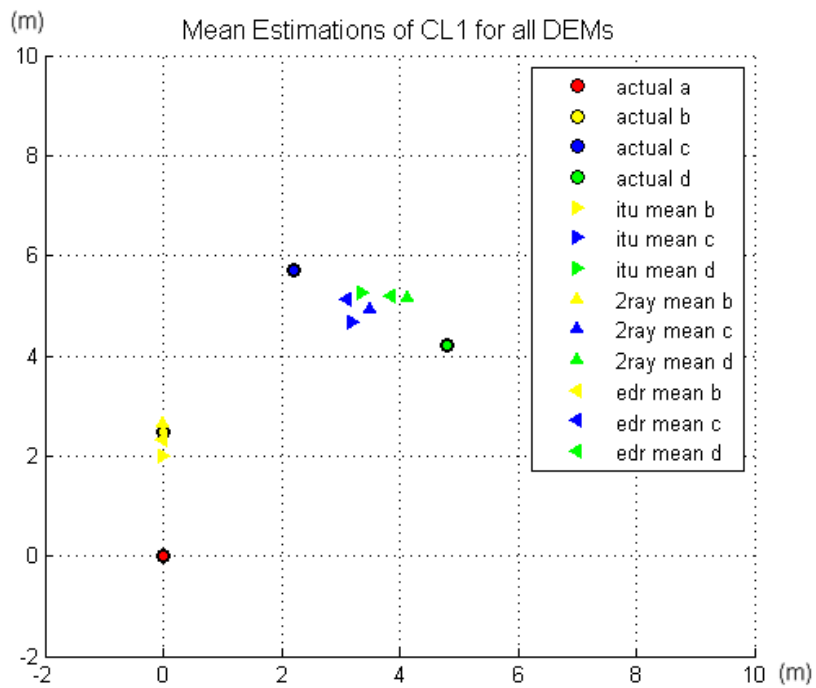


Figure 4.53 Mean positioning results of CL1 for all the distance estimation methods

Table 4.13 Positioning errors of CL1

CL1	client b (m)	client c (m)	client d (m)	mean (m)
ITU	0.4914	1.4390	1.7747	1.2350
Two-Ray	0.1427	1.5036	1.1533	0.9332
EDR	0.1745	1.0804	1.3617	0.8722

The illustrations of the position estimations and the numerical error analysis of the 1<sup>st</sup> CL are presented in the above. According to Table 4.13, it seems that the best position estimations are provided by the distance estimations of EDR Model. Note that the RSSI recordings of this CL are obtained with the 1<sup>st</sup> MM. This is the only CL that is being estimated with the recordings of the 1<sup>st</sup> MM. For the other CLs, the measurement technique is always the 2<sup>nd</sup> MM.

#### 4.2.3.2 Positioning Results of the 2<sup>nd</sup> Client Layout

The results of the NOIP for the 2<sup>nd</sup> CL are presented in the following.

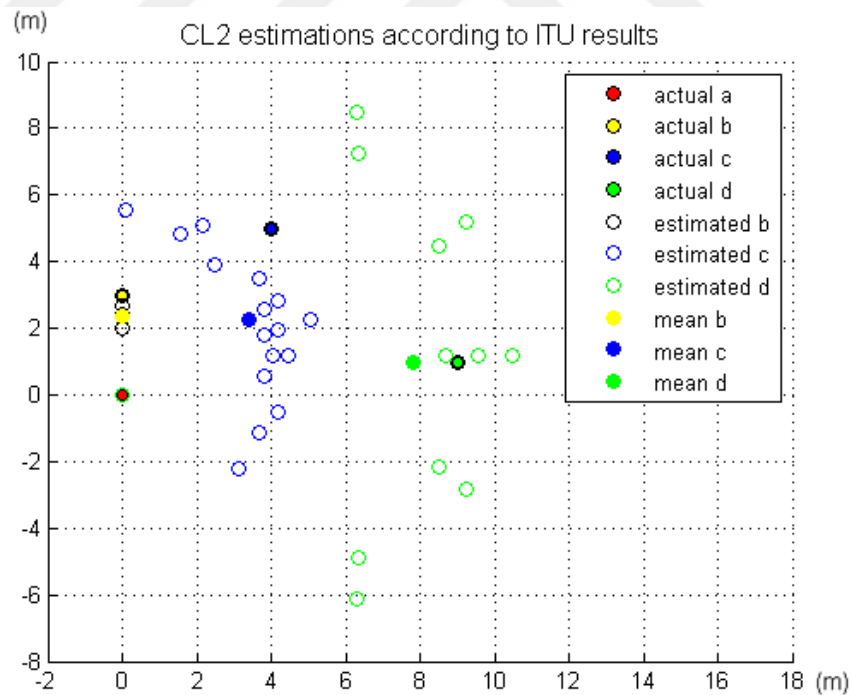


Figure 4.54 Positioning results of CL2 for the distance estimations of ITU Model

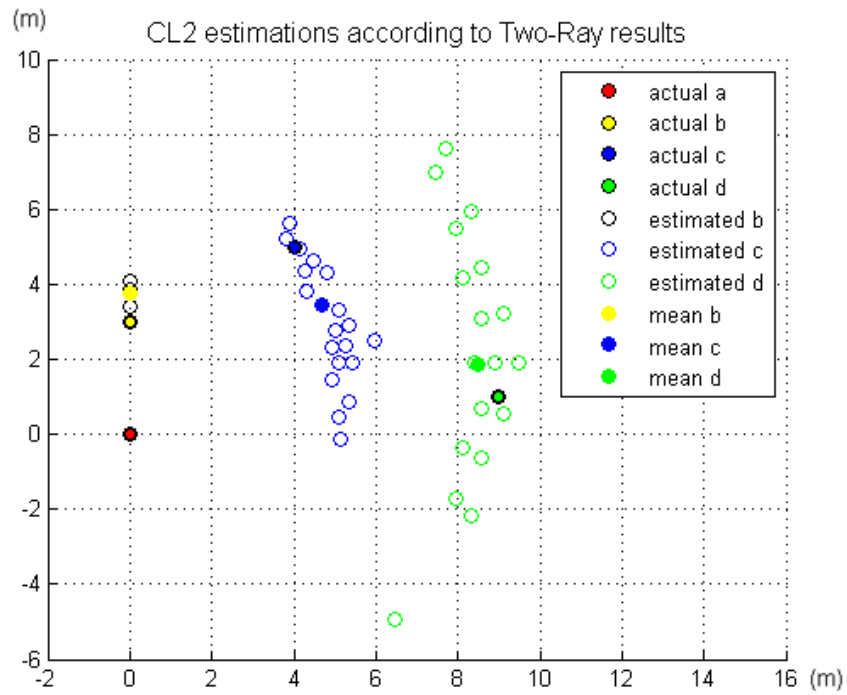


Figure 4.55 Positioning results of CL2 for the distance estimations of Two-Ray Model

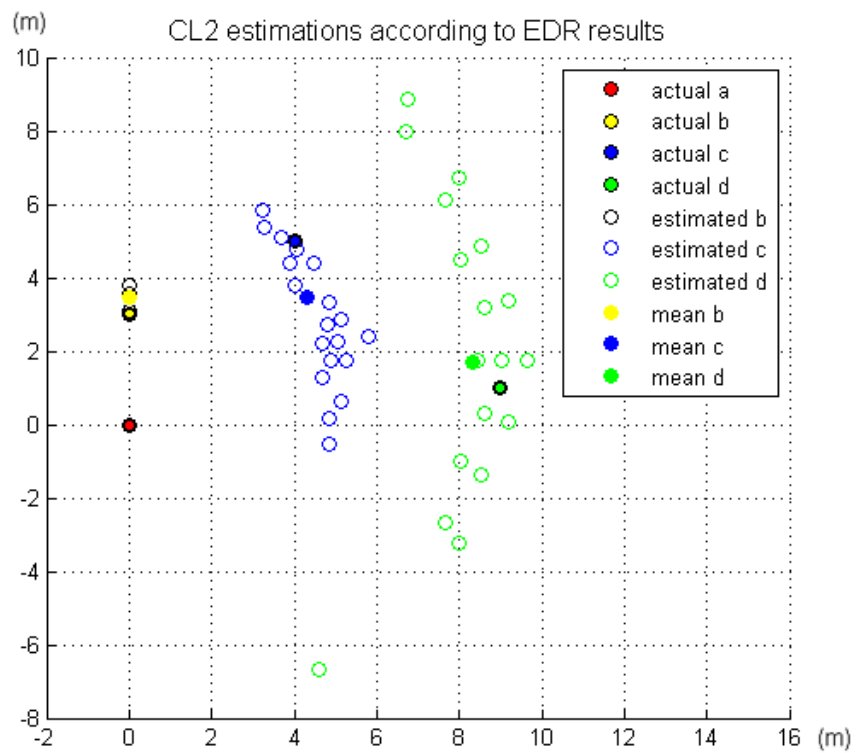


Figure 4.56 Positioning results of CL2 for the distance estimations of EDR Model

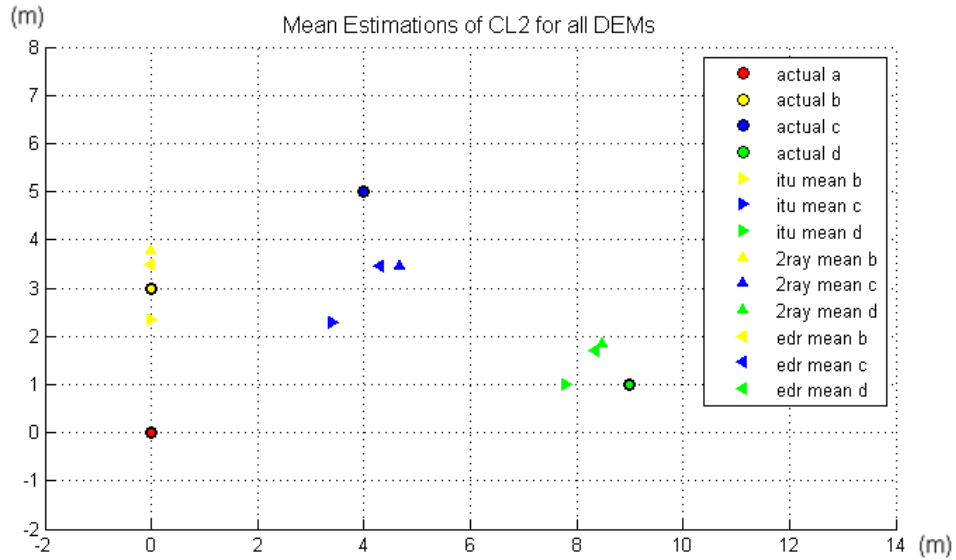


Figure 4.57 Mean positioning results of CL2 for all the distance estimation methods

Table 4.14 Positioning errors of CL2

CL2	client b (m)	client c (m)	client d (m)	mean (m)
ITU	0.6444	2.7821	1.1947	1.5404
Two-Ray	0.7784	1.6832	0.9895	1.1504
EDR	0.4689	1.5763	0.9496	0.9983

The positioning error table yields that, again the performance of EDR Model is better than the other two distance estimation models. Note that, even if the positioning method is the same, the positioning error values of the client *c* are much higher than it is for client *d*. This is originated by both the faulty measurements and the distance estimation errors for the position of client *c*. The estimated distance curves of all the distance estimation methods (see Distance Estimation Results, Section 4.2.2) are alternating over the actual distance curve. For some points, the estimated distance and the actual one are really close but for some it is highly remote. During the RSSI metric measurements, if the distance between the clients is coincide with the remote point of the distance curve, the distance estimation, hence, the position estimation of that client will be faulty, as it is for client *c*.

### 4.2.3.3 Positioning Results of the 3<sup>rd</sup> Client Layout

The position estimations of the 3<sup>rd</sup> CL are presented in the following illustrations. After the graphs, the numerical error comparison of the 3 distance estimation methods can be seen.

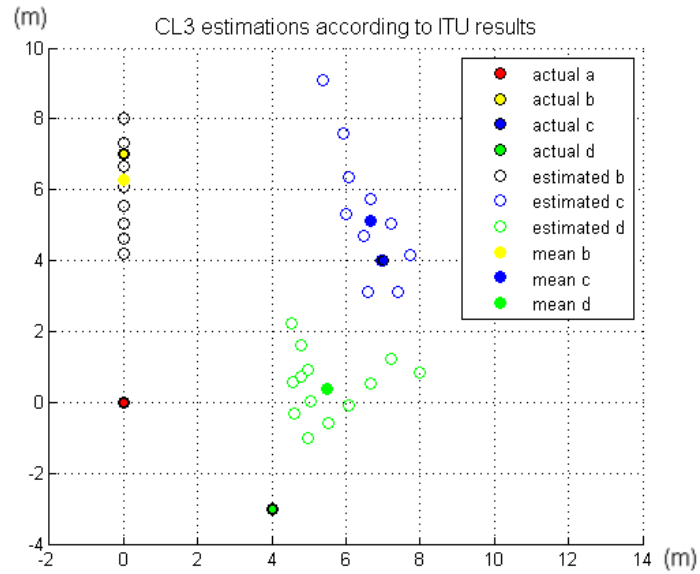


Figure 4.58 Positioning results of CL3 for the distance estimations of ITU Model

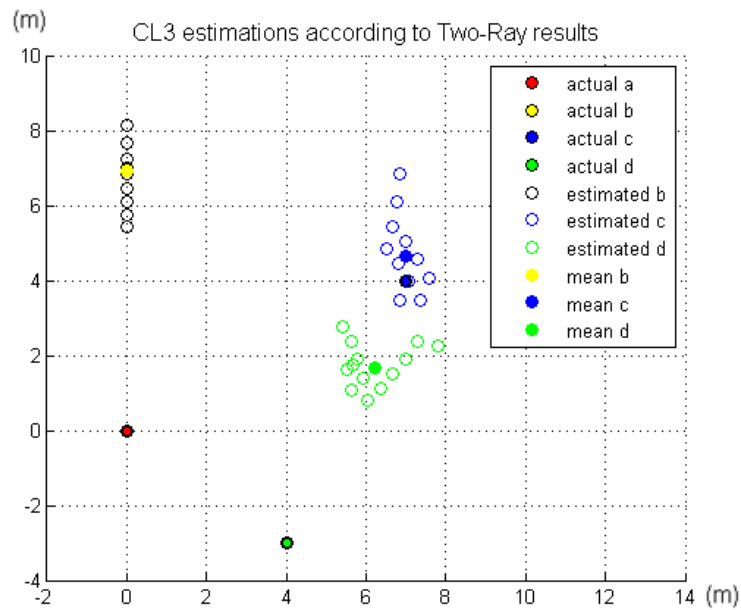


Figure 4.59 Positioning results of CL3 for the distance estimations of Two-Ray Model

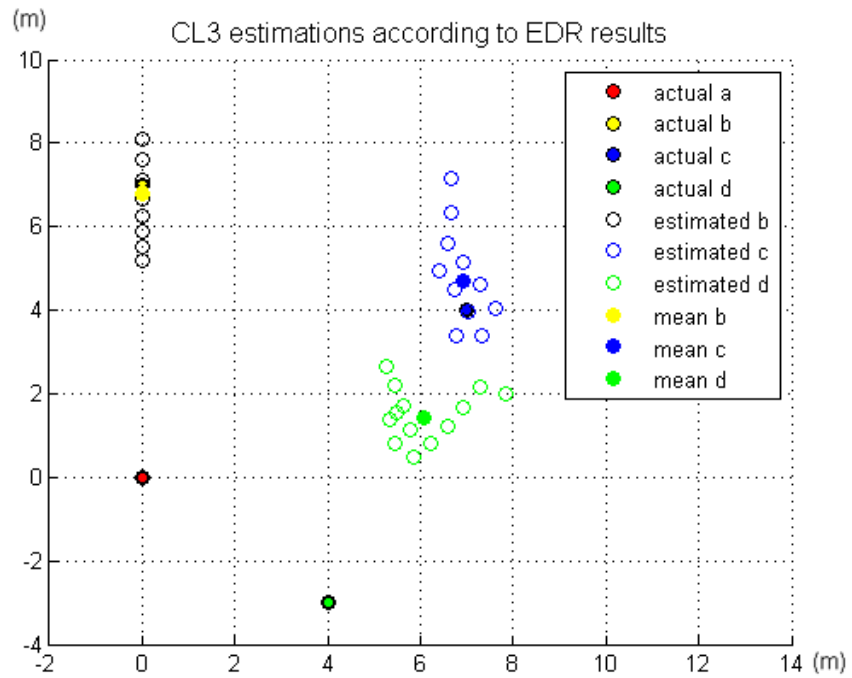


Figure 4.60 Positioning results of CL3 for the distance estimations of EDR Model

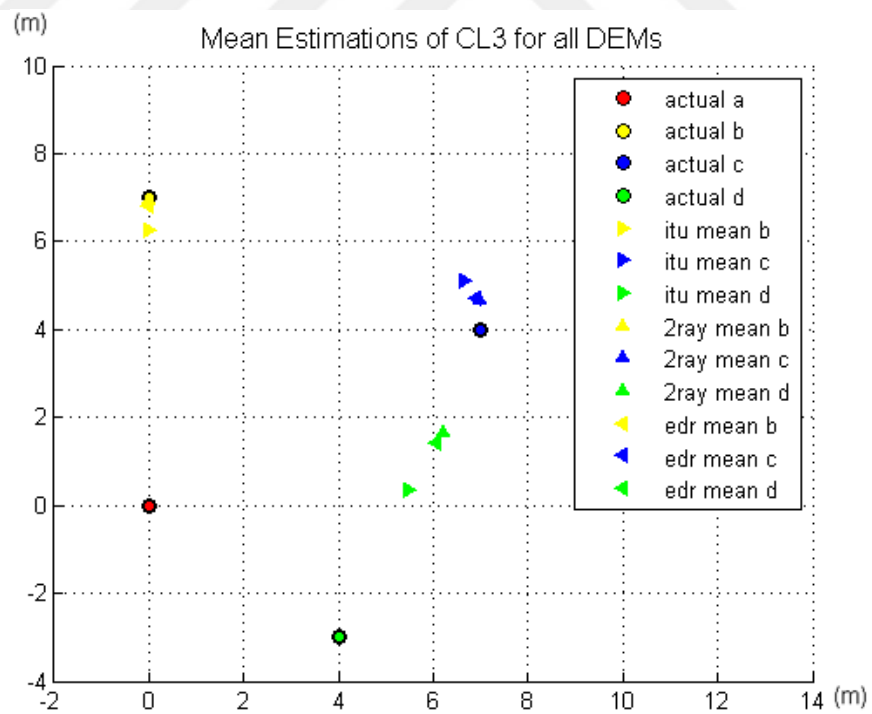


Figure 4.61 Mean positioning results of CL3 for all the distance estimation methods

Table 4.15 Positioning errors of CL3

CL3	client b (m)	client c (m)	client d (m)	mean (m)
ITU	0.7355	1.1522	3.6760	1.8546
Two-Ray	0.0619	0.6507	5.1596	1.9574
EDR	0.2037	0.7148	4.8852	1.9346

Table 4.15 contains the positioning error values for all 3 distance estimation methods and the mean positioning errors. The mean positioning error values are very close to each other and the best condition seems to be the ITU Model where it was EDR Model for the 1<sup>st</sup> and 2<sup>nd</sup> CL. Also it was previously stated that the positioning error of client *c* is very high in the 2<sup>nd</sup> CL, and it was caused by the faulty metric measurements. This time for the 3<sup>rd</sup> CL, the unexpectedly high positioning error belongs to client *d* where client *c* is accurately located considering client *d*.

#### 4.2.3.4 Positioning Results of the 4<sup>th</sup> Client Layout

The results of the NOIP for the 4h and the last CL are presented in this section. Also the numerical positioning error table is given in the end of the section.

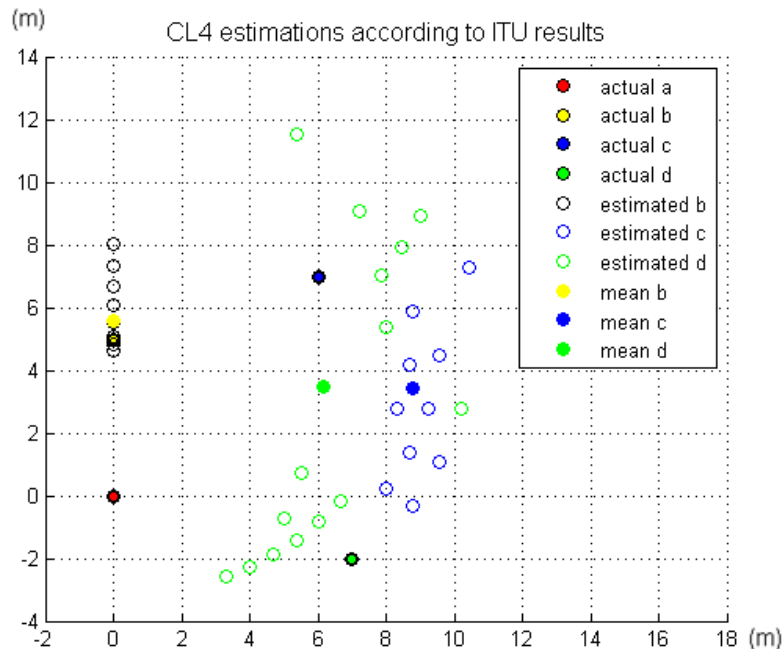


Figure 4.62 Positioning results of CL4 for the distance estimations of ITU Model

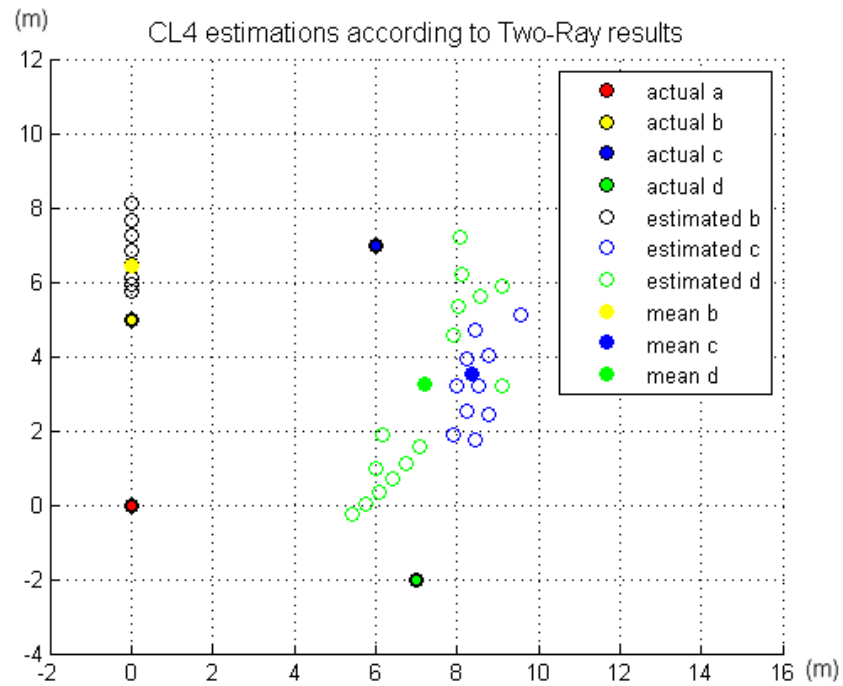


Figure 4.63 Positioning results of CL4 for the distance estimations of Two-Ray Model

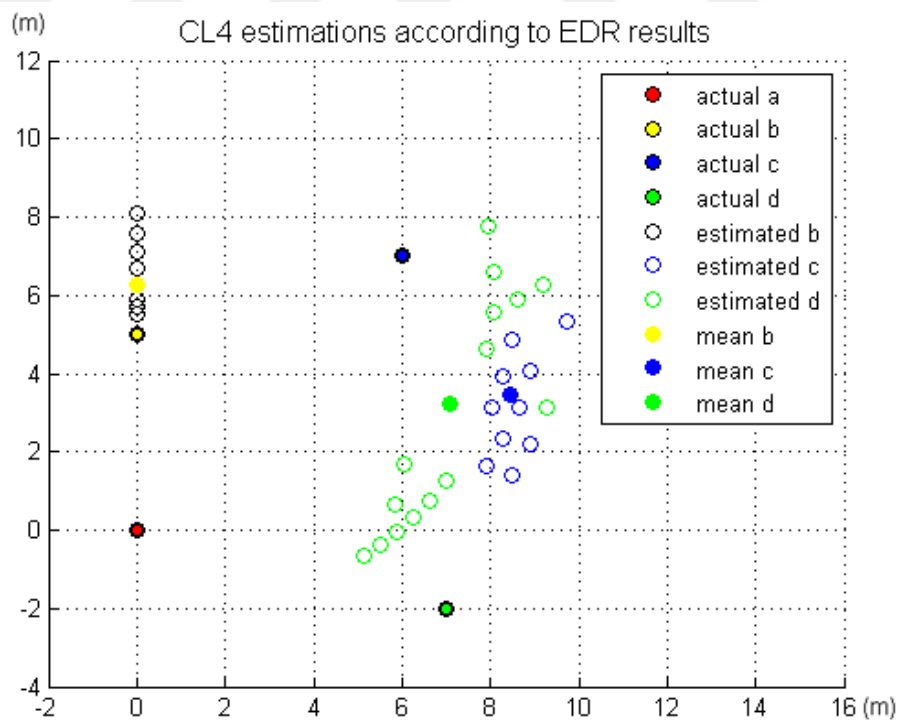


Figure 4.64 Positioning results of CL4 for the distance estimations of EDR Model

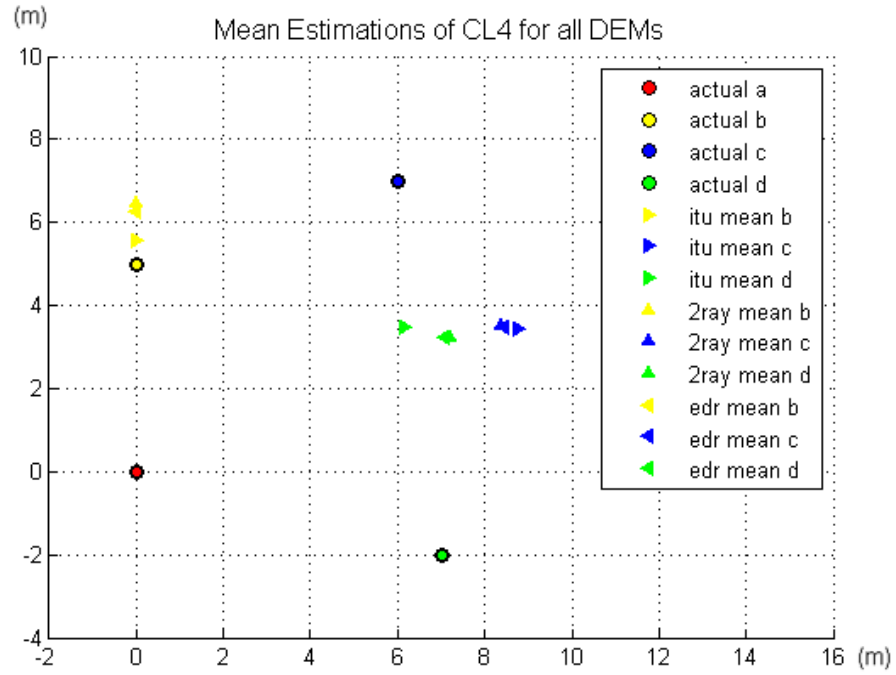


Figure 4.65 Mean positioning results of CL4 for all the distance estimation methods

Table 4.16 Positioning errors of CL4

CL4	client b (m)	client c (m)	client d (m)	mean (m)
ITU	0.5578	4.5251	5.5205	3.5345
Two-Ray	1.4492	4.2063	5.2416	3.6324
EDR	1.2667	4.2827	5.2196	3.5897

For the last CL, Table 4.16 yields the positioning error values for all the distance estimation methods. However, the layout sequence of this CL seems to be improper. For all the position estimations (except for one, ITU *b*), the error is over 1 m where the mean positioning errors of all 3 DEMs also over 3 m. This is highly non preferential for an indoor localization system considering the positions of the clients. On the other hand, this resulting error values are caused by the faulty measurements. The reason that the error values of client *c* and *d* is over 4 and 5 m respectively, is that the distances between the clients *d* to *a* ( $L_{ad}$ ), *d* to *b* ( $L_{bd}$ ), *c* to *a* ( $L_{ac}$ ) and *c* to *b* ( $L_{bc}$ ) are all coincide with the faulty measurement points. The actual distances and the estimations of those points are presented in Table 4.17.

Table 4.17 Actual and estimated distance comparison for the 4<sup>th</sup> CL

<b>CL4</b>	<b>Lab (m)</b>	<b>Lac (m)</b>	<b>Lad (m)</b>	<b>Lbc (m)</b>	<b>Lbd (m)</b>	<b>Lcd (m)</b>
<b>Actual</b>	5.00	9.22	7.28	6.32	9.90	9.05
<b>ITU</b>	5.56	9.69	8.34	9.34	8.47	9.66
<b>Two-Ray</b>	6.45	9.14	8.18	8.94	8.41	9.12
<b>EDR</b>	6.27	9.21	8.18	8.98	8.40	9.19

The differences between the actual distances and the estimated ones show the basis of the unexpectedly high positioning errors. The distances are estimated faulty because of the faulty measurements caused by the intersections of the signals LOSs, hence, it is considered to be normal to estimate a faulty client location.

#### 4.2.3.5 Performance Comparison of the Positioning Results

In this section, the positioning errors of all the CLs are presented together and compared. In Table 4.18 all the error value are shared.

Table 4.18 Error comparison of all CLs for all the distance estimation methods

<b>Positioning Errors</b>		<b>client b (m)</b>	<b>client c (m)</b>	<b>client d (m)</b>	<b>mean (m)</b>
<b>CL1</b>	<b>ITU</b>	0.4914	1.4390	1.7747	1.2350
	<b>Two-Ray</b>	0.1427	1.5036	1.1533	0.9332
	<b>EDR</b>	0.1745	1.0804	1.3617	0.8722
	<b>Mean of CL1</b>	0.2695	1.3410	1.4299	1.0135
<b>CL2</b>	<b>ITU</b>	0.6444	2.7821	1.1947	1.5404
	<b>Two-Ray</b>	0.7784	1.6832	0.9895	1.1504
	<b>EDR</b>	0.4689	1.5763	0.9496	0.9983
	<b>Mean of CL2</b>	0.6306	2.0139	1.0446	1.2297
<b>CL3</b>	<b>ITU</b>	0.7355	1.1522	3.6760	1.8546
	<b>Two-Ray</b>	0.0619	0.6507	5.1596	1.9574
	<b>EDR</b>	0.2037	0.7148	4.8852	1.9346
	<b>Mean of CL3</b>	0.3337	0.8392	4.5736	1.9155
<b>CL4</b>	<b>ITU</b>	0.5578	4.5251	5.5205	3.5345
	<b>Two-Ray</b>	1.4492	4.2063	5.2416	3.6324
	<b>EDR</b>	1.2667	4.2827	5.2196	3.5897
	<b>Mean of CL4</b>	1.0913	4.3380	5.3272	3.5855

Table 4.18 shows that the best error performance is obtained from the 1<sup>st</sup> CL, then comes the 2<sup>nd</sup>, 3<sup>rd</sup> and the 4<sup>th</sup> respectively. The layouts are user defined and it is a

coincidence that the error performance is parallel with the order of layouts. However, it was observed that, even if the mean error performance results show otherwise, the individual positioning errors of the clients yield different performance placements. For client  $b$ , the best error performance is for the 1<sup>st</sup> CL, followed by the 3<sup>rd</sup>, the 2<sup>nd</sup> and the 4<sup>th</sup> CLs where it is the 3<sup>rd</sup>, the 1<sup>st</sup>, the 2<sup>nd</sup>, the 4<sup>th</sup> and the 2<sup>nd</sup>, the 1<sup>st</sup>, the 3<sup>rd</sup> and the 4<sup>th</sup> for clients  $c$  and  $d$  respectively (see Table 4.19).

Table 4.19 Individual and mean error performance comparison of the CLs

	<b>1st</b>	<b>2nd</b>	<b>3rd</b>	<b>4th</b>
<b>client <math>b</math></b>	CL1	CL3	CL2	CL4
<b>client <math>c</math></b>	CL3	CL1	CL2	CL4
<b>client <math>d</math></b>	CL2	CL1	CL3	CL4
<b>mean</b>	CL1	CL2	CL3	CL4

The purpose of Table 4.19 is to show that it does not necessarily mean that the average performance placements do not change for individual performances. Even if the mean performance result of the 1<sup>st</sup> CL is the best that it does not mean all the clients are located at best. Those individual error performances depend on how accurately the distances are estimated.

## CHAPTER FIVE

### CONCLUSION

To solve the indoor localization problem, for a robotic team number of 4, 3 RSS based distance estimation methods and a novel positioning algorithm that needs no initial conditions has been presented. The 3 distance estimation methods, ITU Indoor Path Loss Model, Two-Ray Ground Reflected Path Loss Model and EDR Model are the distance estimation methods based on RSSI measurements which are provided by the SID working with Wi-Fi. For one CL the simulation results and for 4 different CLs the experiment results have been illustrated. Also the error performance of every individual distance estimation method and CL is examined.

The positioning algorithm that needs no initial conditions, the NOIP, is a triangulation based locator. The relative coordinate plane is set on the first two clients,  $a$  and  $b$ , then the positions of the other clients,  $c$  and  $d$ , are estimated on that RCP. This algorithm is based on only the RSSI measurements and therefore the positions of the last two clients have been estimated with an assumption that the  $x$ -axis value of their estimated position would always be positive. This study is a part of a larger project that also includes the AoA information of the clients. In the project, the information of '*which side is the client on x-axis*' is provided by AoA. Also more additive information is provided by an Inertial Measurement Unit (IMU) and by the fusion of all the obtained information, a weighted positioning system is constructed.

The numerical error analyzes of both the distance estimations and the position estimations yields that, the performance of the system is highly depended on the environmental conditions for an RSS based implementation. Additionally, the performance of the system is also influenced by the operating frequency and the supported metric limits of the chosen Wi-Fi IC. The chosen IC can operate smoothly up to 30 m but provides the metrics of RSSI only within 2-12 m. Besides those limits, the RSSI metrics do not change; one can only see the maximum signal strength up to 2 m and the minimum signal strength after 12 m. These limitations are

strictly restricts the resolution of estimations and definitely increase the positioning error. It is observed that environmental and the operating conditions are very important for an RSS based indoor positioning system.

Nevertheless, the NOIP, unlike the other triangulation related algorithms needs no initial conditions, or, likewise, the presented indoor positioning system needs no initial information, implementation etc. Hence, even if the methodology is similar, locating a client with only the information of a set of measurements becomes more effective. The presented system provides the knowledge how the distance estimation methods would be used and also presents a user defined solution for specific utilizations. One can use the self-defined method of distance estimation, EDR, and modify the equation for a specific environment. The reliability of EDR is proven by the results which is considerably consistent with the results of one of the distance estimation methods, Two-Ray Model. Two-Ray Model is also an indoor path loss model. The fact that the results of these two models are similar makes EDR a method of distance estimation, a path loss model such as the predecessors for indoor environments.

The relative coordinate plane that the clients are located on, can be moved to any other known map by using Rotation, Transformation or even Denavit-Hartenberg Matrices although they are used for mainly kinematics. This solution enables to expand the usage of the presented positioning system to a 3D localization system. One can define a map, locate the clients, and then relocate them again without dealing with extra positioning work to any other known map. When the only input was RSSI of the system, the origin displacement and the rotations of each axis would be added as the new inputs. Also by the enlargement of the diversity of the environments where the RSSI metrics are recorded, it is thought to be derive more distance estimation models and in the end, a novel distance estimation model that depends on its' own constants. By recording more measurements in various indoor environments, it is aimed to define those constants that belong to the novel distance estimation model. All improvements that are presented in this paragraph are considered to be our future work.

Last of all, this thesis provides a solution to a problem which has been studied increasingly frequent in the recent years, the indoor localization problem. The wireless communication metrics, indoor distance estimation methods and a novel positioning algorithm are studied, interpreted and the results of all are presented. Both the simulation and experiment procedures are completed, and correlations between them are defined. By the defined correlations and self-impressions new results are provided to improve the conception of this thesis. Consequently, an indoor positioning system based on RSS measurements that needs no initial conditions is presented.



## REFERENCES

- Arslan, H., Chen, Z. N., & Di Benedetto, M.-G. (Eds.). (2006). *Ultra wideband wireless communication*. New Jersey: John Wiley & Sons.
- Chrysikos, T., Georgopoulos, G., & Kotsopoulos, S. (2009). Site-specific validation of ITU indoor path loss model at 2.4 GHz. *2009 IEEE International Symposium on a World of Wireless, Mobile and Multimedia Networks and Workshops, WOWMOM 2009*.
- Cong, L., & Weihua, Z. (2002). Hybrid TDOA/AOA mobile user location for wideband CDMA cellular systems. *IEEE Transactions on Wireless Communications*, *1*(3), 439–447.
- Doğançay, K. (2005). Emitter localization using clustering-based bearing association. *IEEE Transactions on Aerospace and Electronic Systems*, *41*(2), 525–536.
- FN-LINK. (n.d.). *Realtek RTL8723BU USB Wi-Fi+BT Combo Module*. Retrieved January 7, 2017, from <http://www.fn-link.com/downloadRepository/113cd977-6c91-4f69-8b97-63fc138fa254.pdf>
- Gaber, A., & Omar, A. (2015). A study of wireless indoor positioning based on joint TDOA and DOA estimation using 2-D matrix pencil algorithms and IEEE 802 . 11ac. *IEEE Transaction on Wireless Communications*, *14*(5), 2440–2454.
- Galvan, T. G. C. E., Galvan-Tejada, I., Sandoval, E. I., & Brena, R. (2012). Wifi bluetooth based combined positioning algorithm. *Procedia Engineering*, *35*, 101–108.

- Grossmann, U., Gansemer, S., & Suttorp, O. (2008). Rssi-based wlan indoor positioning used within a digital museum guide. *International Scientific Journal of Computing*, 7(2), 66–72.
- Guerrieri, J. R., Francis, M. H., Wilson, P. F., Kos, T., Miller, L. E., Bryner, N. P., et al. (2006). RFID-assisted indoor localization and communication for first responders. In *Antennas and Propagation, 2006. EuCAP 2006. First European Conference on* pp. 1–6). IEEE.
- Gustafsson, F., & Gunnarsson, F. (2003). Positioning using time-difference of arrival measurements. *2003 IEEE International Conference on Acoustics, Speech, and Signal Processing, 2003. Proceedings. (ICASSP '03).*, 6, 553–556.
- Güvenç, I., & Chong, C. C. (2009). A survey on TOA based wireless localization and NLOS mitigation techniques. *IEEE Communications Surveys and Tutorials*, 11(3), 107–124.
- Hara, S., & Anzai, D. (2008). Experimental performance comparison of RSSI- and TDOA-based location estimation methods. *VTC Spring 2008 - IEEE Vehicular Technology Conference*, 0, 2651–2655.
- Indoor Positioning System*. (n.d.). Retrieved January 21, 2017, from [https://en.wikipedia.org/wiki/Indoor\\_positioning\\_system](https://en.wikipedia.org/wiki/Indoor_positioning_system)
- International Telecommunication Union*. (2015). Retrieved January 10, 2017, from [https://www.itu.int/dms\\_pubrec/itu-r/rec/p/R-REC-P.1238-8-201507-I!!PDF-E.pdf](https://www.itu.int/dms_pubrec/itu-r/rec/p/R-REC-P.1238-8-201507-I!!PDF-E.pdf)
- Kaune, R. (2012). Accuracy studies for TDOA and TOA localization. *2012 15th International Conference on Information Fusion (FUSION)*, 408–415.

- Kietlinski-Zaleski, J., Yamazato, T., & Katayama, M. (2010). Experimental validation of TOA UWB positioning with two receivers using known indoor features. *Record - IEEE PLANS, Position Location and Navigation Symposium*, 505–509.
- Kovács, T., Pásztor, A., & Istenes, Z. (2011). A multi-robot exploration algorithm based on a static Bluetooth communication chain. *Robotics and Autonomous Systems*, 59(7–8), 530–542.
- Kumar, P., Reddy, L., & Varma, S. (2009). Distance measurement and error estimation scheme for RSSI based localization in wireless sensor networks. *2009 Fifth IEEE Conference on Wireless Communication and Sensor Networks (WCSN)*, 1–4.
- Laaraiedh, M., Yu, L., Avrillon, S., & Uguen, B. (2011). Comparison of hybrid localization schemes using RSSI, TOA and TDOA. *European Wireless*, 2011, 626–630.
- Larranaga, J., Muguira, L., Lopez-Garde, J. M., & Vazquez, J. I. (2010). An environment adaptive ZigBee-based indoor positioning algorithm. *2010 International Conference on Indoor Positioning and Indoor Navigation, IPIN 2010 - Conference Proceedings*, 15–17.
- Lassabe, F., Canalda, P., Chatonnay, P., Spies, F., & Baala, O. (2005). A Friis-based calibrated model for WiFi terminals positioning. *Proceedings - 6th IEEE International Symposium on a World of Wireless Mobile and Multimedia Networks, WoWMoM 2005*, 382–387.
- Li, J., Han, G., Zhu, C., & Sun, G. (2016). An indoor ultrasonic positioning system based on TOA for internet of things. *Hindawi Publishing Corporation, Mobile Information Systems*, 2016, 1-10.

- Liu, H., Darabi, H., Banerjee, P., & Liu, J. (2007). Survey of wireless indoor positioning techniques and systems. *IEEE Transactions on Systems, Man and Cybernetics Part C: Applications and Reviews*, 37(6), 1067–1080.
- McCrary, D. D., Doyle, L., Forstrom, H., Dempsey, T., & Martorana, M. (2000). Mobile ranging using low-accuracy clocks. *IEEE Transactions on Microwave Theory and Techniques*, 48(6), 938–950.
- Moghtadaiee, V., Dempster, A. G., & Lim, S. (2011). Indoor localization using FM radio signals: A fingerprinting approach. In *Indoor Positioning and Indoor Navigation (IPIN), 2011 International Conference on* (pp. 1–7). IEEE.
- Mondada, F., Bonani, M., Raemy, X., Pugh, J., Cianci, C., Klapotocz, A., et al. (2006). The e-puck , a Robot Designed for Education in Engineering. *Robotics*, 1(1), 59–65.
- Nuaimi, K. Al, & Kamel, H. (2011). A survey of indoor positioning systems and algorithms. In *Innovations in Information Technology (IIT), 2011 International conference on* (pp. 185–190). IEEE.
- Quinlan, M. J., Chalup, S. K., & Middleton, R. H. (2003). Techniques for improving vision and locomotion on the sony aibo robot. *Proceedings of the 2003 Australasian Conference on Robotics and Automation*.
- Rappaport, T. (1996). *Wireless communications: Principles and practice*. United States: IEEE Publications,U.S.
- Rappaport, T. S., Reed, J. H., & Woerner, B. D. (1996). Position location using wireless communications on highways of the future. *IEEE Communications Magazine*, 34(10), 33–41.

*Raspberry Pi*. (n.d.). Retrieved January 7, 2017, from [https://en.wikipedia.org/wiki/Raspberry\\_Pi](https://en.wikipedia.org/wiki/Raspberry_Pi)

Seybold, J. S. (2005). *Introduction to RF Propagation*. New Jersey: John Wiley & Sons.

Sommer, C., & Dressler, F. (2011). Using the right two-ray model? A Measurement based evaluation of PHY models in VANETs. *Proceeding ACM MobiCom*, (3), 1–3.

Türkoral, T., Tamer, Ö., Yetiş, S., & Çetin, L. (2016). Positioning with standart communication metrics without initial position information. *24th Signal Processing and Communication Application Conference (SIU), 2016*, 661–664.

Türkoral, T., Tamer, Ö., Yetiş, S., & Çetin, L. (2017). Indoor localization for swarm robotics with communication metrics without initial position information. *Mechatronics and Robotics Engineering for Advanced and Intelligent Manufacturing*, 207–215.

Türkoral, T., Tamer, Ö., Yetiş, S., İnanç, E., & Çetin, L. (2016). Indoor distance estimation with using received signal strength indicator (RSSI) metric. In *Electrical, Electronics and Biomedical Engineering (ELECO), 2016 National Conference on* (pp. 397-401). IEEE.

Winfield, A. F. T., & Holland, O. E. (2000). The application of wireless local area network technology to the control of mobile robots. *Microprocessors and Microsystems*, 23(10), 597–607.

Xiao, J., Liu, Z., Yang, Y., Liu, D., & Xu, H. (2011). Comparison and analysis of indoor wireless positioning techniques. *2011 International Conference on Computer Science and Service System, CSSS 2011 - Proceedings*, 293–296.

Yamasaki, R., Ogino, A., Tamaki, T., Uta, T., Matsuzawa, N., & Kalo, T. (2005). TDOA location system for IEEE 802.11b WLAN. *IEEE Wireless Communications and Networking Conference, WCNC*, 4, 2338–2343.



## **APPENDICES**

### **ABBREVIATIONS**

AGC – Automatic Gain Control

AoA – Angle of Arrival

AP – Access Point

AWGN – Additive White Gaussian Noise

CL – Client Layout

CPU – Central Processing Unit

EDR – Experimentally Derived Signal Strength – Distance Relation

IC – Integrated Circuit

ISC – Iterations – SNR Combinations

IMU – Inertial Measurement Unit

ITU – International Telecommunication Union

LOS – Line of Sight

MC – Measurement Circle

MM – Measurement Method

NOIP – No Initial Indoor Positioning

NRT – Non-Radio Technologies

RCP – Relative Coordinate Plane

RPi – Raspberry Pi

RSS – Received Signal Strength

RSSI – Received Signal Strength Indicator

RX – Serial Data Receive

SBC – Single Board Computer

SID – Self-Implemented Device

SNR – Signal to Noise Ratio

SSDR – Signal Strength – Distance Relation

TDoA – Time Difference of Arrival

ToA – Time of Arrival

Two-Way ToA – Two-Way Time of Arrival

TX – Serial Data Transmit

WLAN – Wireless Local Area Network

WT – Wireless Technologies

